University of New Hampshire
University of New Hampshire Scholars' Repository

Doctoral Dissertations | Student Scholarship

Fall 2017

# DEVELOPMENT OF NOVEL BIO- AND HETEROGENEOUS CATALYSTS FOR THE PRODUCTION OF BIO- AND GREEN DIESEL

Ye Deng
*University of New Hampshire, Durham*

Follow this and additional works at: https://scholars.unh.edu/dissertation

Recommended Citation
Deng, Ye, "DEVELOPMENT OF NOVEL BIO- AND HETEROGENEOUS CATALYSTS FOR THE PRODUCTION OF BIO- AND GREEN DIESEL" (2017). *Doctoral Dissertations*. 2274.
https://scholars.unh.edu/dissertation/2274

This Dissertation is brought to you for free and open access by the Student Scholarship at University of New Hampshire Scholars' Repository. It has been accepted for inclusion in Doctoral Dissertations by an authorized administrator of University of New Hampshire Scholars' Repository. For more information, please contact nicole.hentz@unh.edu.

# DEVELOPMENT OF NOVEL BIO- AND HETEROGENEOUS CATALYSTS FOR THE PRODUCTION OF BIO- AND GREEN DIESEL

BY

YE DENG

B.S., Tianjin University, 2010

M.S., University of New Hampshire, 2012

DISSERTATION

Submitted to the University of New Hampshire

in Partial Fulfillment of

the Requirements for the Degree of

Doctor of Philosophy

in

Chemical Engineering

September, 2017

This dissertation has been examined and approved in partial fulfillment of the requirements for the degree of Doctor of Philosophy in Chemical Engineering by:

Dissertation Director, Dr. Palligarnai T. Vasudevan
Professor of Chemical Engineering
Senior Vice Provost for Academic Affairs

Dr. Subhash C. Minocha
Professor of Plant Biology and Genetics

Dr. Dale P. Barkey
Professor of Chemical Engineering

Dr. Kang Wu
Assistant Professor of Chemical Engineering

Dr. Harish Vashisth
Assistant Professor of Chemical Engineering

On March 28, 2017

Original approval signatures are on file with the University of New Hampshire Graduate School.

## DEDICATION

I lovingly dedicate this dissertation to my wife and parents.

## ACKNOWLEDGEMENTS

I would like to express my profound appreciation and gratitude to Dr. P. T. Vasudevan, who has provided me guidance and support over the past seven years as my advisor and mentor for both M.S. and Ph.D. programs. He has been a great source of knowledge and wisdom and I have been truly fortunate to have the opportunity to work with him. Thank you.

I would also like to deeply thank Dr. Subhash C. Minocha for his guidance and mentorship and for providing me the opportunity to conduct genetic engineering research in his laboratory. Dr. Minocha also had an excellent research team to whom I would like to express my special thanks: Dr. Swathi Turlapati, Dr. Lin Shao, and Ashley Matthews. I would also like to acknowledge David E. Goudreault and Jonathan Ebba for their assistance and guidance growing the transgenic tobacco plants at the Macfarlane Greenhouse.

I would also like to appreciate the rest of my dissertation committee members, Dr. Dale Barkey, Dr. Kang Wu, and Dr. Harish Vashisth, for their support and help through my academic program. In addition, I would like to thank Dr. Michael Gagnon for help training me to work with the experiments. Thanks to technician John Newell for help assembling the reaction system. And thanks to all the undergraduate students who have assisted me: Nick, Per, Juliana, and Eddlin.

Lastly, I would like to recognize my family for always being there and believing in me. Most importantly, I would like to specially recognize and deeply thank my wife, Xiaoyi, with all of my heart for her love, support, and patience throughout my studies.

## TABLE OF CONTENTS

DEDICATION ..... iv

ACKNOWLEDGEMENTS ..... v

TABLE OF CONTENTS ..... vi

LIST OF FIGURES ..... xi

LIST OF TABLES ..... xiii

ABSTRACT ..... xiv

CHAPTER 1 INTRODUCTION ..... 1

1.1 Energy and Environment ..... 1

1.2 Biodiesel ..... 2

*1.2.1 Mechanism of Biodiesel Production ..... 3*

*1.2.2 Alcohols ..... 4*

*1.2.3 TAGs Sources ..... 4*

*1.2.4 Catalysts ..... 5*

1.3 Challenges and Overview ..... 7

CHAPTER 2 TRANSGENIC EXPRESSION OF LIPASE ON PLANTS FOR THE ENZYMATIC PRODUCTION OF BIODIESEL ..... 10

2.1 Introduction ..... 10

*2.1.1 Current States of Plant Biotechnology ..... 10*

*2.1.2 Genetically Enhancing Oil Accumulation* ..... *13*

*2.1.3 Industrial Lipase Production* ..... *16*

*2.1.4 Recombinant Protein Expression Systems* ..... *18*

2.2 Experimental Section ..... 24

*2.2.1 Strains, Plasmids, and Materials* ..... *24*

*2.2.2 Cloning of T. lanuginosus Lipase cDNA* ..... *25*

*2.2.3 Cloning of C. antarctica Genome DNA* ..... *26*

*2.2.4 Lipase Gene Amplification by Polymerase Chain Reaction (PCR)* ..... *26*

*2.2.5 Agarose Gel Electrophoresis* ..... *27*

*2.2.6 Cloning Vector and Heat-shock Transformation* ..... *27*

*2.2.7 Bacterial Culture and Plasmid DNA isolation* ..... *28*

*2.2.8 Restriction Digestion* ..... *29*

*2.2.9 DNA Sequencing and Analysis* ..... *29*

*2.2.10 Glycerol Stocks* ..... *29*

*2.2.11 Construction of the Final Destination Vectors* ..... *29*

*2.2.12 Electroporation* ..... *30*

*2.2.13 Agrobacterium-mediated Transformation of Tobacco* ..... *31*

*2.2.14 Floral Dip Transformation of Arabidopsis* ..... *32*

*2.2.15 Screening for Transgenic Lines* ..... *32*

*2.2.16 Recombinant Enzyme Extraction* ..... *33*

*2.2.17 Acetone Precipitation* ..... *34*

*2.2.18 Ammonium Sulfate Precipitation and Dialysis* ..... *34*

*2.2.19 His-tagged Protein Purification* ..... *35*

*2.2.20 SDS-PAGE* ..... *36*

*2.2.21 Tributyrin Assay* ..... *36*

2.3 Results and Discussion ..... 37

*2.3.1 Approach and Methodology* ..... *37*

*2.3.2 Cloning of T. Lanuginosus and C. Antarctica Lipase Genes* ..... *39*

*2.3.3 Construction of the Lipase Vectors* ..... *42*

*2.3.4 Transformation of Plants* ..... *50*

*2.3.5 Screening Transgenic Plants* ..... *54*

*2.3.6 Strategy for Homozygotes Achievement of Transgenic Plants* ..... *57*

*2.3.7 Extraction, Purification, and Testing of the Recombinant Lipase in T2 Plants* ..... *59*

2.4 Conclusions ..... 67

CHAPTER 3 HYDRODEOXYGENATION OF BIODIESEL TO GREEN DIESEL VIA CO/-MO CATALYSTS ..... 69

3.1. Introduction ..... 69

3.2. Literature Review ..... 73

*3.2.1 Properties of Biodiesel versus Green Diesel* ..... *73*

*3.2.2 Methods for the Production of Green Diesel* ..... *76*

*3.2.3 Mechanism of Hydrodeoxygenation* ..... *79*

*3.2.4 Catalysts for Hydrodeoxygenation* ..... *82*

3.3. Experimental Section ..... 86

*3.3.1 Materials and Equipment* ..... *86*

*3.3.2 Catalyst Preparation* ..... *86*

*3.3.3 Surface Area and Loading Measurement* ..... *88*

*3.3.4 Equipment System Setup and Reaction Procedure* ..... *89*

*3.3.5 Catalysts Activity Investigation* ..... *94*

3.4. Results and Discusions ..... 96

*3.4.1 Effect of Feedstock* ..... *96*

*3.4.2 Effect of Pretreatment Temperature* ..... *99*

*3.4.3 Effect of Hydrogen Flow Rate* ..... *102*

*3.4.4 Effect of Reaction Temperature* ..... *106*

*3.4.5 Effect of Promoters* ..... *110*

*3.4.6 Effect of Support* ..... *111*

3.5. Conclusions ..... 112

CHAPTER 4 SUMMARY ..... 114

4.1 Overview and Conclusions ..... 114

4.2 Recommendations ..... 116

REFERENCES ..... 118

APPENDICES ..... 124

APPENDIX A GC CALIBRATION CURVES ..... 125

APPENDIX B CALCULATION OF GREEN DIESEL YIELD ..... 127

APPENDIX C MANUFACTURER'S PROTOCOLS ..... 128

APPENDIX D PH-STAT CALIBRATION ..... 137

## LIST OF FIGURES


**1** Production of biodiesel by (a) transesterification and (b) esterification. ..... 3

**2** TAG biosynthetic pathway with the major intermediates and enzymes. ..... 14

**3** Flow chart for the strategy for the production of lipase in transgenic plants ..... 39

**4** Gel analysis results of *C. antarctica* lipase B amplification products using TAKARA Taq polymerase. ..... 42

**5** Plasmid maps of PCR8/GW/TOPO - lipase constructs with annotations of important features and enzyme restriction sites. ..... 44

**6** Gel analysis results from plasmid screening by restriction digest of PCR8/GW/TOPO CAlB constructs with C1, C2 and C3 primers. ..... 45

**7** Plasmid maps of PMDC83-TLl and PGWB408 -CalB constructs with annotations of important features and enzyme restriction sites.. ..... 49

**8** Gel analysis results from plasmid screening of final destination vectors, PGWB408-CAlB 50

**9** Pictures of transgenic and non-transgenic *Arabidopsis thaliana* on kanamycin containing germination media. ..... 52

**10** Gel analysis of PCR screening of T1 transgenic Arabidopsis for *C. antarctica* lipase B gene ..... 55

**11** Gel analysis of PCR screening of T2 transgenic Arabidopsis for *C. antarctica* lipase B gene ..... 56

**12** Gel analysis of PCR screening of T2 transgenic tobacco for *T. lanuginosus* lipase gene .... 56

**13** Gene type map of transgenic plant with self-fertilization ..... 57

**14** SDS-PAGE gel results from initial protein extraction and purification of recombinant lipase from tobaccos ..... 61

**15** Precipitation schemes of recombinant lipase ..... 63

**16** Enzyme hydrolysis of tributyrin ..... 64

**17** The possible pathways in HDO process. ..... 71

**18** NOx and PM exhaust emissions of petrodiesel, biodiesel and some neat components ..... 75

**19** Strategy maps of F-T method. ..... 77

**20** Proposed reaction network for hydrodeoxygenation of palm oil ..... 81

**21** Catalyst developments for hydrodeoxygenation process ..... 82

**22** Reaction system set up ..... 90

**23** Valves set-up for pretreatment step ..... 91

**24** Valves set-up for reaction step ..... 93

**25** Valves set-up for post-reaction cleanup step ..... 94

**26** Overall methyl oleate/biodiesel conversions ..... 98

**27** Effect of pretreatment temperature with Co-/Mo on γ-alumina. ..... 100

**28** Effect of pretreatment temperature with Co-/Mo on Y-zeolite ..... 101

**29** Mass of biodiesel input at different hydrogen flow rate. ..... 102

**30** LHSV of biodiesel input with different hydrogen flow rate ..... 103

**31** Hydrogen pressure effect on HDO process ..... 105

**32** Effect of reaction temperatures with Co-/Mo on γ-alumina. ..... 108

**33** Effect of reaction temperature with Co-/Mo on Y-zeolite. ..... 109

**34** Continuous usage of unpromoted and Co-promoted Mo/γ-Al ..... 110

## LIST OF TABLES


**1** Industrial recombinant proteins produced by transgenic plants ..... 23

**2** PCR conditions for the amplification of *T. lanuginosus* lipase (TLl) cDNA and *C. antarctica* lipase B (CAlB) DNA ..... 27

**3** Lipase information identified by NCBI BLAST ..... 40

**4** Primers for cloning and sequencing of lipases form T. lanuginosus and C. antractica ..... 41

**5** Final destination vectors selected for plant transformation ..... 47

**6** Germination and survival rates for T2 generation transgenic Arabidopsis ..... 52

**7** Germination and survival rates for T2 generation transgenic tobaccos ..... 54

**8** Survival rates of T3 transgenic plants ..... 58

**9** Lipase activity form tributyrin assay ..... 66

**10** Properties of major components of biodiesel (FAME) ..... 73

**11** Properties of major components of green diesel ..... 74

**12** Comparison between gasification/FT process and HDO method ..... 79

**13** Results of BET and XPS ..... 88

**14** Informations of CoMo catalyst on different support ..... 111

**15** Conversion of biodiesel in different supported catalysts ..... 111

## ABSTRACT

## DEVELOPMENT OF NOVEL BIO- AND HETEROGENEOUS CATALYSTS FOR THE PRODUCTION OF BIO- AND GREEN DIESEL

by

Ye Deng

University of New Hampshire, September, 2017

Diminishing petroleum reserves and increasing environmental awareness has led to an urgent need to develop alternative fuels, such as biodiesel. Enzymatic trans/-esterification of waste cooking oils with a lipase catalyst is a promising environmentally-friendly process to produce biodiesel, compared to the current industrial chemical process. Despite several advantages, there are a few technical and economical obstacles that limit this process, such as insufficient availability of large quantities of inexpensive lipase suitable for catalysis, and bad performance at low temperatures due to biodiesel's low cetane number. These limitations are addressed in this dissertation using genetic engineering of plants to produce the enzyme lipase, and hydrodeoxygenation of biodiesel to produce green diesel. The specific objectives include:

- Cloning and over-expressing recombinant lipase from *T. lanuginosus* and *C. antarctica* in tobacco and *A. thaliana* in order to develop an inexpensive biocatalyst.
- Developing and characterizing supported molybdenum and cobalt promoted catalysts in the hydrodeoxygenation reaction of biodiesel for the production of green diesel to promote oils' performance.

The major findings are: (i) Lipase genes can be constitutively expressed in tobacco and *A. thaliana* without adversely affecting plant growth. Plants offer a promising platform for producing recombinant enzymes for biodiesel production; (ii) Optimization of hydrodeoxygenation process parameters such as reduction temperature, hydrogen gas flow rate, and reaction temperature can significantly increase green diesel yield; (iii) Cobalt added as a promoter in the supported molybdenum catalysts can significantly increase the catalytic activity, selectivity, and stability; and (iv) The choice of support in the heterogeneous molybdenum catalysts can also have a considerable effect on the green diesel yield.

# CHAPTER 1

# INTRODUCTION

## 1.1 Energy and Environment

Over the past decade, there has been a dramatic increase globally in the production and consumption of energy. According to the Energy Information Administration (EIA)[1], current estimates of worldwide recoverable reserves of petroleum and natural gas are estimated to be 1.34 trillion barrels and 6,289 trillion cubic feet, respectively. 87.3 million barrels of oil is consumed per day along with 112.6 billion cubic feet of natural gas. If current consumption rates continue, the worldwide reserves of oil will be exhausted in approximately 40 years, whereas the reserves of natural gas will be exhausted in approximately 60 years. As a result of this increase in consumption, the price of petroleum has increased dramatically over the past decade. A record high was achieved in July 2008 when the price per barrel of crude oil reached $147.27.[1] The price of crude oil has since dropped; however, the impact that this level of consumption has had on the environment is undeniably serious.

One impact of this increased consumption of fossil fuels, which include oil, coal, and natural gas, is that scientists are seeing higher levels of carbon dioxide ($CO_2$) than ever before. $CO_2$ is a heat-trapping greenhouse gas that is primarily produced by the combustion of fossil fuels. Scientists have determined that $CO_2$ levels naturally fluctuate from around 180 ppm to 300 ppm; however, human activities have changed the atmospheric concentrations of $CO_2$.[2] Higher levels of $CO_2$ along with an increase in greenhouse gases and deforestation directly correlate with an increase in the Earth's surface temperature, which has been seen throughout the 20$^{th}$

century. The second warmest temperature on record was just recorded in 2010.[2] The issue of climate change is one of the key challenges facing humans and it is imperative that steps are taken to reduce greenhouse gas emissions.

Recently, an urgent need has developed to produce alternative, renewable, and environmentally friendly biofuels such as biodiesel. This is partially due to an increased awareness of the environmental problems plaguing the world. Additionally, the combination of diminishing oil reserves, non-renewable resources, and unpredictable prices involved with petroleum fuels has fueled the need to develop biodiesels. As a result of this increased interest in biofuels, the International Energy Agency (IEA) has predicted that liquid biofuels will dominate the energy sector by 2030.[3]

**1.2 Biodiesel**

Biodiesel, as defined by the United States National Biodiesel Board, is a vegetable oil- or animal fat-based diesel fuel, which consists of mono long-chain alkyl esters (methyl, propyl or ethyl), that meets the requirements of the American Society for Testing Materials (ASTM) D6751.[4] The ASTM standard specifications denote the necessary physical and chemical properties of pure biodiesel as determined by chemical analysis.[5] For example, ASTM standard specifications indicate that pure biodiesel or B100 can be used as a blending component with petroleum diesel at ratios of 2% (B2), 5% (B5), or 20% (B20). The ASTM specifications are in place to ensure that biodiesel meets a specific minimum quality standard for commercial use with existing diesel engines that are less than 15 years old and that do not have any engine modifications. Older engine systems may require replacement of fuel lines and other rubber components in order to operate as a biodiesel engine within ASTM standards.

1.2.1 Mechanism of Biodiesel Production

The production of biodiesel occurs by the transesterification reaction of triglycerides (TAGs) or by the esterification of free or unesterified fatty acids (FFAs).[6] TAGs are the main component of grease, vegetable oil, and animal fat. The transesterification of TAGs with an alcohol and a catalyst will result in fatty acid esters (FAAE, biodiesel) with glycerol as a by-product (Figure 1a). FFAs are naturally present in virgin vegetable oils in small quantities. Cooking oils and fats that have already been used, such as restaurant grease, spent frialator oil, and trap grease, have higher levels of FFAs due to the hydrolysis and decomposition of TAG molecules.[5] The esterification of FFAs with an alcohol and a catalyst will result in the production of biodiesel with water as a by-product (Figure 1b).

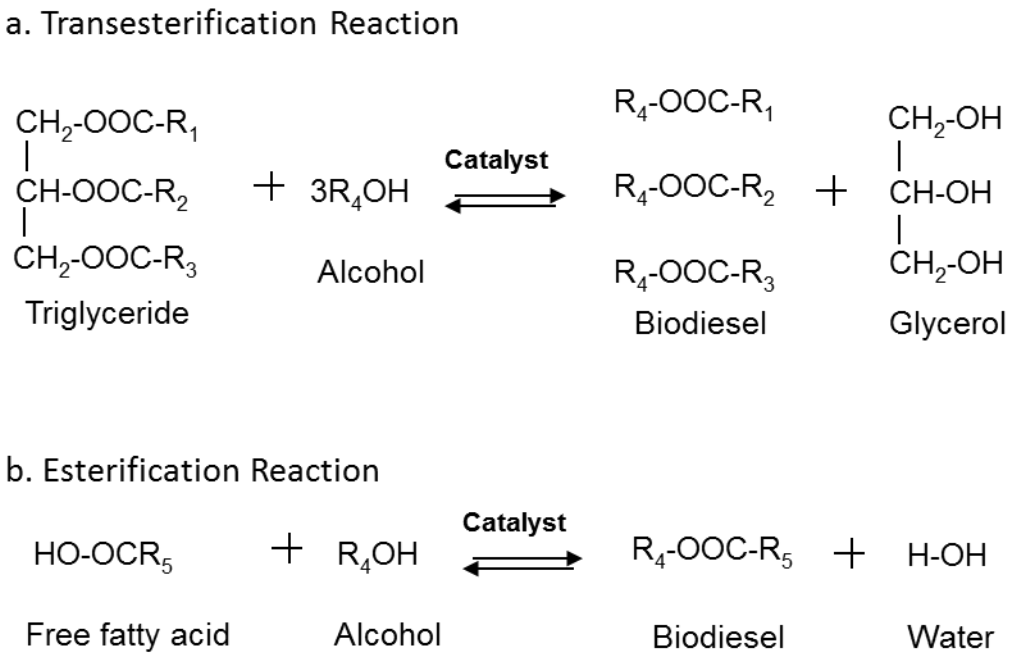


**Figure 1** Production of biodiesel by (a) transesterification and (b) esterification.

### 1.2.2 Alcohols

Typically, a short-chained alcohol (such as methanol, ethanol, propanol or butanol) works as an acyl-acceptor for biodiesel synthesis. Methanol is the most commonly used acyl-acceptor in research and in industry because of its low cost.[6] The process by which methanol is used in a transesterification reaction is referred to as methanolysis. This process results in the production of fatty acid methyl esters (FAME) as biodiesel. All of the commercial biodiesel currently available in the United States is FAME. After methanol, ethanol is the next most used acyl-acceptor because it can be produced from biomass via fermentation, whereas methanol is mainly produced from fossil fuels.[6] As a result, biodiesel produced from ethanol is more of a renewable fuel and has a higher energy content than biodiesel produced from methanol. The drawback of ethanol is that its cost is about twice as much as the price of the same quantity of anhydrous methanol. Recently, the use of acetates as a replacement for methanol has been investigated, because they prevent the formation of glycerol that can have some detrimental effects on the post-react separation process. However, the cost becomes the main factor in finding a replacement for methanol. The price of acetates is approximately fourfold the price of the same quantity of methanol, which limits their application.[5,6]

### 1.2.3 TAGs Sources

There are many TAGs sources available for biodiesel production, such as virgin vegetable oils, biomass, algae, and waste oils.[6] A considerable amount of the research to produce biodiesel has been done using edible sources of virgin vegetable oils, such as soybean, rapeseed, sunflower seed, and canola. Most of these sources vary with location, climate, and growing conditions. Soybean oil is currently the dominant feedstock for the production of

biodiesel in the United States.[7] This has resulted in soybeans being sold for fuel instead of for food-related purposes. This has resulted in increased prices of soybean oil from 2001 (16.46 cents/lb.) to 2011 (54.5 cents/lb.).[7] Moreover, an United Nations report (2008)[8] stated that the global rushed to switch from oil to energy derived from plants would drive deforestation, push small farmers off their land, increase poverty, and lead to serious food shortages unless it could be carefully managed. This has been reported as the "food versus fuel" controversy. Nevertheless, biodiesel production needs to focus on the production of more sustainable feedstocks, such as waste oils and greases, animal fats, and non-edible vegetable oil sources.

Waste cooking oils and animal fats are available in huge quantities throughout the world, especially in developed countries.[9] Disposal of these waste oils and fats pose a significant challenge because of possible contamination of water and land resources. The use of waste cooking oil as a feedstock offers significant advantages over virgin vegetable and algae oils because it enhances the economic viability of biodiesel production. Used vegetable oils are typically collected from restaurants and fast-food establishments, and can amount to almost three billion gallons per year as estimated by the EPA.[3] Food processing and service facilities also produce greases, fats, and oils in large quantities, some of which are currently sold as inexpensive animal feed. All of these waste oils, fats, and greases provide an economic opportunity to take a sustainable, low cost waste product and turn it into a viable feedstock for use in a growing biodiesel market.

### 1.2.4 Catalysts

Most of the biodiesel that is commercially produced today is by alkali-catalyzed transesterification of vegetable oils, using a homogenous base catalyst, such as sodium hydroxide (NaOH) or potassium hydroxide (KOH).[10] Due to solubility considerations, NaOH is used as

the catalyst when methanol is the acyl acceptor, and KOH is used when ethanol is the acyl acceptor. This method has proven to be the most economical because of the high conversion rate (upward of > 98% ester yield) within a short reaction time (< 1 h) at a low temperature (66°C) and low pressure environment (1.4 atm). The main drawback of this process is the sensitivity of alkaline catalysts with respect to feedstock purity. The vegetable oil and alcohol must be substantially anhydrous and have low FFA content because water and FFA promote soap formation. This formation of soap lowers the yield of esters and renders the downstream separation of the products difficult. Thus, a pretreatment step becomes necessary before the transesterification process to reduce the acid and water concentrations below an optimum threshold limit (FFAs < 1.0 wt% and water < 0.5 wt%). Other than pretreatment, alkaline transesterification also requires multi-step purification of the end products. The glycerol by-product contains some of the excess methanol, most of the catalyst and soap, which makes the alkaline transesterification process expensive and harmful to the environment.[5,6]

The second most commonly used commercial process to produce biodiesel is acid-catalyzed transesterification.[10] The most commonly employed acid catalysts are sulfuric acid ($H_2SO_4$) and hydrochloric acid (HCl). Acid catalysis is considered a viable alternative to alkaline catalysis because it is not susceptible to soap formation due to strong catalytic activity for esterification, resulting in easier product separation and a relatively high quality glycerol by-product. However, low transesterification reaction rates (50-60% of alkaline catalysis) and the high reaction temperature (100°C) that is required for acid catalysis, makes it typically used for esterification reactions only. Both the alkali and acid catalysis processes are energy intensive and require extensive downstream processing.[5,6]

A relatively new and attractive method for biodiesel production is by enzymatic transesterification and esterification.[6] Enzymes offer several advantages over chemical catalysts, such as high substrate selectivity and operation at a mild temperatures (20–60°C), pressure (1 atm), and pH conditions.[11] Unlike homogeneous chemical catalysts, enzymes are often immobilized, which simplifies the separation of products, produces a high quality glycerol, and allows for the reuse of the catalyst.[12] Waste oils, greases, lard, and other low cost feedstocks that are higher in FFAs can be used for biodiesel production without extensive processing. Moreover, enzymes require much less alcohol to perform the reaction when compared to chemical catalysts, usually close to the stoichiometric ratio, which benefits the by-product glycerol separation.

Lipases are enzymes that naturally catalyze the hydrolysis of lipids and are also a versatile biocatalyst with activities as phospholipase, cholesterol esterase, and amidase.[6, 12] The commonly used lipases in biodiesel production have triacylglycerol activity (EC 3.1.1.3 group) and are capable of catalyzing both transesterification and esterification reactions. Several microbial strains of lipases have been found to have trans/-esterification activity, such as *Candida antarctica, Pseudomonas cepacia*, and *Thermomyces lanuginosus*.[6, 9, 12]

### 1.3 Challenges and Overview

The production of biodiesel by enzymatic trans/-esterification has been extensively studied; however, this technology has not received much commercial attention due to various challenges. One challenge is the high cost of lipase due to insufficient quantities.[5,12] Currently, there are a limited number of lipases from microorganisms that have been screened for trans/-esterification activity and even fewer that are acceptable for biodiesel catalysis. Production of lipases in sufficient quantities from these microorganisms is very expensive and requires

purification and immobilization. A second challenge are the poor properties of biodiesel related to its low cetane number.[66] The cetane number of fatty esters depends on chain length and the degree of unsaturation. The presence of polyunsaturated fatty esters causes oxidative stability problems with biodiesel, and the presence of higher amounts of saturated fatty esters results in a bad low-temperature performance. Thus, the key to the economic feasibility of commercializing this technology is to lower the cost associated with using enzymes, and/or enhance the biodiesel properties by modifying/optimizing fatty esters composition. This dissertation will try to offer solutions to the current problems and examine new perspectives in the production of biofuels. The organization of this dissertation is as follows:

Chapter 2 reports the results of genetically engineering plants to constitutively over-express lipase for biodiesel production from spent oils. The genes of lipase with known trans/-esterification activity were cloned from a thermophylic fungus, *Thermomyces lanuginosus,* and a well-studied yeast, *Candida antarctica.* These genes were inserted into a cloning vector, sequenced to confirm their identity, and then inserted into a plant destination vector. The transformed plasmids were inserted into *Agrobacterium tumefaciens*, which was used to insert the genes into *Nicotiana tabacum* (tobacco) and *Arabidopsis thaliana* by the floral dip method. The recombinant enzyme was collected from transgenic plants, purified, and tested for its activity. This approach should provide a relatively cheap and environmentally safe source of lipase for use as biocatalyst.

Chapter 3 reports the hydrodeoxygenation study of unpromoted and Co-promoted reduced molybdenum catalysts for upgrading biodiesel into green diesel. In this chapter, four supported molybdenum catalysts ($Mo/Al_2O_3$, $Co\text{-}Mo/Al_2O_3$, Mo/Zeolite, and Co-Mo/Zeolite) were synthesized, and an auto-sampling PFR-bubbler reaction system was designed and

assembled. The effects of two feedstock sources (methyl oleate and commercial biodiesel B100), five pretreatment temperatures (250, 300, 350, 400, and 450 °C), four hydrogen flow rates (20, 30, 40 and 60 mL/min), and five reaction temperatures (250, 300, 350, 400, and 450°C) were investigated to find the optimal conditions for the hydrodeoxygenation of biodiesel using these supported molybdenum catalysts. The effect of cobalt as a promoter was also studied. Additionally, the activities of Co/-Mo catalysts with different supports (γ-alumina and Y-zeolite) as well as the commercial CoMo catalyst (Harshaw CoMo catalyst) were compared to get an idea of the function of various supports.

Chapter 4 details an overview, conclusions, and recommendations for future work.

# CHAPTER 2

# TRANSGENIC EXPRESSION OF LIPASE ON PLANTS FOR THE ENZYMATIC PRODUCTION OF BIODIESEL

## 2.1 Introduction

As mentioned briefly in Chapter 1, despite several advantages, there are a few technical and economical obstacles that limit enzymatic trans-/esterification processes for the production of biodiesel. These include such issues as insufficient availability of large quantities of inexpensive lipase suitable for catalysis, and resistance from farmers to provide a sufficient triacylglycerol source. These challenges can be addressed by the development of biological technologies, which provide a variety of innovative tools to manipulate biomolecular structures and properties for advanced applications. These tools include genetic engineering, metabolic engineering, protein and enzyme engineering, and recombinant DNA technology.[13] Currently, most of these technologies use expression systems based on bacterial cells (*Escherichia coli* or *E.coli*), yeast cells (*Saccharomyces cerevisiae* or *S. cerevisiae*) or mammalian cells (Chinese hamster ovary or CHO cells). The ability to identify novel genes, clone them and alter their sequences allows for versatile expression systems (such as *Nicotiana tabacum* or tobacco cell and *Arabidopsis thaliana* or *A. thaliana*) with the capability of large-scale production.

### 2.1.1 Current States of Plant Biotechnology

The first plant-derived pharmaceutical protein was produced by Sijmons et al. in 1990.[14] In that study, Sijmons et al. successfully expressed human serum albumin proteins in transgenic tobacco and potato plants. From then on, advances in plant biotechnology and genomics have resulted in the alteration of plants to aid in the areas of nutrition, herbicide resistance, insect

tolerance, and abiotic stress tolerance.[13] For example, Bettini and Santangelo (2016)[15] successfully increased the tolerance of transgenic tomato plants to the phytopathogenic fungus *Fusarium oxysporum* by transforming *Agrobacterium rhizogenes rol* genes. Macknight, Laing, and Bully (2017)[16] successfully increased the ascorbate (vitamin C) levels in rice and tomatoes to enhance their nutritional value for humans; this increased ascorbate level was also proved to benefit plant abiotic stress tolerance. Current plant biotechnology development can also result in the production of large amounts of selected proteins including animal, human and bacterial proteins.[13] Plant genetic transformation has been successful with hundreds of different plant species, including *Nicotiana tabacum* (tobacco), *Arabidopsis thaliana*, *Solanum lycopersicum* (tomato), and *Zea mays* (maize). The technique for producing transgenic plants is either by indirect or direct methods. Direct methods involve the physical insertion of genes by penetrating the plant's cellular wall. Indirect methods involve the use of bacterial systems such as *Agrobacterium*-mediated transformation technology.[13, 14]

Direct gene transfer methods originated in the 1980s and have evolved to include several different technologies that are used today. The most commonly used method is biolistics, which is also known as particle bombardment, and is sometimes referred to as a "gene gun." Biolistics was initially developed in 1987 at Cornell University.[17] In this technique, high density carrier particles are covered with exogenous DNA, accelerated and are inserted directly into the plant cell. The initial delivery system consists of firing a 0.22 caliber nail gun cartridge as a propellant. Today a more sophisticated system is used, which consists of a high and low pressure chamber separated by a rupture disc and compressed helium or nitrogen gas. One of the first to use this technique was Klein and Fromm[18] who successfully expressed the β-glucuronidase gene in a tobacco plant by incorporating a chloramphenicol acetyltransferase gene into maize using

biolistic transformation in 1987. Since then, many other transgenic plants have been successfully created using biolistic transformation, such as wheat, poplar, rice, algae, and soybean. Tseng, Yang, and Liu (2014)[19] successfully applied the biolistic method to modify *Brassica oleracea L. var. capitata L.* (cabbage) with introducing new agronomic and horticultural traits. In 2017, Ribeiro et al.[20] used the biolistic method to increase the pest tolerance of a genetically modified cotton plant. In his study, Cry10Aa toxin, a protein encoded by the entomopathogenic *Bacillus thuringiensis* (Bt) gene was successfully expressed in cotton plants by biolistic transformation to provide a high resistance to the cotton boll weevil.

Indirect methods of plant transformation use specialized bacteria to transform target DNA fragments into plant genomes. The most commonly used technology is *Agrobacterium*-medicated transformation, which uses a gram-negative soil bacteria *Agrobacterium tumefaciens*.[13] This bacterium contains a large tumor-inducing plasmid (Ti plasmid) that consists of two main sets of genes that are vital for plant tumorigenesis.[21] One set works as a segment of DNA that would be integrated into the plant genome, called the transfer-DNA or T-DNA. There are two border sequences located beside the T-DNA region that consist of 24 bp imperfect repeats and genes responsible for directing opine biosynthesis and uncontrolled cell division. The other set are virulence (*vir*) genes which are responsible for T-DNA transferring. The *vir* genes consist of at least eight genetically identified operons, marked as A, B, C, D, E, F, G, and H. The protein expressed by the virA gene can be activated the phenolic compounds (such as acetosyringone) and sugars (monosaccharides) released by wounded plants, and are then phosphorylated. This subsequently activates the expression of the *vir*G protein, which induces expression of all other *vir* genes located on the Ti plasmid to facilitate T-DNA transfer.[21,22]

In recent years, progress has been made in understanding the mechanisms of gene transfer in *A. tumefaciens*. For example, it has been discovered that most of the natural sequence in T-DNA can be removed and replaced with the desired gene to encode proteins of interest in plants. Furthermore, Curtis et al.[23] and Nakagawa et al.[24] have developed a series of new vector systems for Agrobacterium-mediated transformation. These vectors have been developed to facilitate fast and reliable DNA cloning with a collection of functional parameters, such as different promoters, terminators, and antibiotic resistances. This method also allows for gene fusion of a variety of reporter/purification tags. Yang, Deng, and Zhang (2016)[25] developed a twin T-DNA vector (pTRIDT313-g) containing two independent T-DNA cassettes. These two T-DNA cassettes can be independently inserted in different regions of the plant genome and could potentially be a valuable tool for producing marker-free transgenic lines. An alternative to *A. tumefaciens* is *Agrobacterium rhizogenes* which can infect the root system of a hairy root plant.[21] Besides *Agrobacterium*, there are a limited number of organisms capable of inter-kingdom gene transfer. A recent patent (US 7,888,552 B2)[26] used different *Rhizobium* strains *(Rhizobium* sp., *Sinorhizobium* sp., and *Mesorhizobium* sp) to transform various crops including soybean, canola, corn, and cotton.

2.1.2 Genetically Enhancing Oil Accumulation

Triacylglycerol (TAG) works as an energy reserve in developing seeds, pollen, grains, anthers, flower petals, and fruit mesocarp in a number of plant species.[27] As shown in Figure 2, the metabolic pathway involved in the biosynthesis of TAG is comprised of three major steps: (1) fatty acid (FA) synthesis in the plastids; (2) FA acyl chain elongation and development of a fatty acyl-CoA pool in the cytoplasm; and (3) TAG formation in the endoplasmic reticulum (ER).[27, 28]

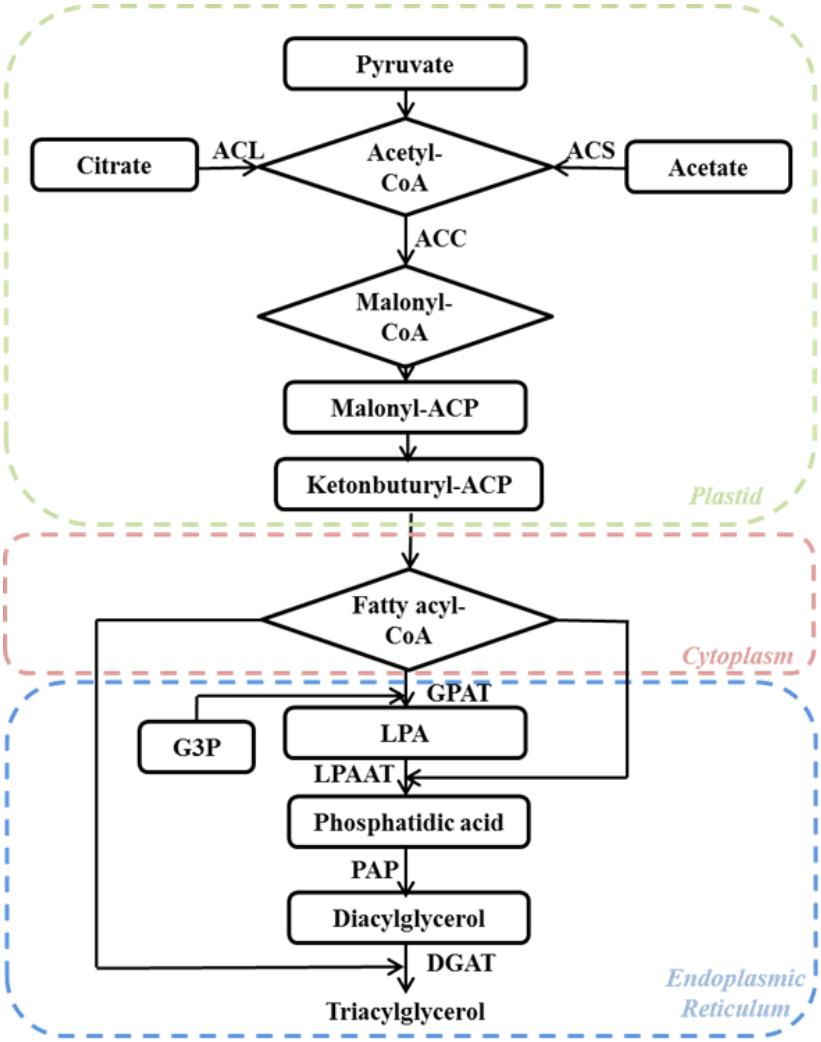


**Figure 2.** TAG biosynthetic pathway with the major intermediates and enzymes.[27]

Initially, FAs are synthesized *de novo* in the stroma of the plastid. These FAs are synthesized using an initial precursor known as acetyl coenzyme A (acetyl-CoA). This is then carboxylated by an acetyl-CoA carboxylase enzyme (ACC) and ATP to form malonyl-CoA. The next step involves linking the malonyl CoA to the acetyl-CoA by using a malonyl-CoA:ACP transacylase enzyme, and the resulting complex is then transferred to an acyl carrier protein (ACP) of the fatty acid synthase or FAS complex. Next, 4-carbon intermediates are formed when the acetyl-CoA undergoes a condensation reaction with the malonyl-ACP, after which 2-carbon subunits catalyzed by FAS are sequentially added. This results in a process known as FA

elongation. Finally, hydrolysis of acyl moieties by acyl-ACP desaturase concludes the synthesis step resulting in FAs that are around 16–18 carbons long, which form the core of the fatty acetyl-CoA found in the cytoplasm.

The next step involves the formation of TAG in the ER by the acylation of glycerol 3-phosphate (G3P0 with an acetyl-CoA, which results in the formation of lysophosphatidic acid (LPA). The LPA is catalyzed by glycerol 3-phosphate acyltransferase or GPAT, and is then further acylated to form phosphatidic acid or PA by a process known as lysophosphatidic acid acyltransferase (LPAAT). This process ends with the dephosphorylation of PA by phosphatidic acid phosphatase (PAP) to form diacylglycerol, and the last FA is transferred from the acetyl-coA pool to form TAG by a diacylglycerol acyltransferase enzyme (DGAT).

Over the past decade, numerous studies have been conducted to gain a better understanding of the biosynthesis of TAG and the enhancement in TAG accumulation. Different species of plants have been investigated by over-expressing different key enzymes in order to enhance TAG accumulation while only limited success was achieved. In 2007, Rangasamy and Ratledge[29] introduced a modified rat liver ACL gene into the genome of tobacco. This over-expression of ACL resulted in a fourfold increase of CL activity and a 16% increase in FA. In 2015, a 6% increase in FA content was reported by Kubala et al.[30] after over-expressing an ACC gene from *Arabidopsis* in *Brassica napus*. However, the increase of FA in these studies did not affect the TAG content, which suggests the limiting step is the conversion of FA to TAG. In 2001, Jako et al.[31] were the first to report enhanced seed oil content and seed weight by over-expression of a DGAT in plants. Over-expression of a seed-specific DGAT gene in wild-type *Arabidopsis* resulted in an increased activity of 10–70%, which correlated with a 40–100 wt% increase in TAG content. Dinamarca (2017)[32] also reported an increase in TAG content by 15%

with the overexpression of a specific DGAT gene in *Phaeodactylum tricornutum*. In 2015, Zou et al.[33] reported that enhancing LPAAT expression can also result in a seed oil content increase. The over expression of the LPAAT gene in *Arabidopsis thaliana* and rapeseed resulted in an 8–48 % increase in seed oil content.

Many researchers have focused on TAG synthesis pathways in the plant cell that have common substrates and precursors. They found that a multi-gene approach (over-expressing more than one key enzyme as well as down-regulating competed enzymes) may lead to substantial increases in oil content. Coleman and Lee discovered that the biosynthesis pathway for phospholipids competes with TAG biosynthesis for a common substrate PA.[34] TAG production can be increased by down-regulating the phosphatidate cytidylyl transferase (CTP) enzyme, which converts PA to CDP-diacylglycerol, a precursor of phospholipid synthesis. In 2015, Chen *et al.* were able to down-regulate the CTP enzyme by expressing antisense CTP in rapeseed, which resulted in a 6–18 % increase in oil content.[35]

2.1.3 Industrial Lipase Production

The global industrial enzyme market has evolved continuously due to numerous mergers and acquisitions. According to the data of Research Gate, the 2016 global industrial enzyme market was $6.5 billion, which was a marked increase from $3.9 billion in 2011.[36] The majority of the enzyme market consists of hydrolytic enzymes, such as protease, amylases, amidases, esterases, and lipases.

Currently, most of the industrial lipase is produced from microorganisms, such as bacteria, yeast, and fungi. Despite a relatively high number of available microbial lipase sources, only limited amounts are commercially available due to the complex growth condition requirements.[37] As a result, these lipases are unavailable in sufficient quantities due to high

production costs, which limit their potential applications in industry. Recombinant DNA technology, by which the gene of a suitable lipase is selected and cloned into an appropriate expression system, can be used to overcome these limitations. The amount of raw materials such as water, steam, and electricity that is required by recombinant lipase production can be reduced by 40% when compared with original species.[38] Lipolase produced by the Novozymes Company in 1988 was the first lipase to be commercially produced by recombinant DNA technology.[39] The lipase originating from *Thermomyces lanuginosus* was cloned and over-expressed in *Aspergillus oryzae*.

There can be specific property requirements for industrial biocatalysts that are different from those found in nature. These property requirements can include selectivity, thermostability, and stability in organic media. An attractive approach to modify the properties of existing wild-type enzymes is to use protein engineering technologies, such as rational protein design and directed evolution. Rational protein design technique uses the available knowledge of enzyme to develop molecular models to predict and plan changes to the amino acid sequence of the protein. The site-directed mutagenesis method is then used to generate mutant genes, and the recombinant variants are collected, purified, and analyzed for the desired characteristics.[37] Lipolase Ultra and LipoPrime are two variants of Lipolase produced by the Novozymes Company that were developed using rational protein design.[40] Both lipase variants are more effective cleansers than the original and are also expressed in *Aspergillus oryzae*. An alternative to rational protein design is directed evolution, which is used when the function, mechanism, and structure are not known for a particular enzyme.[39,42] This technology uses random mutagenesis of genes to produce molecular diversity. Zhang et al. (2015)[41] successfully improved the tolerance of *C. antarctica* lipase B towards irreversible thermal inactivation through directed

evolution. Two of the mutants resulted in over a 20-fold increase in half-life at 70 °C compared with the wild-type lipase.

Recombinant DNA technology and protein engineering can enhance lipase production and improve catalytic characteristics. These strategies have already successfully been applied in industry to produce several commercial lipases. In order to develop a competitive strategy for the enzymatic production of biodiesel, it is imperative to develop an appropriate and effective biocatalyst system using both genetic engineering and biochemical strategies.

2.1.4 Recombinant Protein Expression Systems

With the development of genetic and protein engineering technologies, recombinant proteins can be expressed in a wide variety of host cells, including in bacterial, yeast, mammalian, and plant systems. Each of these systems has its inherent advantages and drawbacks which must be considered when choosing an appropriate expression system. These factors include recombinant protein function, structure, quality, quantity, and costs.

The bacterial expression system is the first commercially applied expression system for recombinant protein production. In the early 1980s, recombinant human insulin from *E. coli* became the first recombinant pharmaceutical protein to enter the market.[43] The biological and genetic information of bacteria has been well documented, and currently bacterial expression systems for transgenic protein expression represent approximately 30% of the enzymes produced commercially.[44] The advantage of using bacterial cells are their ability to be rapidly grown with relative ease in high biomass concentrations on inexpensive media. Currently *E. coli* is the most commonly used bacterium for recombinant protein expression.[43] Despite being an effective expression host for simple proteins, *E. coli* lacks the ability to perform post-translational modifications, which are often required in more complex proteins, such as glycosylation,

acylation, and phosphorylation. Moreover, due to the fact that gram-negative bacterium such as *E. coli* do not naturally secrete proteins in high amounts, some recombinant proteins expressed in *E.coli* can form inclusion bodies. These inclusion bodies are often inactive, insoluble, and difficult to isolate without denaturing, which increases the cost in recombinant protein production.[45]

Yeast and molds are currently the most commonly used expression systems in the recombinant protein industry, which have produced > 50% of the commercial enzymes for the past two decades.[44] Yeast are single cell eukaryotic fungal organisms that are often used to produce recombinant proteins that cannot be expressed in *E. coli*.[46] Similar to bacteria, yeast are simple to cultivate and can rapidly achieve high cell density levels in fairly inexpensive media. Moreover, yeast also have the machinery to perform post-translational modifications and can secrete recombinant proteins from the cell into the fermentation broth.[46] The most common yeast strain for producing recombinant protein is *Saccharomyces cerevisiae*, which has been used throughout history to make bread and alcoholic beverages.[45] In as early as 1986, a vaccine for hepatitis B was licensed and produced from cell cultures of recombinant strains of *S. cerevisiae*.[47] The drawback of using yeast lies in the process of protein glycosylation as mammalian proteins expressed in yeast cells tend to be over-glycosylated. Mannose sugar residues synthesized in the glycosylation process can affect the activity of the recombinant proteins. Methylotrophic yeasts, such as *Pichia pastoris*, have become a very attractive alternative to *S. cerevisiae* because they create much shorter chain lengths of mannose during glycosylation.[45, 47-49]

The mammalian expression system is particularly useful for more complex proteins, like vaccines, which require mammalian post-translational modifications, and provide about 8% of

industrially available enzymes.[44] The reason mammalian cells are sometimes preferable to yeast cells is that they properly fold and secrete glycosylated proteins in their native form without the addition of excessive sugar residues.[50] The most commonly used mammalian expression system during the past two decades is the Chinese hamster ovary (CHO) cell. In 1987, tissue plasminogen activator was the first recombinant therapeutic protein produced by a mammalian system using CHO cells that was approved for clinical trials.[51] Despite the wide variety of cell lines available, there is currently only a small number of mammalian expression systems used commercially, such as baby hamster kidney (BHK) cells, human embryonic kidney (HEK) cells, and mouse L-cells.[50] Mammalian cells are more suited for the production of high valued products, such as pharmaceuticals and therapeutics, rather than for large quantities of inexpensive proteins, such as enzymes. The cultivation process of mammalian cells is extremely complex and expensive, and the resulting product often contains a large percentage of low level proteins.[52] Therefore, mammalian cell cultures would not be well suited for producing biocatalyst for biodiesel production.

The plant system is a fairly new recombinant protein expression system that was only developed in the 1990s.[13] In 1997, the first commercial plant-based recombinant protein was produced by ProdiGene and Sigma.[53] The chicken oviduct avidin gene with an ubiquitin promoter was transformed in maize. It resulted in the over-expression of avidin proteins in maize seeds and a final yield of 230 mg/Kg of extractable protein from the seeds. Moreover, this recombinant avidin protein could maintain activity for up to three months if stored in the cracked and flaked kernels. Although currently plant expression systems for transgenic protein expression only represents about 5% of the enzymes produced commercially, they are gaining

attention due to the advantages in cost, easy of handling and the ability to post-modify proteins.[44]

When compared to microbial and mammalian expression systems, transgenic plants are theorized to offer a number of advantages in terms of cost, protein complexity, storage, and distribution.[13] The amount of recombinant proteins can be easily scaled up by using current agricultural technologies since only soil and light are required. Plant cells can also support the folding of proteins and post-translational modifications.[54] There are over 300 types of post-translational modifications that have been identified in plant cells, which can fulfill the specific requirements of the recombinant protein and organism. In 2006, a vaccine for Newcastle disease known as Concert became the first vaccine made in transgenic plants which was approved by the USDA.[55] Concert was produced by Dow AgroSciences, and was transgenically expressed in tobacco plants as a poultry viral antigen.

When compared to yeast cells, an advantage of the plant expression system is the highly efficient glycosylation process, which is almost as high as in mammalian cells.[54] The only deficiency lies in the N-terminal glycosylation, which has no terminal sialic acids and contains xylose residues. This deficiency is significant for pharmaceutical proteins production because of the immunological concerns. However, when producing large quantities of inexpensive enzymes, this slight deficiency is not important because usually the protein activity, function and stability are not affected. Moreover, this deficiency in pharmaceutical recombinant proteins was recently overcome by Yang et al. (2012)[56]. They were able to demonstrate mammalian glycosylation in transgenic tobacco plants by expressing a *P. aeruginosa* Glc(NAc) C4-epimerase and a human polypeptide GalNAc-transferase. Although further improvements are needed, they believe that

transgenic plants are capable of producing mammalian glycoproteins for pharmaceuticals and therapeutics.

Plant cells also have the ability to regenerate from a single cell into an entire plant in a process known as totipotency.[13, 53] This ability makes plants and plant cells versatile production systems which allow for the targeting of different organelles and subcellular compartments, such as the endoplasmic reticulum (ER), chloroplast, cytoplasm, or vacuole. Moreover, plant expression systems can encompass a diversity of forms which the other systems cannot, such as in the whole plant, suspension cell cultures, and root cultures.[54] Although whole plants offer unlimited scalability, there is a resistance from farmers to provide a sufficient grown area. This issue can be addressed by cell suspensions or hairy root cultures, where recombinant protein production can take place in bioreactors with relative high cell density and performs similarly to that of bacterial and yeast cultures. Moreover, hairy root cultures are preferred over suspension cultures due to their genetic, biochemical, and relatively low-cost culture requirements (no sunlight required).[54, 57-58]

The production of recombinant proteins has always been of utmost importance because of the high production value in the pharmaceutical industry. However, the cost of producing pharmaceutical products, of conducting clinical trials, and of proving safety and efficacy in humans, limit the use of this system. On the other hand, industrial enzymes do not have the same weaknesses and are infinitely cheaper than recombinant proteins. As inexpensive enzymes and proteins are required on much larger scales, the use of transgenic plants is ideal due to their ease of transformation, expression versatility and the speed of the scale-up process. A wide variety of non-pharmaceutical proteins have been produced in transgenic plants, illustrating the reliability of this process (Table 1).[59]

**Table 1.** Industrial recombinant proteins produced by transgenic plants[59]

| Protein | Gene Source | Host Plant | Company |
|---|---|---|---|
| Peroxidase | Fungus | Maize | Applied Biotechnology |
| Laccase | Fungus | Maize | Applied Biotechnology |
| Cellulase | Fungus | Maize | Applied Biotechnology |
| Cellulase | Fungus | Maize | Infinite Enzymes |
| Aprotinin | Bovine | Tobacco | Large Scale Biology |
| Thyrotropin Receptor | Human | Melon | Nexgen |
| Avidin | Chiken | Maize | ProdiGene |
| Aprotinin | Bovine | Maize | ProdiGene |
| GUS | Bacteria | Maize | ProdiGene |
| Trypsin | Bovine | Maize | ProdiGene |
| α-amylase | Microbial | Maize | Synhenta |
| Lactoferrin | Human | Rice | Ventria Bioscience |
| Lysozyme | Human | Rice | Ventria Bioscience |

In terms of biofuel production, transgenic plants have been widely thought as the key to a sustainable and successful future. Genetic modifications to various metabolic and biosynthesis pathways have enhanced plants to become more suitable for use as biofuel feedstocks, which can thrive in a variety of environmental conditions, including temperature, water availability, and salinity. Moreover, organisms have been genetically engineered to produce enzymes that are used in the catalytic process to produce biofuels. The majority of these enzymes are produced in microorganisms, such as bacteria and yeasts. Plant expression systems allow us the versatility and almost unlimited scalability to produce recombinant enzymes required for cellulosic ethanol and enzymatic biodiesel. Currently, companies like Infinite Enzyme, ProdiGene and the Applied Biotechnology Institute are taking advantage of plant-based expression system to produce cellulases for ethanol production.[58] However, to the best of the author's knowledge, there is no research being done to produce lipases in plants for the enzymatic production of biodiesel.

In this chapter, we examine the results of genetically engineering plants to constitutively express lipase for biodiesel production from spent oils and non-edible plant oils. The genes of two well-studied lipases, which are naturally from *Thermomyces lanuginosus* and *Candida antarctica*, were cloned and inserted into *Nicotiana tabacum* (tobacco) and *Arabidopsis thaliana* plant using *Agrobacterium*. The recombinant enzyme was collected from the genetically engineered plants, purified, and tested for its activity.

## 2.2 Experimental Section

### 2.2.1 Strains, Plasmids, and Materials

*Thermomyces lanuginosus* (strain 200065), *Candida antarctica* (strain 28323) and *Agrobacterium tumefaciens* (strain GV3101) were purchased from the American Type Culture Collection (ATCC). Endura$^{TM}$ Chemically Competent *E. coli* was supplied by Lucigen (Cat. No. 60240-0). The plasmid PCR8/GW/TOPO used for gene cloning and sequencing was purchased from Invitrogen (Cat. No. K250020). Plant expression plasmid vectors, PGWB408 and PMDC83, were supplied by Tsuyoshi Nakagawa (Shimane University) and Mark Curtis (University of Zurich), respectively.

Luria Broth (LB) medium (ultrapure), soluble starch (hydrolyzed potato), and Tris (ultrapure, grade MB) were purchased from Affymetrix. Agar (type A, plant cell culture tested), Gamborg's vitamin solution 1000x, 6-benzylamino-purine (BAP), Murashige and Skoog basal salt mixture (MS), Triton X-100, protease inhibitor cocktail for plant cell and tissue extracts in DMSO solution (Cat. No. P9599), protease inhibitor cocktail for use in purification of Histidine-tagged proteins (Cat. No. S8830), and lipases from *Thermomyces lanuginosus* and *Candida antarctica* solution (>100,000 U/g) were purchased from Sigma-Aldrich.

Prestained SDS-PAGE broad range standards (Cat. No. 161-0318), β-mercaptoethanol (Cat. No. 161-0710), Laemmli sample buffer (Cat. No. 161-0737), 10x Tris/Glycine/SDS buffer (Cat. No. 161-0732), Bio-safe Coomassie G-250 stain (Cat. No. 161-0786) and mini-PROTEIN TGX Gels (Cat. No. 456-1034) were purchased from Bio-Rad. Sodium phosphate dibasic heptahydrate (ACS grade), sodium hydroxide solution N/10 (Certified 0.1000 N), $MgSO_4 \cdot {}_7H_2O$, and Spectrum Spectra/Pro 3 RC Dialysis Membrane Tubing 3500 Dalton MWCO (Cat. No. 08-670-5A) were purchased from Fisher Scientific. Tributyrin (98%) and D(+)-sucrose were purchased from Acros Organics. Spectinomycin dihydrochloride (Cat. No. S742) and carbenicillin (Cat. No. C346) were purchased from Phyto Technology Laboratories. Other chemicals used are Seakem LE agarose (Lonza, Cat. No. 50000), S.O.C. medium (Invitrogen, Cat. No. 15544-034), yeast extract (Bacto, Cat. No. 212750), kanamycin monosulfate (MP Biomedicals, Cat. No. 150029), hygromycin B (Plant Media, Cat. No. 4081000-1), TAE 50x buffer (Eppendorf, Cat. No. 95515533-5), ammonium sulfate (ICN Biomedicals, Inc., Enzyme grade), and acetone (Alfa Aesar, HPLC grade).

2.2.2 Cloning of *T. lanuginosus* Lipase cDNA

Freeze-dried *T. lanuginosus* obtained from ATCC was rehydrated with deionized (DI) water and grown on PDA medium containing: 50.0 g/L yeast extract, 20.0 g/L soluble potato starch, 18.3 g/l olive oil, 5.0 g/L $K_2HPO_4$, 0.15 g/L $CaCl_2$, 1.0 g/l $MgSO_4 \cdot 7H_2O$, and 15.0 g/L bacterial agar (grade A) for 48 - 72 h at 50 °C. The fungal tissue was then frozen in liquid nitrogen and used for total RNA extraction using the ZR plant RNA MiniPrep Kit according to the manufacturer's protocol (Zymo Research, Cat. No. R2024), as described in Appendix C. The concentration and quality of mRNA was confirmed by characterization using NanoDrop spectrophotometer 2000c (Thermo-Fisher Scientific). The total RNA was reverse-transcribed to

synthesize complementary DNA (cDNA) immediately after isolation using qScript cDNA Supermix kit according to the manufacturer's protocol (Quanta Biosciences, Cat. No. 95048-100) and a PTC 100 Programmable Thermal Controller (MJ Research Inc.), as described in Appendix C. The RNA and resultant cDNA were stored at -80 ºC and -20 ºC, respectively.

2.2.3 Cloning of *C. antarctica* Genome DNA

Freeze-dried *C. antarctica* used in this study was rehydrated with deionized (DI) water and grown on yeast growth medium containing: 10.0 g/L yeast extract, 20.0 g/L peptone, 18.3 g/l olive oil, 100 mL/L glucose, and 15.0 g/L bacterial agar (grade A) for 48–72 h at 30 °C. The cells were then harvested and disrupted with glass beads (0.75–1.00 mm) using a Retsch-mill (Retsch, Cat. No. MM2000) for 30 min. The proteins were precipitated with 2% of SDS at 65°C and centrifugated at 13,000x g. Afterwards, the genomic DNA was precipitated from the supernatant with 0.3 M sodium acetate and 2-propanol, and finally re-suspended in 100 µL TE buffer (Tris 100 mM, EDTA 10 mM, and pH 8.2) supplemented with 0.1% of RNase. The genomic DNA was stored at -20ºC and prepared for lipase gene amplification by PCR, as described below.

2.2.4 Lipase Gene Amplification by Polymerase Chain Reaction (PCR)

A PCR was performed to amplify the lipase gene using the PTC 100 Programmable Thermal Controller (thermocycler). A typical reaction was 50 µL total volume with a final concentration of 1x buffer ($Mg^{2+}$), 200 µM dNTP mix, 0.2 µM forward and reverse primers, 2 ng/µL of total plasmid DNA or 2-3 ng/µL of genomic DNA, and 1.25 units of Takara Ex Taq DNA polymerase (Takara Bio Inc, Cat. No. RR001A).

Typical PCR conditions for various lipase DNA amplifications are described in Table 2. Other Taq polymerases and thermocycles were also used for screening purpose with similar reaction conditions.

**Table 2.** PCR conditions for the amplification of T. lanuginosus lipase (TLl) cDNA and C. antarctica lipase B (CAlB) DNA

| Step | TLl | CAlB |
|---|---|---|
| **1-Initiation** | 94 ºC for 1 min | 94 ºC for 1 min |
| **2-Denaturation** | 94 ºC for 30 s | 94 ºC for 30 s |
| **3-Anneealing** | 52 ºC for 1 min | 63 ºC for 1 min |
| **4-Elongation** | 72 ºC for 1 min | 72 ºC for 1 min |
| **Repeat steps 2-4** | 30 cycles | 35 cycles |
| **5-Final elongation** | 72 ºC for 2 min | 72 ºC for 2 min |
| **6-Final hold** | 4 ºC for 24 h | 4 ºC for 24 h |

2.2.5 Agarose Gel Electrophoresis

Analyses of DNA fragment sizes were performed using agarose gel electrophoresis. The gels consisted of 1% LE agarose dissolved in 1x TAE buffer (40 mM Tris-acetate, 1 mM EDTA). Samples were mixed with 6x loading dye and then loaded into the gel along with an appropriated DNA size standard (e.g. NEB 2-log DNA Ladder or NEB 1kb DNA Ladder). The gel was electrophoresed at 90–100 V for 45–60 min. and then stained in 0.5 µL/mL of ethidium bromide (EtBr) for 15 min. followed by 15 min. of destaining in distilled water. Afterward, the gel was visualized and photographed using Fotodyne gel-documentation system. The DNA fragments were analyzed visually in comparison to bands of molecular weight standards from a DNA ladder.

2.2.6 Cloning Vector and Heat-shock Transformation

After the PCR amplification and DNA band confirmation, *T. lanuginosus* lipase and *C. antarctica* lipase B genes were cloned into the PCR8/GW/TOPO vector according to the

manufacturer's protocol (Invitrogen, Cat. No. 45-0642), as described in Appendix C. The plasmid was inserted into bacterial cells using the heat-shock transformation protocol, where 150 ng of the plasmid DNA was added into 50 µL of chemically competent *E. coli* cells (Endura$^{TM}$ 60240), mixed gently, and placed on ice for 30 min. The cells were then placed in the Eppendorf Thermomixer at 42ºC for 30.0 sec. (with no shaking) and put on ice for 2 min. Then 250 µL of room temperature Super Optimal broth with Catabolite (S.O.C.) medium was added to the cell culture tube and placed horizontally in a New Brunswick Scientific Controlled Environment Incubator Shaker at 37ºC and 200 rpm for 1 h. Afterward, 50 µL of cell culture was spread onto two pre-warmed LB gar plates with the appropriate antibiotic and incubated overnight at 37 ºC.

2.2.7 Bacterial Culture and Plasmid DNA isolation.

Liquid cultures of *E. coli* and *Agrobacterium* were grown in LB medium containing appropriate antibiotics, depending on the selection gene (ampicillin 100 µg/mL, spectinomycin 100 µg/mL, kanamycin 50 µg/mL, or hygromycin 50 µg/mL). Sterile pipette tips or applicators were used to start a 3 mL liquid culture of *E. coli* or 5 mL liquid culture of *Agrobacterium* from glycerol stocks or plates. For solid cultures, 1.3% agar was added to the medium prior to autoclaving. Solid or liquid culture of *E. coli* and *Agrobacteriu*m were incubated at 37ºC for 16–18 h and 28 ºC for 48–72 h, respectively. Liquid cultures were grown on a shaker at 200 rpm.

Individual cell colonies from a successful transformation were randomly selected and grown overnight in separate test tubes containing 3–5 mL liquid LB culture with the appropriate antibiotic and placed in the incubator shaker at 200 rpm and at their optimum temperature (37 or 28ºC). The plasmid DNA isolation from the transformed *E. coli* was performed using the Zyppy Plasmid Miniprep Kit, according to the manufacturer's protocol (Zymo Research, Cat. No.

D4020), as described in Appendix C. The plasmid DNA was then quantified by the NanoDrop 2000c, and stored at -20ºC.

2.2.8 Restriction Digestion

Typical restriction digestion was performed using enzymes from New England Biolabs (NEB). A reaction mixture contained a final concentration of 1x of the appropriate buffer, 1x bovine serum albumin (if required), 2 units/µg DNA of the enzyme, 150–200 ng of plasmid DNA, all brought to a volume of 10 µL by sterile distilled water. The reaction was incubated at 37ºC for 3 h and used immediately for gel electrophoresis or stored at -20 ºC.

2.2.9 DNA Sequencing and Analysis

Two sequencing reactions were prepared containing 300 ng of plasmid DNA, 5 pmol of primer (forward primer in one tube and reverse primer in the other), and diluted to 6 µL with sterile water. The sequencing was done at the University of New Hampshire Hubbard Genome Center using an ABI 3130 DNA Analyzer, and the results obtained from sequencing were aligned and analyzed with the target sequences using the BioEdit Sequence Alignment Editor.

2.2.10 Glycerol Stocks

Liquid cultures containing 3 mL of LB medium with appropriate antibiotics from the desired colonies were grown overnight at 200 rpm at their optimum temperature (37 or 28ºC). Equal parts liquid culture and glycerol were thoroughly mixed in two cryo-vials and stored at -80ºC. The glycerol stock solution contained a 3:2 ratio (v/v) of LB medium and glycerol which was then sterilized.

2.2.11 Construction of the Final Destination Vectors

Gateway compatible destination vectors contained the bacterial ccdB gene, which encodes an anti-DNA gyrase protein (ccdB). This binds the DNA gyrase so that it was unable to

reseal the DNA resulting in bacterial death. The *E. coli* strain DB3.1 contains a mutation in the DNA gyrase gene so that the ccdB protein was unable to bind and was used to amplify the stock vectors to provide sufficient quantities for transformation. The DB3.1 cells were transformed with the stock vector using the heat-shock method followed by plasmid isolation. The plasmid DNA was confirmed by restriction digestion and gel electrophoresis.

After the gene was inserted into the cloning vector (PCR8/GW/TOPO) and confirmed through restriction digestion, electrophoresis, and sequencing, it was then subsequently transferred into two Gateway compatible destination vectors (PGWB408 and PMDC83) using Gateway LR Clonase II enzyme mix according to the manufacturer's protocol (Invitrogen, Cat. No. 11791-020), as described in Appendix C. The plasmid was transformed into *E. coli* by heat-shock method and confirmed by plasmid isolation, restriction digestion, and gel electrophoresis. Afterward, the plasmids were transformed into *Agrobacterium tumefaciens* by electrophoration.

2.2.12 Electroporation

Electroporation of *Agrobacterium* was performed using an Eppendorf model 2510 electroporator. A 2 µL of the isolated plasmid form the final destination vector was added to 50 µL aliquot of *Agrobacterium* glycerol stocks thawed on ice. The mixture was mixed gently and transferred to pre-chilled cuvettes (1 mm gap) and electroporated at 1800 V. This was quickly followed by addition of 250 µL S.O.C medium and incubation in the New Brunswick Scientific G24 Environmental Incubator Shaker at 28 ºC for 3–4 h at 200 rpm. Afterward, 10–30 µL of the cell culture was spread on solid LB medium with appropriate antibiotics and incubated at 28ºC for 48–72 h. The resulting colonies were selected and grown in liquid LB medium with appropriate antibiotic at 28ºC for 48–72 h and 200 rpm.

Screening of the transformed *Agrobacterium* was performed by centrifuging 500 µL of culture at 12,000 x g for 30 sec, discarding the supernatant, and resuspending the pellet in 50 µL sterile water. The suspension was then heated to 99ºC in the thermomixer for 10 min, centrifuged at 12,000 x g for 5 min, and 5 µL of the supernatant was used to run a PCR with the appropriate primers. Gel electrophoresis confirmed a successful transformation.

2.2.13 Agrobacterium-mediated Transformation of Tobacco

Small aliquots of transformed *Agrobacterium tumefaciens var. Xanthi* (tobacco) were used to initiate 3 mL liquid LB medium with appropriate antibiotic overnight at 28ºC and 200 rpm. Agrobacterium cultures were subcultured to 30 mL fresh medium and grown 24–48 h at 28ºC for 48–72 h and 200 rpm. Acetocyringone was added at a final concentration of 50 µM within 12 h prior to transformation. The entire culture was pelleted at 4ºC for 5 min at 10000 rpm. The supernatant was discarded and the pellet was resuspended with 0.9 w/v% NaCl to adjust the $OD_{600}$ to 0.65 ± 0.05 before transformation.

For transformation, non-transformed (NT) tobacco leaves (from plants grown in Magenta boxes; no more than one month old) were cut into 1 $cm^2$ pieces and submerged in the *Agrobacterium* suspension for 15 min after wounding the tissue several times with the tip of a scalpel. The leaf was then blotted dry with sterile paper towels (twice) and carefully placed onto basal media plates (30 g/L sucrose, 4.3 g/L MS basal salts, 500x vitamin solution, 1.0 mg/L BAP, 0.1 mg/L NAA, 8 g/L plant agar, and pH 5.6 ± 0.1). These plates were placed in the growth room for two days; then the leaves were washed in a 300 mg/L carbenicillin solution for 10 min, blotted dry, placed onto selection plates containing basal media and the appropriate plant hormones and antibiotics, and put back into the growth room. The leaf segments were subcultured on the same medium at 4–6 week intervals.

2.2.14 Floral Dip Transformation of Arabidopsis

*Arabidopsis thaliana* (ecotype Columbia - 0) plants were transformed by *Agrobacterium* using modified floral dip method.[61] Seeds of wild type *Arabidopsis* were planted in four pots per transformation six weeks before dipping. By week six, the plants were prepared by clipping the primary bolt to encourage synchrony in branching and flowering. A week later, 320 mL culture of *Agrobacterium* was started in liquid LB with antibiotic hygromycin and grown at 28ºC for 24 h and 200 rpm. The entire culture was pelleted at 4ºC for 10 min at 5000x g. The supernatant was discarded and the pellet was resuspended with 5% (w/v) final concentration of L-77 Silwet (Lehle Seeds, #VIS-02) to adjust the $OD_{600}$ to 0.8 ± 0.2 before dipping.

The unopened flower buds along with flowers were dipped into the bacterial suspension for 8–10 sec, avoiding contact with the basal leaves and soil. The pots were placed on their sides in a flat, covered with a clear plastic to prevent desiccation, and left overnight. In the next morning, these plants were rinsed thoroughly under cold water and moved to their normal growth conditions. The same plants were re-dipped in a similar fashion after seven days. The seeds (T1) were harvested from each pot separately after the siliques matured. Seeds were desiccated at room temperature for 5–7 days followed by sterilization and storage at 4ºC.

2.2.15 Screening for Transgenic Lines

After transformation of tobacco leaves, only the transgenic cells would grow and multiply in the presence of the antibiotic. For transgenic tobacco, shoots were randomly selected from individual events growing on the selection media and subcultured onto fresh basal shooting media: 4.3 g/L MS basal salts (Murashige and Skoog, 1962) with 30 g/L sucrose (Sigma), 1.0 mg/L BAP (Sigma), 8 g/L plant agar (Sigma), and pH 5.6 ± 0.1. Each event was clearly labeled and placed in the growth room for 2–4 weeks.

For transgenic *Arabidopsis*, T1 seeds were surface-sterilized with by 70% ethanol with 1% Triton X-100 for 30 sec, followed by desiccation on the filter paper at room temperature. The washed seeds were separately placed onto an *Arabidopsis* germination media:1 g/L sucrose, 0.5 g/L MES, 4.3 g/L MS basal salts, 8 g/L plant agar, and pH 5.7 ± 0.1 with appropriate antibiotic. The plates were kept in the dark at 4ºC for two days and transferred to growth room for two weeks until almost all seeds germinated. Non-transgenic *Arabidopsis* would die on the antibiotic containing germination medium, and the survivor one was then transferred onto soil and placed in the growth chamber (20°C, daylight in 24 h per day) until flowering.

An alkali treatment procedure was used to rapidly obtain DNA for PCR screening. Tobacco or *Arabidopsis* tissue (about 1 gram) was collected into sterile microfuge tubes. To the tube was added 40 µL of 0.25 M NaOH and the plant tissue was punctured several times with a pipette tip until the solution turned slightly green. The sample was incubated at 99ºC for 30 sec in the thermomixer and subsequently neutralized by 40 µL of 0.25 M HCl and 20 µL of 0.5 M Tris-HCl (pH 8.0 with 25% Nonidet P-40), before boiling for an additional 2 min. The tissue sample was centrifuged at 10,000 x g for 10s and 5 µL was used immediately for PCR with the appropriate primers. Gel electrophoresis confirmed a successful transformation.

2.2.16 Recombinant Enzyme Extraction

Young leaf tissue of tobacco from the greenhouse or leaf tissue of *Arabidopsis* from the growth chamber was collected and immediately frozen in liquid $N_2$. The tissue was then transferred to a pre-chilled mortar and pestle, and ground into a fine powder, using additional liquid $N_2$ to prevent thawing. The powdered tissue was quickly transferred into a sterile 50 mL conical centrifuge tube, weighing the tube before and after in order to determine the mass of tissue collected. Afterward, an extraction buffer with a 3:1 ratio (mL buffer/gram tissue) was

added to the tissue and vortexed vigorously and left at room temperature for 10–15 min. A protease inhibitor cocktail (Sigma-Aldrich, 41010) was added to selected buffers at a ratio of 0.5 mL/g tissue to the extraction buffer. Both the buffer and the protease inhibitor cocktail were cooled to 4ºC on ice prior to extraction. The tissue was pelleted at 12,000 x g for 25 min at 4ºC. The collected supernatant (crude extract) was use for protein precipitation and purification.

2.2.17 Acetone Precipitation

A 4:1 volume ratio of cold acetone (-20 ºC) was slowly added to the crude extract. The mixture was inverted gently and left for 12–16 h at 4ºC to allow for proteins to precipitate. Afterwards, the proteins were pelleted at 13,000x g for 10 min at 4ºC. The acetone was removed by decanting and the tube was left open to allow any residual acetone to evaporate. Before the pellet was completely dry, it was resuspended in one-fifth the volume of the original volume of the buffer with the extraction buffer.

2.2.18 Ammonium Sulfate Precipitation and Dialysis

The volume of crude extract was carefully measured and the amount of solid ammonium sulfate was calculated for 30% saturation at 4ºC. The solid ammonium sulfate was ground into a fine powder with a mortar and pestle and weighed to the calculated amount. The crude extract was placed into a 100 mL glass beaker with stir bar in a cold room at 4ºC. At a moderate mixing rate, the ammonium sulfate was slowly added to the extract, a process that took 20–40 min. Afterwards, the solution was allowed to mix for 1 h to equilibrate. The solution was placed into a sterile centrifuge tube and the proteins that precipitated were pellet at 13,000x g for 10 min at 4 ºC. The supernatant was decanted into another sterile tube and the volume determined. The pellet was resuspended in 1/10 the volume of the crude extract. The amount of ammonium sulfate was

recalculated for 60% saturation at 4ºC and the process was repeated on the supernatant, and then again for 90% saturation.

Dialysis tubing (18 mm flat diameter, MWCO 3.5 kDa, Sigma-Aldrich) was rehydrated in buffer solution 1–2 h prior to dialysis. After rehydration, the dialysis tubing was tied off on one end and the precipitation fraction was added into the tubing with a pipette. A dialysis tubing clamp was used to seal the open end, ensuring that the solution was tightly packed in the tubing with minimal air bubbles. A string was tied to each dialysis tubing clamp, labeled with a tag, and placed into a large container of buffet (1–2 L) containing a stir bar. Using a low mixing speed, the strings attached to the dialysis tubes were taped to the outside of the container to ensure the stir bar did not contact the tubing. The tubes were left on the buffer solution for 12–16 h, with one buffer change within the first 4 h. The dialysis procedure was conducted entirely in the cold room at 4ºC. After dialysis, the tubes were removed from the buffer and the outside of the tubing was patted dry. The clamp was removed and the solution was removed via pipette onto a sterile tube and used for purification, SDS-PAGE, western-blot, or tributyrin assay immediately.

2.2.19 His-tagged Protein Purification

The His-tagged lipase was purified using His-Spin Protein Miniprep kit by Zymo Research (Cat. No. P2002). 450 µL of the crude extract sample was added to an equal volume of binding buffer. Three aliquots of 300 µL were added to the spin column and binding matrix, in case the concentration of lipase was very dilute. The spin column was centrifuged at 13,000 x g for 10s following the manufacturer's protocol, as described in Appendix C. The purified protein was eluted with 150 µL of elution buffer.

### 2.2.20 SDS-PAGE

Samples were prepared by adding 25 µL of the sample with 25 µL sample buffer. The sample buffer was prepared by adding 950 µL Laemmli Sample Buffer to 50 µL β-mercaptoethanol. The prepared sample was heated to 95ºC for 5 min in the Thermomixer and quickly vortexed and centrifuged. The Mini-PROTEAN Tetra Cell (Cat. No. 165-8000) and Mini-PROTEIN TGX gel was set up in accordance with the manufacturer's instruction, as described in Appendix C. 6 µL of the broad protein standard and 10–30 µL of the prepared samples were loaded into the gel wells. Gel electrophoresis was performed at 200 V for 30 min and was carefully removed from the plastic container and washed three times in 200 mL of DI water for 5 min. 50 mL of Bio-Safe Coomassie G250 stain was applied to the gel and placed on a rocker for 1 h. Afterwards, the stain was removed and 200 mL of DI water was added to destain the gel, which was placed back on the rocker for 3–12 h. The destaining process was aided by the addition of a Kim Wipe paper.

### 2.2.21 Tributyrin Assay

A solution of 2 mL tributyrin and 5 mL of 100 mM potassium phosphate buffer, pH 7.3, and 20 mL of DI water were added to a 100 mL plastic beaker (Mettler Toledo, Cat. No. 22006). The beaker was attached to the Mettler Toledo T50 pH-stat and a jacketed 250 mL reactor containing 200 mL of DI water was raised to encase the plastic beaker. The jacketed reactor was attached to a Fisher Scientific Isotemp Refrigerated Circulator (Model 9100), which maintained a constant reaction temperature of 40ºC. The pH electrode was rinsed and placed into the sample holder, along with the autoburette tip and rotational motor containing a plastic mixing impeller.

The program was activated and the pH-stat automatically adjusted the pH of the solution to 7.5 using 0.1 M NaOH certified solution. Once the pH 7.5 was maintained, the program

indicated when to add the sample containing the lipase. The enzyme was added through a hole intop of the pH-stat and the start button on the touch pad was immediately pressed, starting the program, as described in Appendix C. After the program was completed, the R2 value displayed was the mL of titrant per min used through testing (mL/min). This value and the mass of sample added were used to determine the enzyme activity in tributyrin units per gram (TBU/g) based on the calibration slope that was generated using enzymes with a known activity, as shown in Appendix C. 1 TBU unit = 1 μmol butyric acid released per minute / g lipase.

## 2.3 Results and Discussion

### 2.3.1 Approach and Methodology

A relatively high number of microbial lipase sources have been found to have high trans/-esterification activity that are suitable for biodiesel production. The genes for a number of these lipases have been identified, and their sequences made publicly available. Genetic and protein engineering has allowed a few of these lipases to be produced commercially in bacteria and yeast. The recent advances in plant biotechnology and genomics have allowed us to transgenically express recombinant protein and enzymes in plants as well. However, no one has taken advantage of the plant expression system to produce microbial lipases; leading to the motivation for this research. Our aim was to generate a proof-of-concept for the long-term goal of developing transgenic plants to express various lipases for testing and producing large quantities of lipase for the enzymatic biodiesel production.

The initial approach was to start with a known lipase from a microbial source that has high trans/-esterification activity, detailed genetic information, and has been successfully cloned, transformed, and expressed in a host organism. As a result, lipases from *Candida antarctica* and *Thermomyces lanuginosus*, two thermophilic fungi, were chosen for this research. Although the

transformation of plants was fairly straightforward, the transgenes had to be expressed in an appropriate fashion, since the origination hosts were microorganisms. In some cases, the expression of transgenes could result in metabolic energy waster, negative pleiotropic effects, and potential gene escape. Moreover, we did not know if the accumulation of lipase within the plant cell would interfere with the plant's metabolic and biosynthesis pathways, which could adversely affect growth and development. Therefore, a considerable amount of planning and experimental design was needed in order to properly express a recombinant enzyme without detrimental effects on the plants.

We focused on over-expressing cloned lipase genes in plants to produce a biocatalyst for biodiesel production using genetic engineering and biochemical strategies. The specific goals and objectives of the research were: (1) to clone and characterize genes of two lipases with known trans/-esterification activity, *Candida antarctica* lipase B (CAlB) and *Thermomyces lanuginosus* lipase (TLl); (2) to genetically engineer the cloned lipase genes into higher plants, like tobacco and Arabidopsis thaliana; (3) to subculture the transgenic plants into the 3$^{rd}$ generation to obtain transgenic plants with hereditary stability; and (4) to extract and purify the recombinant lipase from the transgenic plants followed by activity analyses. An outline of the steps in the experimental approach is shown in Figure 3.

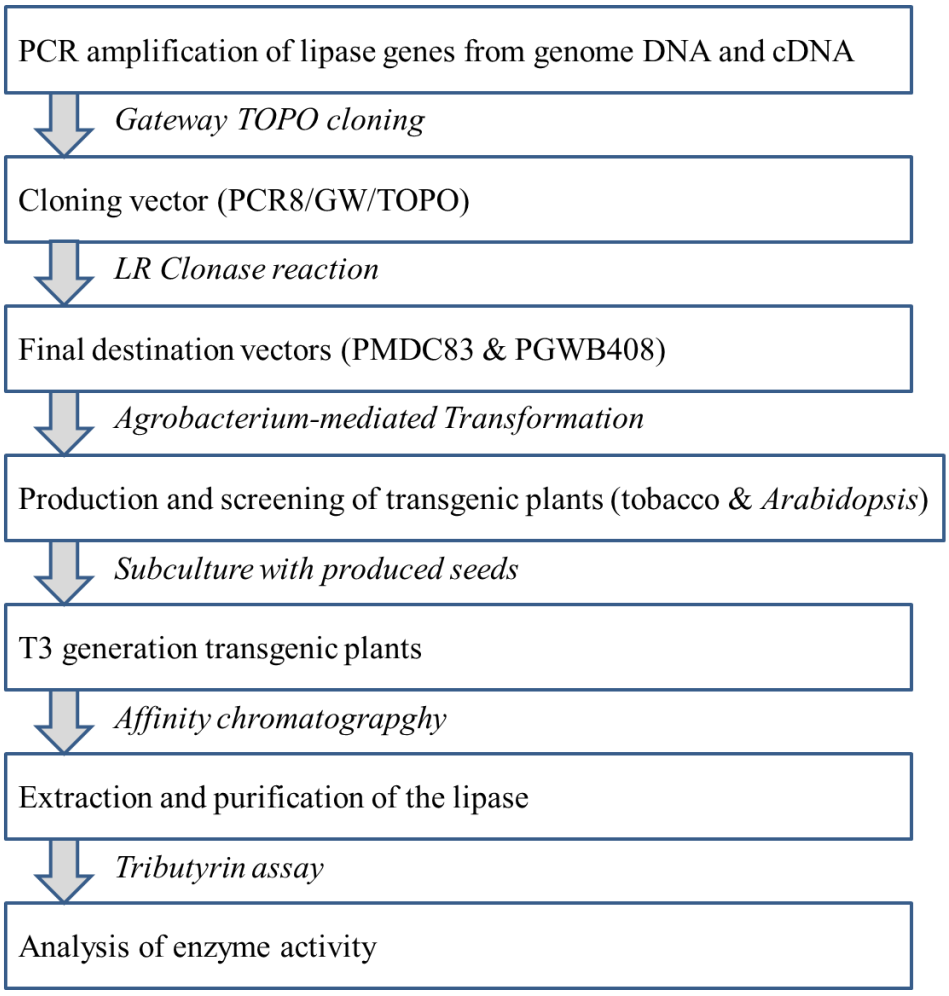


**Figure 3.** Flow chart for the strategy for the production of lipase in transgenic plants

2.3.2 Cloning of *T. lanuginosus* and *C. antarctica* lipase genes

There are currently 114 nucleotide listings on NCBI for lipases from *T. lanuginosus* and *C. antarctica* and numerous other literature references. However, different strains of fungi can have slightly different genomic sequences and many of the strains referenced are locally acquired by research groups or provided by a company. Not having the correct fungal stain with the corresponding genetic information could cause difficulties in gene cloning. Currently, the entire genomes for commercially available strains of *T. lanuginosus* (ATCC Strain 200065) and *C. antarctica* (ATCC Strain 32657) were already sequenced, annotated, and made accessible

online in 2011 and 2008, respectively. Analysis of their database identified two lipases (*T. lanuginosus* lipase, TLl, and *C. antarctica* lipase B, CAlB) that corresponded with other reported lipases listed on NCBI, matching both their coding sequence (CDS) and protein sequence, as reported in Table 3.

**Table 3.** Lipase information identified by NCBI BLAST

| Name | Protein ID | Gene Length | Protein Length | NCBI Access Number |
|---|---|---|---|---|
| **TLl** | Thela2p4_000466 | 1061 | 291 | CS793911 |
| **CAlB** | P41365 | 1029 | 342 | DF830068 |

The sample of *T. lanuginosus* and *C. antarctica* we received from ATCC came free-dried in a glass vial and was rehydrated following protocol provided by ATCC. The rehydrated *C. antarctica* was cultured onto a universal yeast medium and was incubated at 30ºC for 72 h. The genome DNA of C. antarctica was then extracted and stored at -20ºC, preparing for amplification by PCR.

The rehydrated *T. lanuginosus* was cultured onto potato dextrose agar (PDA) medium containing olive oil to induce lipase expression and was incubated at 50ºC for 72 h. The fungus was collected and frozen using liquid nitrogen in order to isolate the total RNA. The genomic DNA of *T. lanuginosus* indicated there were three introns in the genomic sequence, ranging between 58–74 bp each. Although these introns were removed during the transcription process within the fungi, it was not guaranteed that they would be properly removed within plant cells. Therefore, cloning required isolating the total RNA and the reverse transcription of the mRNA into complementary DNA (cDNA) using reverse transcriptase.

The lipase genes were amplified by PCR using specific primers. The primers were designed to construct three variations of the lipase gene, as shown in Table 4. The first constructs,

B1 & C1, include the entire CDS with the predicted signal peptide that was 17 aa in length. The signal peptide at the N-terminus of the protein helped direct the protein to the proper post-translational pathway. The lipases of *T. lanuginosus* and *C. antarctica* are extracellular and the signal peptides direct the lipases to be secreted from the cell. However, it is unknown if the signal peptide or protein would function properly in a plant cell since the secretion mechanisms are different from that in yeasts. Therefore, constructs B2 & C2 were developed, in which the signal peptide was removed from the CDS. Since this removed the start codon (ATG), the primers were designed to add the start codon to the beginning of the sequence. Recognition of initiator codons by eukaryotic ribosomes as the translational start site could also be affected by the removal of the signal peptide. Therefore, the third constructs, B3 & C3, were designed to replace the signal peptide with the Kozak sequence: AGA ACC ATG GGC. This sequence was determined by Marilyn Kozak to improve translational recognition of the ribosome by introducing a modest amount of secondary structure to the beginning of the CDS. Reverse primers removed the stop codon to allow for gene fusion with reporter/purification tag to the C-terminus.

**Table 4.** Primers for cloning and sequencing of lipases form T. lanuginosus and C. antarctica

| No./Lipase | Forward Primer | Reverse Primer | TM (Fwd/Rvs) |
|---|---|---|---|
| **B1/TLl** | ATGAGGAGCTCCCTTGTGCT | AAGACATGTCCCAATTAACCCGAA | 58.5/56.6 |
| **B2/TLl** | ATGAGTCCTATTCGTCGAGAGGT | AAGACATGTCCCAATTAACCCGAA | 56.9/56.6 |
| **B3/TLl** | AGAACCATGGGCAGTCCTATT | AAGACATGTCCCAATTAACCCGAA | 56.0/56.6 |
| **B4/TLl** | AGTCCTATTCGTCGAGAGGTC | TACCATAGGTGCGCAGGGATA | 56.6/57.7 |
| **C1/CAlB** | ATGAAGCTACTCTCTCTGACCGGT | GGGGGTGACGATGCCGGA | 59.0/63.0 |
| **C2/CAlB** | ATGGCCACTCCTTTGGTGAAGCGT | GGGGGTGACGATGCCGGA | 63.2/63.0 |
| **C3/CAlB** | AGAACCATGGGCGCCACTCCT | GGGGGTGACGATGCCGGA | 63.7/63.0 |
| **C4/CAlB** | TTGCAGCCACTCCTTTGGTGAA | AGGGTTGCAGTCCGTAATGCCATA | 59.6/60.5 |

The fourth pair of constructs, A4 & B4, were exploratory primer sets to amplify a conserved section of the CDS. These were designed in case we were unable to amplify the lipase

gene using the other primer sets. In addition, these primers could be used for screening purposes for all three of the previous constructs. After optimizing PCR conditions (with respect to annealing temperature), we were able to successfully clone all eight constructs. The optimum annealing temperature was found to be 52ºC for all TLl primers, and 63ºC for CAlB primers. The results were determined by gel electrophoresis, as shown in Figure 4. In a collaborative effort, the works of TLl gene amplification and TOPO vectors' construction were finished and shown in Michael Gagnon's dissertation[12], while I focused on the CAlB one.

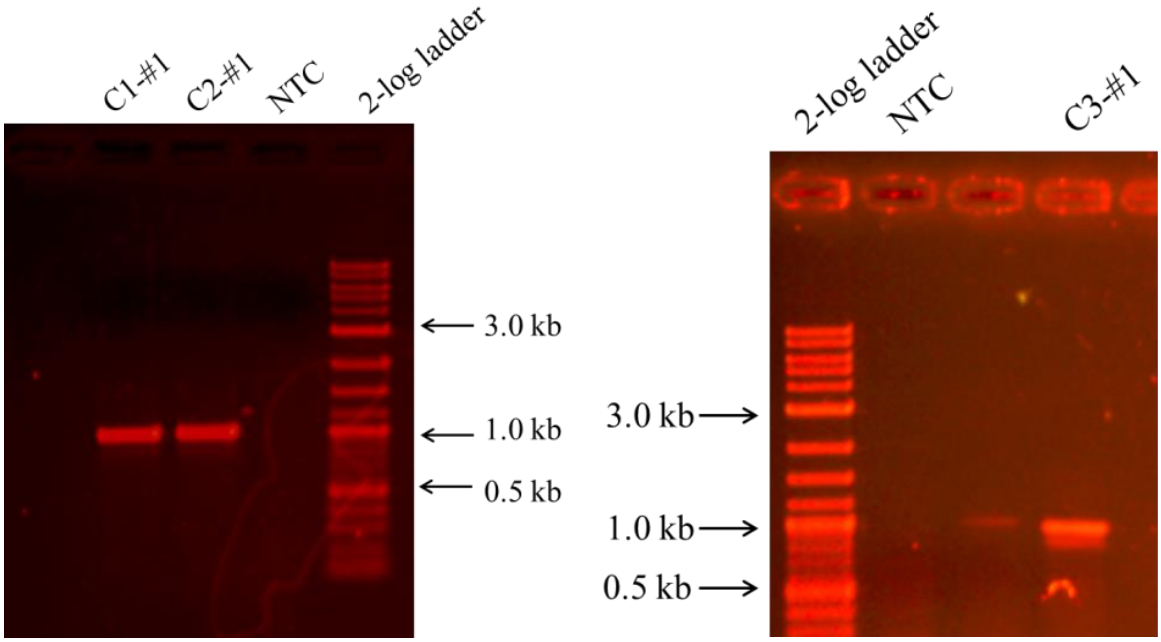


**Figure 4.** Gel analysis results of C. antarctica lipase B amplification products using TAKARA Taq polymerase. PCR conditions: (1) initialization for 1 min at 94 °C, (2) denaturation for 30 sec at 94°C, (3) annealing for 1 min at 63 °C, (4) elongation for 1 min at 72 °C. Steps 2–4 was repeated for 35 cycles, and (5) final elongation for 2 min at 72°C. The products are stored at -20°C for future use. Expected PCR product size: C1 1026 bp, C2 975 bp, and C3 991 bp.

### 2.3.3 Construction of the Lipase Vectors

The *taq* polymerase used for PCR had a non-template dependent terminal transferase activity which added a single deoxyadenosine (A) to the 3' ends. This feature allowed us to

insert our PCR products into a linearized Gateway recombination cloning vector platform, due to 3'-T overhangs for direct ligation. Insertion into a cloning entry vector (PCR8/GW/TOPO) offered att sites for recombination into a variety of Gateway compatible destination vectors without tedious sub-cloning. The PCR8/GW/TOPO - lipase constructs were transformed into chemically competent *E. coli* cells and grown overnight on LB media containing spectinomycin. The cloning vector contained the gene for spectinomycin resistance (SpnR), which is efficient for selection of transformed *E. coli*. However, directionality of the gene was important later for insertion into Gateway destination vectors and the simplicity of the PCR8/GW/TOPO allows the gene to be inserted backwards. Therefore, colonies growing on the selection medium need to be screened to ensure proper orientation.

Several individual colonies were chosen at random and grown overnight in liquid LB medium containing spectinomycin. These cultures were used to isolate and characterize the plasmid for purity and concentration. A restriction digest used restriction enzymes to cleave DNA molecules at specific sites. A plasmid map was generated for each construct using pDRAW32 and analyzed to select the most appropriate enzymes to determine proper insert size and correct orientation. The plasmid maps for PCR8/GW/TOPO - lipase constructs are shown in Figure 5 and the gel pictures form the corresponding plasmid restrictions are shown in Figure 6. Also due to the gel pictures for TLl finished and already shown in M. Gagnon's dissertation[12], Figure 6 only shows the results of CAlB.

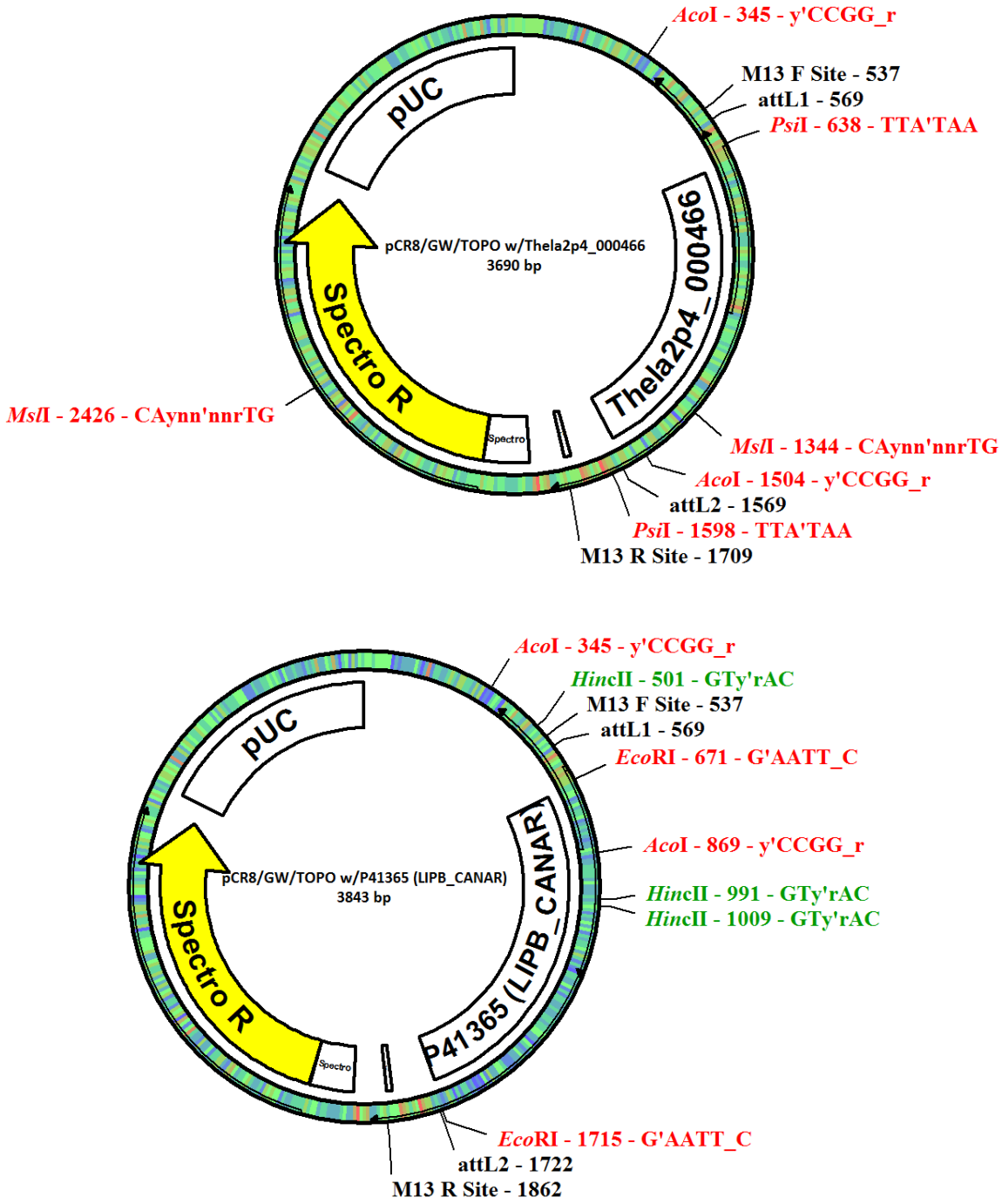


**Figure 5.** Plasmid maps of PCR8/GW/TOPO - lipase constructs with annotations of important features and enzyme restriction sites. For TLl case, fragments of restriction digest for correct orientation: AcoI: 2531, 1159 bp, and MslI: 2608, 1082 bp; fragments of wrong orientation: AcoI: 3301, 389 bp, and MslI: 2158, 1532 bp. For CAlB case, fragments of restriction digest for correct orientation: HincII: 3319, 524 bp; fragments of wrong orientation: HincII: 2962, 881 bp.

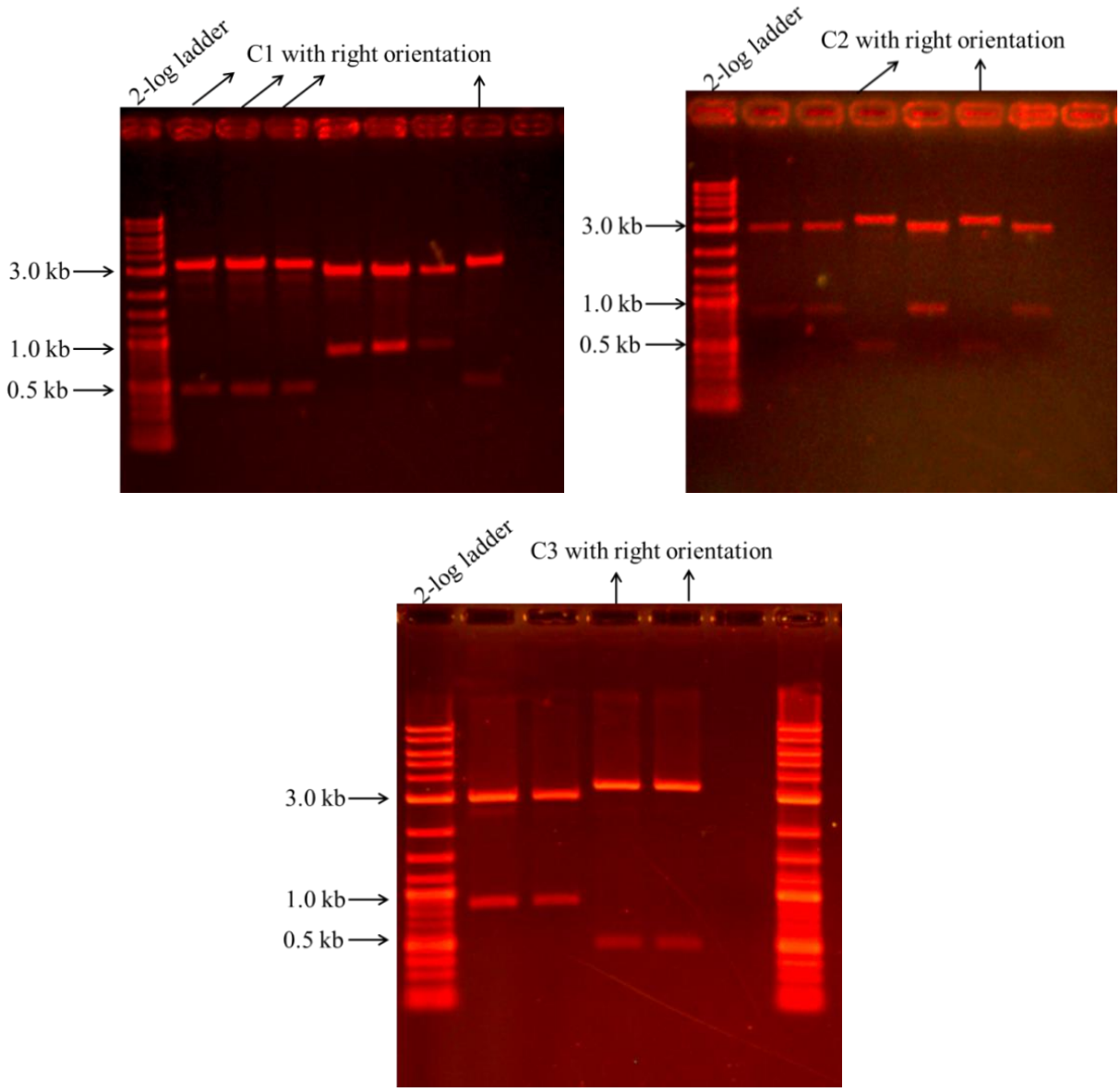


**Figure 6.** Gel analysis results from plasmid screening by restriction digest of PCR8/GW/TOPO - CAlB constructs with C1, C2 and C3 primers.

The isolated plasmids that indicated the correct insert size and proper orientation by gel were sent for sequencing at the University of New Hampshire's Hubbard Center for Genome Studies (HCGS) DNA Sequencing Core Facility. While several of the sequences indicated some substitutions and deletions of the known sequence, there were a few colonies from constructs C1, C2 and C3 that matched 100% with the reported sequence from the Genozymes Project database,

the results of which are shown in Appendix C. After sequencing, glycerol stocks were made of each *E. coli* culture containing the cloning vector with the correct lipase gene (orientation and sequence).

Final destination vectors, in this case vectors for plant transformation, were used for Agrobacterium-mediated transformation of tobacco and *Arabidopsis*. These vectors were able to replicate in *Agrobacterium* and *E. coli*, contain selectable markers to identify successfully transformed bacteria and plants, and possess the left and right border sequence for *Agrobacterium*-mediated transformation to ensure proper integration of the genes of interest into the plants' genome.

Producing transgenic plants is often hindered by conventional cloning technology (i.e., restriction digestion and ligation), which is rather labor intensive. However, several research groups have developed several series of final destination vectors that are Gateway compatible and are freely available for academic purposes. These vectors were used for the expression of protein fusions to reporter/purification tags, such as GFP, β-glucuronidase (GUS), 6x Histidines (His), and glutathione S-transferase (GST). In addition, these vectors could also be used to generate different promoter::reporter constructs to facilitate constitutive or inducible transgene expression.

Gateway Technology is a universal technology used to clone DNA sequences for functional analysis and expression in multiple systems using site-specific recombination properties of bacterioghage lambda. This provides a rapid and highly efficient way to transfer DNA sequences by allowing recombinant sites to provide high specificity and activity. The use of the λ site-specific recombination system allows site attL1 and attL2 (from the TOPO vector) to react only with the corresponding attR1 and attR2 (LR Clonase reaction), respectively, on the

final destination vector by a mixture of lambda and *E.coli*-encoded recombination proteins. Therefore, unlike the PCR8/GW/TOPO vector transformation, the orientation of the transferred gene was maintained. To ensure the desired vector was obtained, a negative selectable marker consisting of the bacterial *ccdB* gene was located between att sites, which encoded an anti-DNA glyrase protein. The DNA gyrase enzyme relieves the strain while double-stranded DNA is being unwound by helicase during transcription and replication. Disruption of this enzyme results in bacterial death; however, *E. coli* strain DB3.1 contains a mutated DNA glyrase protein which was not susceptible to *ccdB* protein and used to replicate the stock untransformed vector.

The two final destination vectors selected for this study were PGWB408 and PMDC83, which were developed by Nakagawaand Matsuoka (2007)[23] and Curtis Grossniklaus (2003)[24], respectively. These two vectors both constitutively express the recombinant protein with a fused 6x His tag for rapid purification. The main difference between the two vectors is that the PMDC83 vector fuses a GFP reporter gene to the C-terminus before the 6x His tag, while the PGWB408 vector just has a fused 6xHis tag on the C-terminus. Additional details on the two vectors are shown in Table 5. While the addition of GFP fused onto the lipase could interfere with its activity, it also allowed us to visually observe expression in transgenic plants. Furthermore, the GFP and 6xHis tag can be enzymatically cleaved and separated from lipase after purification.

**Table 5** Final destination vectors selected for plant transformation

| Vector | Lipase Source | Size | Bacterial/Plant Resistance | Promoter | Reporter Gene | Purification Tag |
|---|---|---|---|---|---|---|
| **PMDC83** | TL | 12,513 | Kanamycin/Hygromycin | 2x35S | GFP | 6xHis |
| **PGWB408** | CA | 11,703 | Spectinomycin/Kanamycin | 35S | N/A | 6xHis |

After confirmation by sequencing, the lipase gene was inserted into the final destination vectors (TLl was inserted into PMDC83 and CAlB was inserted into PGWB408) by a LR Clonase reaction, transformed into *E. coli* by heat-shock method, and grown on an LB plate containing the appropriate bacterial antibiotic overnight. Similar to the cloning vector, five individual colonies were selected and grown in liquid media overnight and the plasmids were isolated, characterized, and size confirmed by restriction digests. The plasmid maps for PGWB408/PMDC83 - lipase constructs are shown in Figure 7 and the gel pictures are shown in Figure 8. Also due to the gel pictures for TLl finished and already shown in M. Gagnon's dissertation[12], Figure 8 only shows the results of CAlB. Glycerol stocks of each *E. coli* culture were made containing the destination vector with each lipase construct.

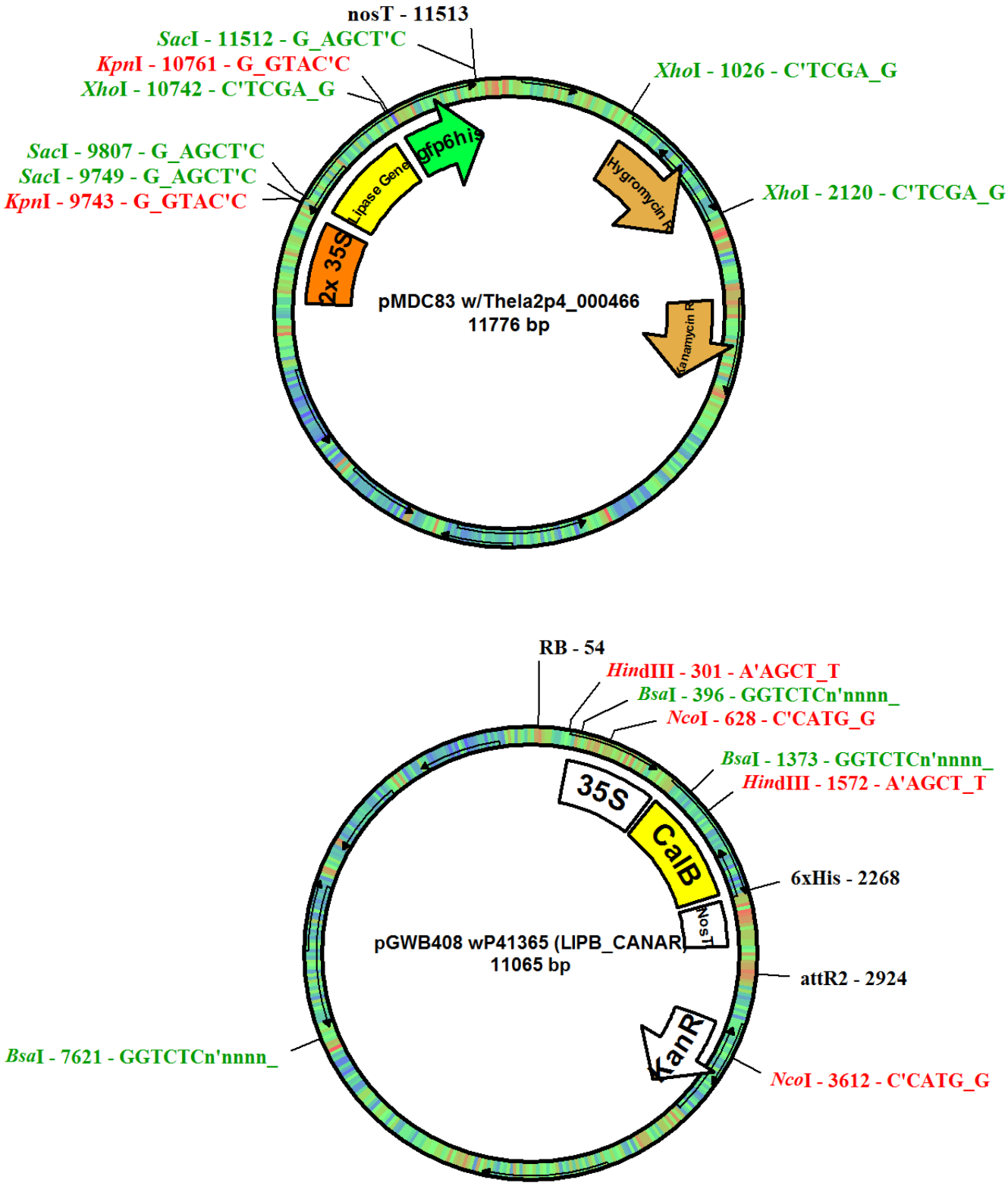


**Figure 7.** Plasmid maps of PMDC83-TLl and PGWB408 -CalB constructs with annotations of important features and enzyme restriction sites. Restriction expected size for PGWB408 -CalB: NcoI: 8081, 2684 bp; HindIII: 9794, 771 bp.

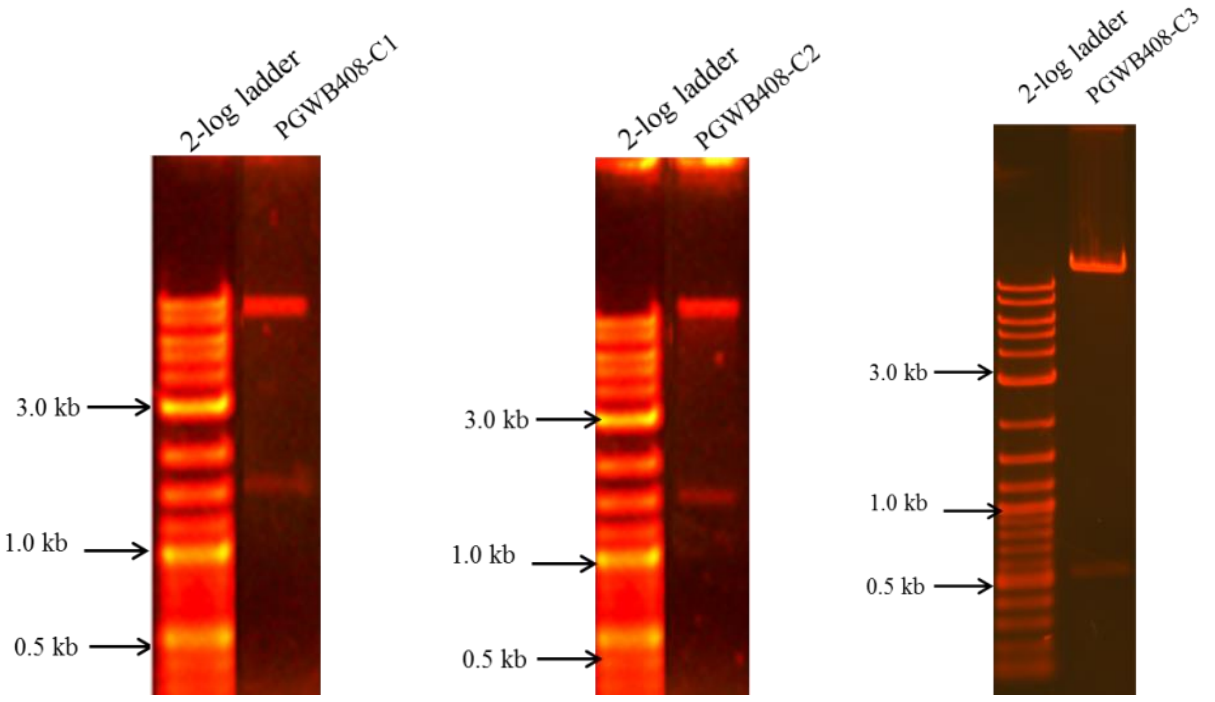


**Figure 8.** Gel analysis results from plasmid screening of final destination vectors, PGWB408-CAlB. The results of C1 and C2 were digested by NocI, while C3 was digested by HindIII.

2.3.4 Transformation of Plants

Each of confirmed final destination vector constructs was transformed into *agrobacterium tumefaciens* (strain GV3101) by electroporation and grown on LB plate media with the appropriate bacterial antibiotic at 27 ºC for 48–72 h. A final verification was performed on selected Agrobacterium colonies to ensure the presence of the vector and the lipase gene. The individual colonies were screened by PCR after a crude DNA extraction using the corresponding lipase construct primer set (Table 4). Glycerol stocks were made of each Agrobacterium culture containing the destination vector with each lipase constructs.

*Arabidopsis thaliana* was transformed using *Agrobacterium* containing the final vectors PGWB408-C1, PGWB408-C2 and PGWB408-C3 by the floral dip method. Non-transgenic seeds of *Arabidopsis* were sown in moist soil mix for 3–4 weeks. For each lipase construct, three

pots were prepared one week prior to dipping by clipping the primary bolt to encourage synchrony in branching and flowering. The *Agrobacterium* preserved in glycerol stocks were used to grow 500 mL of culture in liquid LB medium with the antibiotic 100 µg/mL spectinomycin. The solutions were pelleted in a centrifuge and resuspended in a solution of 5 w/v% sucrose and 0.05 vol.% of L-77 Silwet to an OD600 of 0.8 ± 0.2 before dipping. The unopened flower buds along with flowers were dipped into the solution of *Agrobacterium* for 8–10 sec, avoiding contact with the basal leaves and soil. The pots were laid on their side overnight and covered with clear plastic wrap to prevent desiccation. The plants were then rinsed in cold water to remove any residual sugars and placed in a growth room. This dipping process was repeated seven days later to ensure sufficient transformation. Afterward, the plants remained in the grow room for 4–6 weeks to allow for seed (T1 transgenic *Arabidopsis*) development. The seeds were collected and desiccated at room temperature for 2–3 days, followed by sterilization and storage at 4ºC.

The seeds were spread evenly on solid germination media containing the antibiotic of 50 µg/mL kanamycin. The plates were covered and placed in a dark room at 4ºC for 2 days. Afterwards, they were removed from the cold storage and placed in the growth chamber. As expected, the vast majority of the seeds did not germinate or died on the kanamycin containing media after one week, while the survived ones were picked to soil and placed to the grow room for 4–6 weeks. The pictures of successful transgenic Arabidopsis and the non-transgenic Arabidopsis on the kanamycin containing media are shown in Figure 9. The transgenic plants were verified with the PCR screening method, as described in part 2.3.5, and in total five T1 generation transgenic Arabidopsis plants were obtained, with the mark of PGWB408-C1-1, C2-1, C3-1, C3-2, and C3-3.

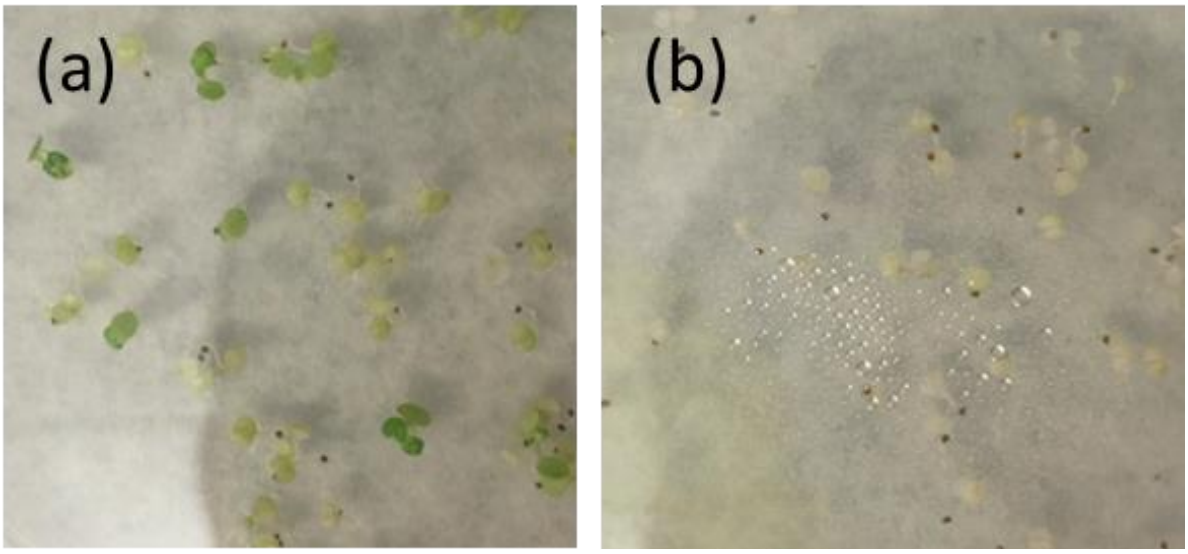


**Figure 9.** Pictures of transgenic and non-transgenic Arabidopsis thaliana on kanamycin containing germination media: (a) transgenic Arabidopsis, successfully transformed Arabidopsis survived on the media, (b) non-transgenic Arabidopsis, all plants dried to die on the medium.

In order to obtain the hereditary stable transgenic plants, seeds of the T1 transgenic *Arabidopsis* were collected and germinated for T2 generation transgenic with the same strategy did for T1 *Arabidopsis*. The germination rates and survival rates of every T1 generation *Arabidopsis* were recorded and shown in Table 6.

**Table 6.** Germination and survival rates for T2 generation transgenic Arabidopsis

| T1 Plant | Germination Rate | Survival Rate |
|---|---|---|
| **PGWB408-C1-1** | 104/128 | 44/104 |
| **PGWB408-C2-1** | 116/132 | 48/116 |
| **PGWB408-C3-1** | 84/120 | 32/84 |
| **PGWB408-C3-2** | 96/108 | 36/96 |
| **PGWB408-C3-3** | 112/144 | 44/112 |

*Nicotiana tabacum* (tobacco) was transformed using *Agrobacterium* containing the final vectors PMDC83-B1, PMDC83-B2 and PMDC83-B3, which was finished and shown in M. Gagnon's dissertation[12], and three T1 generation transgenic tobaccos (PMDC83-B1-A1, PMDC83-B1-C7, and PMDC83-B2-B4) were obtained. However, Dr. M. Gagnon was unable to

successfully isolate the lipase protein from any of these T1 transgenic tobaccos before he graduated. Therefore, in order to see if there is a result in other generations as well as to obtain the hereditary stable transgenic plants, subculture of the T1 generation transgenic tobaccos into T2 generation was necessary.

After growth in Magenta boxes for 4–6 weeks, the transgenic tobacco was transferred into soil and placed in a 6" round pot. These pots were then transported to the University of New Hampshire's Macfarlane Greenhouse Facility for 2–4 months until tobaccos flowered. Tweezers were used to touch the plant's stamens and pistil to make it self-fertilized, followed by covering the whole plant with a gauze bag to prevent cross-fertilization. The seeds (T2 generation transgenic tobacco) were harvested after 2 weeks and desiccated at room temperature for 2–3 days, followed by sterilization in the 70% ethanol for 10 sec. A wet pre-sterile filter paper was used to germinate these tobacco seeds. After being put in wet paper at room temperature for about 7 days, the germinated tobacco seeds were transferred onto MS-basal medium plate containing the antibiotic of 50 μg/mL hygromycin for 1–2 weeks. The vast majority of the seeds died on the hygromycin containing media and the survived tobaccos were transfer onto solid MS-basal medium in Magenta boxes wrapped with microporous tape and placed in growth room for 4–6 weeks. The germination and survival rates were also recorded and shown in Table 7.

**Table 7.** Germination and survival rates for T2 generation transgenic tobaccos

| T1 Plant | Germination Rate | Survival Rate |
|---|---|---|
| **PGWB408-C1-1** | 104/128 | 64/104 |
| **PGWB408-C2-1** | 116/132 | 68/116 |
| **PGWB408-C3-1** | 84/120 | 52/84 |
| **PGWB408-C3-2** | 96/108 | 46/96 |
| **PGWB408-C3-3** | 112/144 | 64/112 |

2.3.5 Screening Transgenic Plants

When the transgenic *Arabidopsis* grew the fourth leaf or the leaves of transgenic tobacco were larger than 5 mm in size, one leaf was removed and screened for the presence of a lipase gene in its genome. A rapid DNA isolation was performed on the tissue followed immediately by a PCR with the corresponding lipase primers (Table 4). The results of the screening indicated that the majority of the plants did in fact have the lipase gene present. Gel results of T1 generation *Arabidopsis* were shown in Figure 10, T2 generation *Arabidopsis* in Figure 11, and T2 generation tobacco in Figure 12.

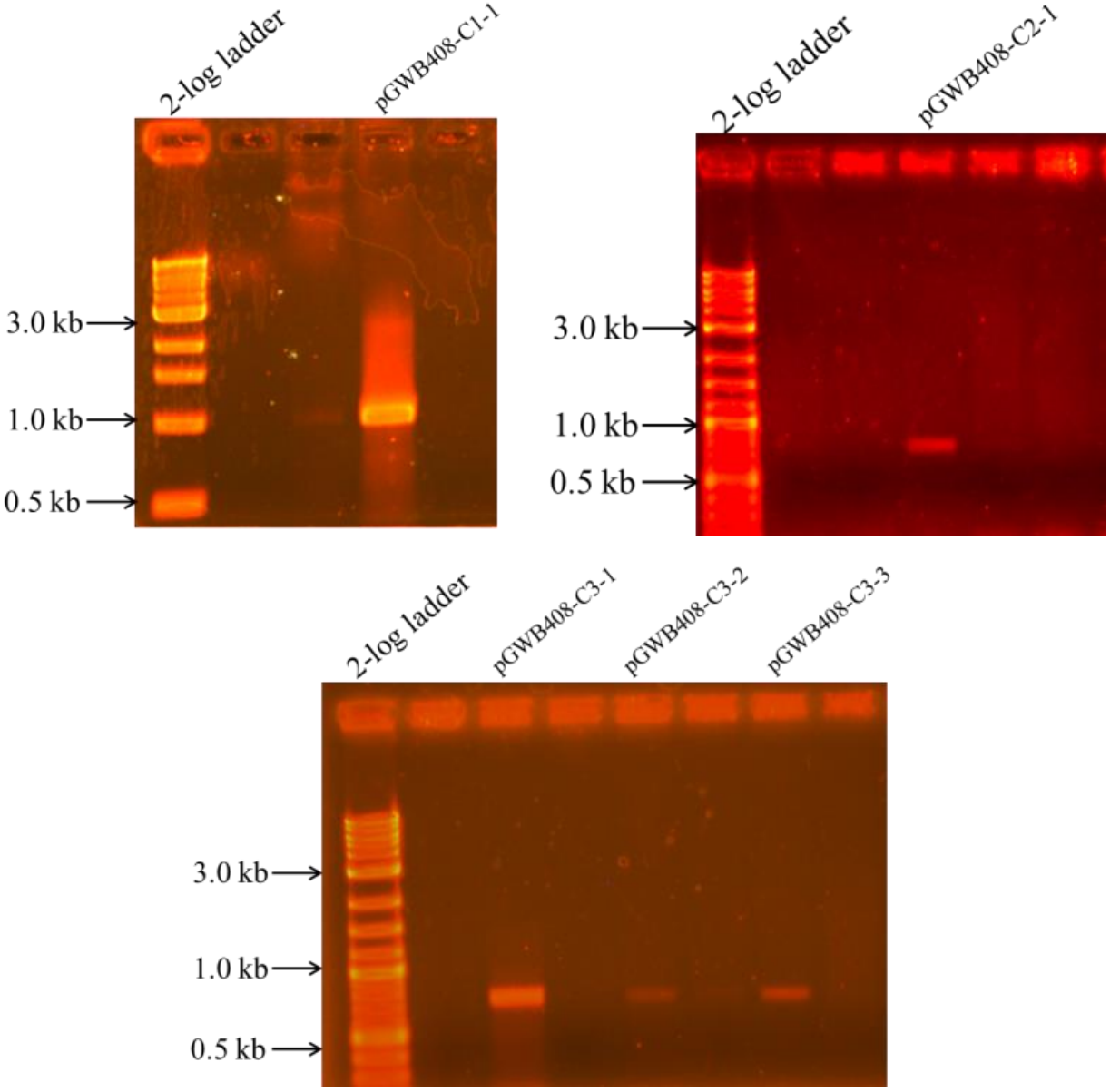


**Figure 10.** Gel analysis of PCR screening of T1 transgenic Arabidopsis for C. antarctica lipase B gene. PCR product sizes: C1 975 bp, C2 962 bp, and C3 967 bp.

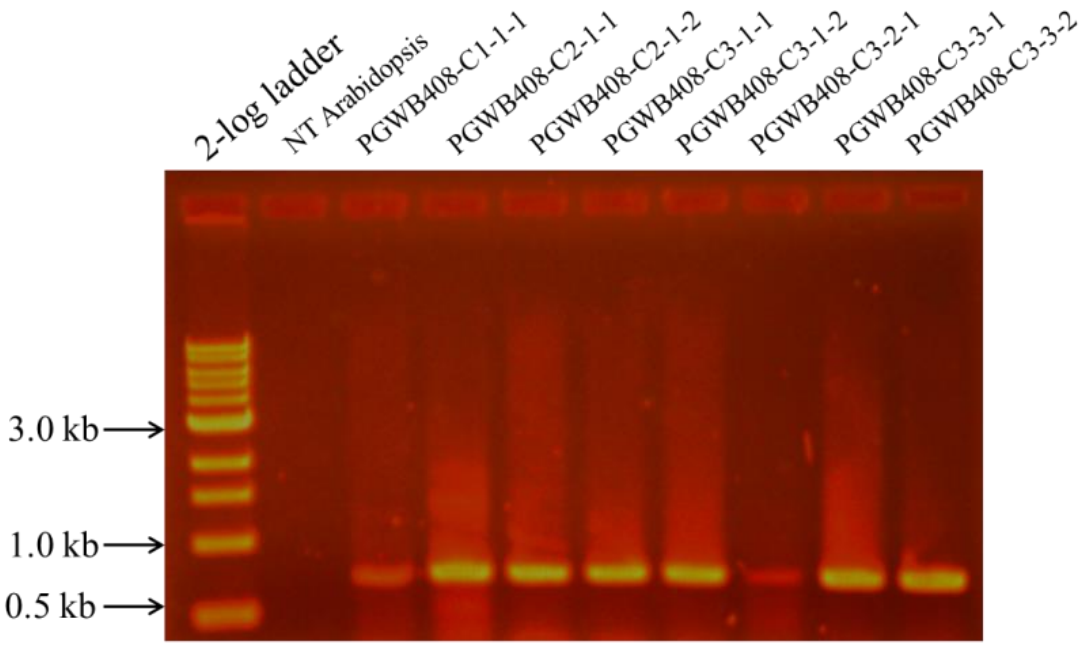


**Figure 11.** Gel analysis of PCR screening of T2 transgenic Arabidopsis for C. antarctica lipase B gene. PCR product sizes: C1 975 bp, C2 962 bp, and C3 967 bp.

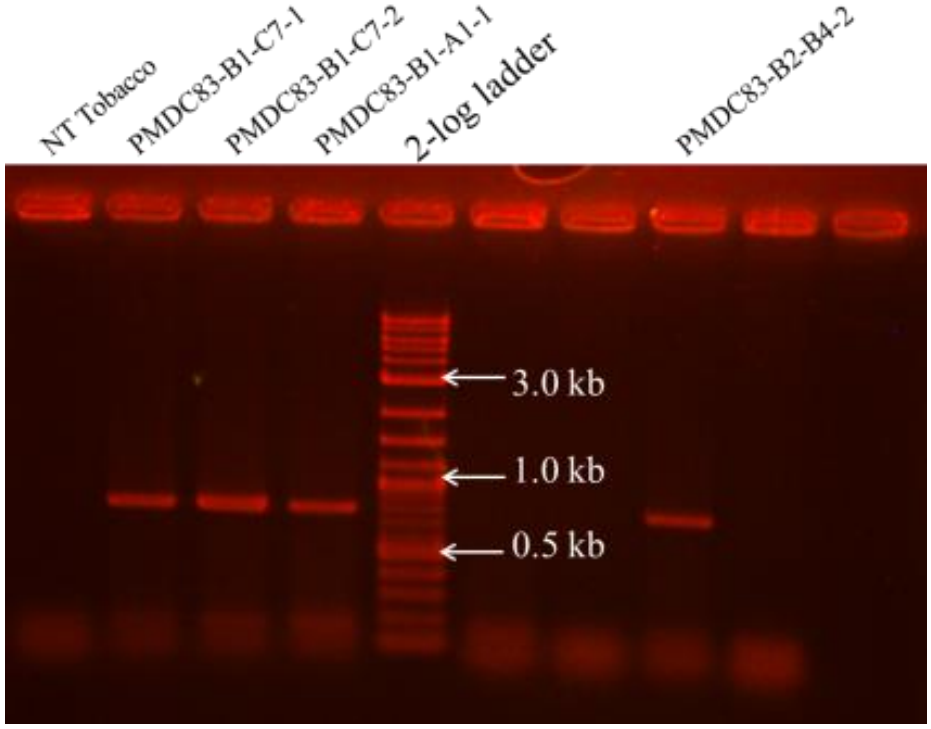


**Figure 12.** Gel analysis of PCR screening of T2 transgenic tobacco for T. lanuginosus lipase gene. PCR product sizes: B1 873 bp, C2 825 bp, and C3 834 bp.

From the results eight T2 generation transgenic *Arabidopsis* plants were obtained marked with: PGWB408-C1-1-1, PGWB408-C2-1-1, PGWB408-C2-1-2, PGWB408-C3-1-1, PGWB408-C3-1-2, PGWB408-C3-2-1, PGWB408-C3-3-1, and PGWB408-C3-3-2. And four T2 generation transgenic tobaccos were selected: PMDC83-B1-A1-1, PMDC83-B1-C7-1, PMDC83-B1-C7-2, and PMDC83-B2-B4-2. The fake transgenic plants were removed from the growth medium/soil, and the transgenic plants were grown 2–4 more weeks for lipase protein extraction.

2.3.6 Strategy for Homozygotes Achievement of Transgenic Plants

If we marked the plant genome inserted with lipase and antibiotic resistance gene sequence as "A," while its sister genome without insertion as "a," the typical gene type of T1 transgenic plants should be "Aa." After self-fertilization, the gene type of T2 plants could be "AA" and "aa," the homozygote, as well as the hybrid "Aa." And only "AA"- and "Aa"- typed plants can survive on the antibiotic-containing media. According to the Mendel's theory, after self-fertilization, the seeds of the homozygote transgenic plants (T3 generation) should have a 100% survival rate, while the hybrid one has a rate of about 75%, as shown in Figure 13.

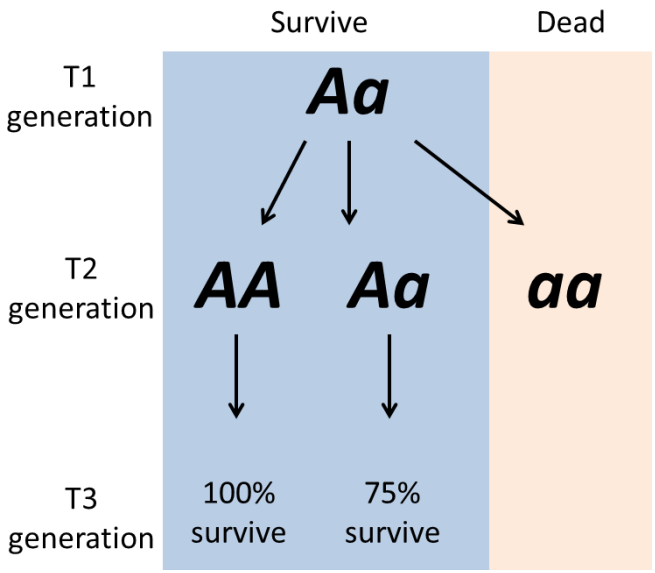


**Figure 13.** Gene type map of transgenic plant with self-fertilization.

All achieved eight T2 generation *Arabidopsis* and four tobaccos were then self-fertilized and seed-collected with the method introduced in part 2.3.4. Seeds were then germinated in an antibiotic-containing medium and the survival rates were counted, as shown in Table 8. The result proved that all these 12 lines of T2 transgenic plants were hybrid gene type. And in order to achieve the hereditary stable plant, more T2 generation plants need to be investigated.

**Table 8.** Survival rates of T3 transgenic plants

| Plant | *Arabidopsis thaliana* | | | | | | | | tobacco | | | |
|---|---|---|---|---|---|---|---|---|---|---|---|---|
| Number | C1-1-1 | C2-1-1 | C2-1-2 | C3-1-1 | C3-1-2 | C3-2-1 | C3-3-1 | C3-3-1 | B1-A-1 | B1-C-1 | B1-C-2 | B2-2-4 |
| Survival rate | 52/84 | 64/96 | 56/96 | 42/68 | 44/72 | 72/104 | 48/76 | 52/88 | 68/92 | 72/92 | 44/68 | 40/64 |

### 2.3.7 Extraction, Purification, and Testing of the Recombinant Lipase in T2 Plants

When extracting recombinant proteins from plant tissues, there are a wide variety of techniques, buffers, and protocols available to researchers. However, there are no real set of rules or guidelines in choosing one method over another and the procedure is usually tailored to the protein and expression system being used. Extraction methods for the recombinant expression of lipase in yeasts were fairly straightforward because the yeast normally secretes the lipase into medium from which it can be easily filtered and purified. Lipases have also been extracted from the seeds of plants, where the early stages of germination produce the largest amount of lipase. This procedure usually required steps to remove residual TAG molecules, since it is a major constituent of the seed and a substrate for the lipases. However, the easiest and most desired method to extract recombinant proteins that showed constitutive over-expressed in transgenic tobacco and Arabidopsis is through the leaf tissue.

In general, the processing of recombinant proteins from plant expression systems consists of four steps: (1) extraction; (2) solid-liquid separation; (3) pretreatment/conditioning; and (4) purification. Extracts from green leaves contain large amounts of proteases, phenol oxidases, and thousands of other plant phenols and polyphenols, some of which can degrade or modify recombinant proteins. Therefore, the process of extraction involves collecting the plant tissue and disrupting either fresh or deeply frozen tissue as quickly as possible by grinding, pressing, or homogenization of the leaf tissue and extracting the protein during and after extraction buffers containing protease inhibitors, reducing agents, detergent, and antichelating agents. The ionic strength and pH of the extraction buffer can also reduce protein and phenol interactions. However, many of the strategies commonly used to prevent recombinant protein degradation and increase product yield are also detrimental to the typical methods for purification, such as

affinity chromatography. Therefore, great care was needed to develop an effective extraction and purification strategy.

Several common themes in protein extraction were observed in the literature, a weak extraction buffer (phosphate or Tris) of pH 7–8 and a reducing agent, such as β-mercaptoethanol, sodium bisulfate, or dithiothreitol (DTT). However, strong reducing agents, such as DTT, and metal-chelating agents, such as ethylenediaminetetraacetic acid (EDTA), cannot be used in conjunction with the nickel (Ni) affinity columns used for His tag purification. Therefore, the buffer containing 25 mM Tris-HCl pH 7.5, 50 mM NaCl, 2mM β-mercaptoethanol, and a plant protease inhibitor cocktail was used to extract the recombinant lipase. Leaves from transgenic tobaccos and Arabidopsis were frozen in liquid $N_2$ and ground with a mortar and pestle containing the extraction buffer with a ratio of 3:1 (mL buffer/ g tissue FW). Afterward, the extract was centrifuged and the supernatant collected. A portion of the extract was mixed with the binding buffer from the purification kit and then run through the spin columns in accordance with the manufacturer's instruction. To maximize purification, three column volumes of the sample were run through the column before elution. The crude extract and column elution sample were analyzed by SDS-PAGE. Unfortunately, no bands were observed on the purified sample of the SDS-PAGE gel for any of the samples analyzed, as shown in Figure 14. Several other plants, which were from both tobaccos and *Arabidopsis*, were investigated then, with similar results.

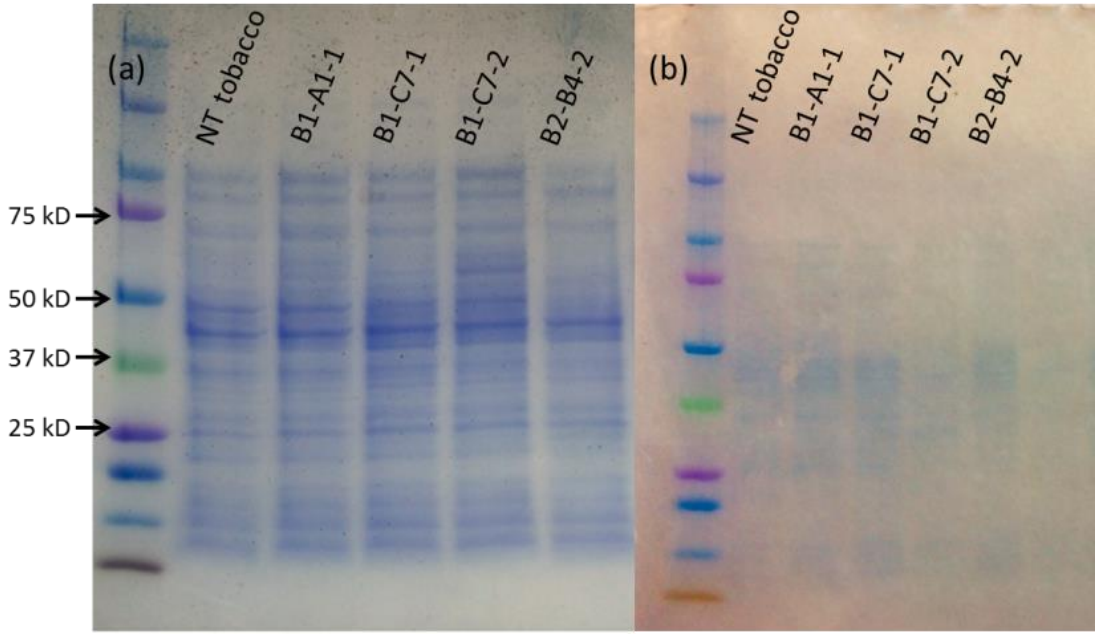


**Figure 14.** SDS-PAGE gel results from initial protein extraction and purification of recombinant lipase from tobaccos: (a) crude extract, (b) purified sample. Expected fragment size is 61.4 kDa.

After these results, we decided to backtrack and re-screen these transgenic plants to determine if the lipase gene was being expressed. The results indicated that all these plants had a recombinant lipase gene in the genome and expressed the gene properly. Afterward, the protein precipitation was applied on the crude extracts to increase the concentration. Although there were many options available to accomplish this, two of the methods most commonly seen in the literature were used: ammonium sulfate and acetone precipitations.[60]

Ammonium sulfate precipitation acts upon the electrostatic forces of the water molecules surrounding a protein and accounts for about 60% of the precipitation schemes conducted by researchers.[61] An excess amount of salt can cause a protein to precipitate by a phenomenon called *salting-out*. As the salt concentration increases, the ionic strength of the solution increases and the proteins will begin to precipitate out of solution depending on the properties of the specific protein. Usually, different fractions with varying amounts of ammonium sulfate are

collected sequentially in order to remove some of the unwanted proteins. Performing the procedure at lower temperatures (4°C) increases the protein's stability and decreases the amount of ammonium sulfate required. Fractions of ammonium sulfate saturation levels were performed on the crude extract at 0-30 %, 30-60 %, and 60-90% levels. The precipitated proteins were pelleted by centrifugation and resuspended in buffer and the ammonium salts were removed by dialysis.

Precipitation by organic solvents, such as acetone, accounts for about 35% of the precipitation schemes conducted by researchers.[61] The general explanation is that the addition of a water-soluble organic solvent reduces the dielectric constant of the solution and increases the interaction between the proteins' charged groups on the surface, thus leading to agglomeration and precipitation. The organic solvents were generally added to the solution cold, around -20–0 °C, in order to prevent inactivation and denaturing of the enzymes. The precipitated proteins were pelletized by centrifugation and resuspended in buffer after the acetone was removed.

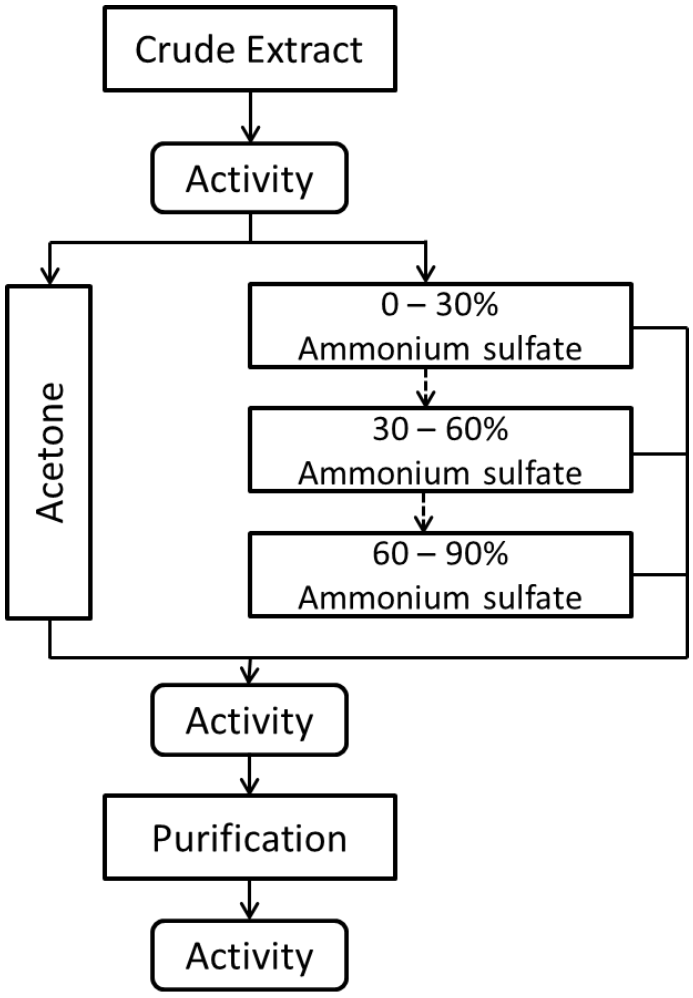


**Figure 15.** Precipitation schemes of recombinant lipase

The overall precipitation process is shown in Figure 15. Ammonium sulfate was ground to a fine powder and slowly added to half of the crude extract, which was at a moderate mixing speed. After each fraction was completed, the solution was left to mix for 1 h and then centrifuged at 13,000 x g for 10 min. The supernatant was transferred to another container and the pellet was resuspended with buffer at one-tenth the volume of crude extract. This procedure was repeated with the supernatant for the next fractions. The resuspended pellet was placed inside dialysis tubing with a 3.5–5 kDa molecular weight cut off (MWCO). The tubing was

closed tightly and placed in a large container (1–2 L) of the corresponding buffer for 12–16 h, with one buffer change.

The other half of the crude extract was used for acetone precipitation. The acetone was chilled to -20°C and added slowly to the extract at a 4:1 volume ratio and left for 12–16 h at 4°C to precipitate out. Afterward, the mixture was centrifuged at 13,000 x g for 10 min to pelletize the protein. Acetone was decanted out and the pellet was left open which allowed the residual acetone to mostly evaporate. The same volume of cold acetone was added and the solution was vortexed and left for 1 h. Then the protein was re-pelleted and the acetone was removed and evaporated. The pellet was then resuspended in one-fifth the volume of the crude extract.

The samples collected were analyzed using the well-known pH-stat method, which was generally used to determine lipase activity.[62] The pH-stat titrator consists of an autoburette, pH electrode, and propeller stirrer that connect to a computer to run the titration program, record results, and perform calculations of lipase activity. There were several commonly available TAG substrates used to determine lipase, such as triolein, tributyrin, and triocatanoin. Tributyrin was selected in this research because of its cost.

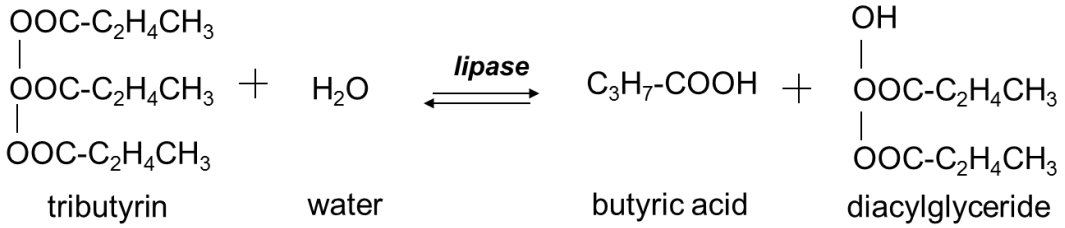


**Figure 16.** Enzyme hydrolysis of tributyrin

The pH-stat method was based on the rate at which the lipase hydrolyzes the tributyrin and forms butyric acid as a byproduct, as shown in Figure 16. The butyric acid was then titrated

by pH-stat with 0.1 N sodium hydroxide (NaOH) in order to maintain the pH at 7.5 for 3–30 min. The consumption of NaOH was recorded as a function of time and was used to determine the tributyrin units per gram enzyme (TBU/g). A TBU was defined as the amount of lipase which release 1 µmol titratable butyric acid per minute at pH 7.5 and 40°C. The activity of a sample was calculated by:

$$Enzyme\ activity\ (TBU/g)\ = \frac{(R2) * (M) * 1000}{W}$$

where R2 is the average titrant rate (mL/min), M is the molarity of the titrant (mol/L), and W is the weight of sample (g).[63] A standard curve was generated with series of different dilutions of T. lanuginosus lipase in an aqueous solution with known activity of 100,000TBU/g, as determined by Sigma-Aldrich, and plotted as TBU vs. R2, details of which are shown in Appendix C. The associated mean slope was used to determine the corresponding enzyme activity of the unknown samples.

The tributyrin assay results of T2 transgenic plants are shown in Table 9. The procedure was also carried out on NT plants (both tobacco and Arabidopsis) as a control and as expected, indicated no activity (data not shown). Although each sample was analyzed twice, the results were inconclusive. As we can see from the table, only the *Arabidopsis* C3-3-1 showed a consecutive activity of 75.8 and 52.1 TBU/g in the crude and 30-60% ammonium sulfate precipitation sample. The problem may have been that the samples were too dilute for an accurate reading on the pH-stat.

**Table 9.** Lipase activity form tributyrin assay

| Sample (TBU/g) | Arabidopsis thaliana | | | | | | | | Tobacco | | | |
|---|---|---|---|---|---|---|---|---|---|---|---|---|
| | C1-1-1 | C2-1-1 | C2-1-2 | C3-1-1 | C3-1-2 | C3-2-1 | C3-3-1 | C3-3-1 | B1-1-1 | B1-7-1 | B1-7-2 | B2-2-4 |
| **Crude** | 0 | 86.3 | 0 | 0 | 183 | 0 | 75.8 | 0 | 0 | 68.6 | 0 | 0 |
| **Acetone** | 0 | 0 | 0 | 0 | 0 | 0 | 0 | 0 | 0 | 0 | 0 | 0 |
| **0-30 %** | 0 | 0 | 0 | 0 | 0 | 0 | 0 | 0 | 0 | 0 | 0 | 0 |
| **30-60%** | 0 | 0 | 0 | 0 | 0 | 0 | 52.1 | 0 | 0 | 0 | 0 | 0 |
| **60-90%** | 0 | 0 | 0 | 0 | 0 | 0 | 0 | 0 | 0 | 0 | 0 | 0 |
| **Purified** | 0 | 0 | 0 | 0 | 0 | 0 | 0 | 0 | 0 | 0 | 0 | 0 |

The problems associated with detection and activity of the lipase could be due to several factors. Plant cells are very complex in comparison to bacteria or yeasts. Therefore, even though the transgene has been transcribed by the plant, it may not be properly translated by the ribosome.[63] Alternatively, the plant cell may have proteases or other mechanisms to break down and destroy the foreign protein after translation. There could have been problems with the extraction from the green tissue. Proteases, phenolic compounds, and secondary metabolites can interact, inactivate, or denature the recombinant protein. Lastly, Hey and Zhang (2012)[64] also had problems in purifying proteins (antibodies) from green leafy tissue using Protein A affinity chromatography. This was because green tissue contains large quantities of ribulose-1,5-biohosphate carboxylase oxygenase (RuBisCO), which is involved in carbon fixation. One of the RuBisCO sub-units has a molecular weight of 55 KDa, which is close to the expected size of recombinant lipase, 61 KDa. This RuBisCO sub-unit was in the elution samples of Hey and Zhang, and detected in the SDS-PAGE gels as well. Therefore, the resulting band in the control sample could mask any trace band of lipase from the transgenic plants.

## 2.4 Conclusions

In this chapter, we have genetically engineered plants to constitutively express a lipase for biodiesel production from spent oils and non-edible plant oils. The genes of lipase with known trans-/esterification activity was cloned from *Thermomyces lanuginosus* and *Candida antarctica*. Cloning involved isolation of total RNA and genome DNA, reverse transcription of mRNA to cDNA, and PCR amplification of lipase gene using specific primers. Three lipase constructs were designed for gene fusion on the C-terminus: (1) entire CDS with signal peptide; (2) deletion of the signal peptide; and (3) addition of the Kozak sequence after signal peptide removal. The gene was inserted into a cloning vector (pCR8/GW/TOPO) and sequenced to confirm its identity. Each of the gene constructs were then inserted into *Agrobacterium*-compatible plant destination vectors via LR Clonase reaction: pGWB408 which fuses a 6xHis tag, and pMDC83 which fuses GFP and a 6xHis tag. *Agrobacterium tumefaciens* (strain GV3101) was used to transform genes into *Nicotiana tabacum* (tobacco) by *Agrobacterium*-mediated transformation and into *Arabidopsis thaliana* by floral dip method. The transgenic plants were screened using selection media and PCR.

Extraction and purification of the transgenic lipases proved to be more complex and difficult. Green plant tissue contains a myriad of phenolic compounds and secondary metabolites which can interact and deactivate recombinant proteins. Several extraction and purification methods were employed and analyzed by SDS-PAGE and tributyrin assay. The results showed no conclusive evidence for enzymatic activity or presence of lipase. However, there were positive indications that the transgene was being expressed within the transgenic plants.

In this research, we showed a proof-of-concept that a lipase gene with high trans/-esterification can be cloned from microbial sources, genetically transformed into plant host, and

over-expressed. Although we were unable to successfully purify the enzyme, we did demonstrate a method to develop an inexpensive biocatalyst for biofuel production that had not previously been attempted. The use of plant expression system could grant us the versatility and almost unlimited scalability that cannot accomplished by other expression systems.

# CHAPTER 3

# HYDRODEOXYGENATION OF BIODIESEL TO GREEN DIESEL VIA CO/-MO CATALYSTS

## 3.1. Introduction

The enhancement of biodiesel fuel properties by modifying/optimizing fatty ester composition is an issue of nascent and ongoing research. Methods for upgradation of biodiesel can be broadly classified into physical and chemical methods.[65] Physical upgrading methods include char removal, hot vapor filtration, solvent addition, and extraction of organic acids. Chemical upgrading methods include catalytic hydrodeoxygenation process (HDO), hydrothermal liquefaction, Ficsher-Tropsch synthesis (F–T synthesis), and super-critical modification. Currently, catalytic hydrodeoxygenation process for converting biodiesel into renewable petrodiesel-like fuels substitutes is gaining considerable importance.[65,66]

Hydrodeoxygenation is the process of increasing the energy value of the oil by the removal of oxygen as water.[66] The first review on hydrodeoxygenation process was published by Edward Furimsky in 1983.[67] In that paper, several works on hydrodeoxygenation of coal-derived liquids (CDLs) were studied and noted. However, due to limited information on various aspects of HDO process available at that time, some conclusions had to be based on the assumptions and/or on the information extrapolated from hydrodesulphurization and hydrodenitrogenation processes. Also from that time, numerous studies on the hydrodeoxygenation of CDLs, oil shale liquids and bio-oils were conducted and published. Moreover, phenol had been widely used as a model compound in hydrodeoxygenation research

for its simple structure.[68] Currently a database of the experimental results can now be accessed and used to clarify several issues in HDO process, such as effects of the catalyst type and feed composition, processing conditions, etc.

In recent years, the HDO process was drawing attention in upgradation of bio-oils into fuel to solve energy issues. Typical feedstocks in such research were local vegetable oils with high energy content, such as soybean oil, sunflower oil, palm oil, and Camelina oil.[65, 69] Since most of these vegetable oils are edible, it can also lead to the "food vs. fuel" problem introduced in Chapter 1. In 2013, Liu et al.[70] studied Ru and Pt catalysts supported on SBA15 in hydrodeoxygenation of Jatropha oil, a non-edible oil, and achieved a final yield of 98%. However, there is no compatible production of Jatropha oil, which limits its application in the industry.[66] Biodiesel based on waste cooking oil is a good potential for the hydrodeoxygenation feedstock. However, to the best of the author's knowledge, there is limit research being done to upgrade biodiesel by hydrodeoxygenation process.

Oxygen content of the biofuels plays a major role in assessing the fuel properties.[71] The high oxygen content of biodiesel (up to 50 wt%) has adverse effects, such as low heating value, thermal and chemical instabilities, corrosivity, immiscibility with fossil fuels, and increase in a tendency towards polymerization.[72] During the HDO process, oxygen is removed in the form of water at an elevated temperature and pressure, and unsaturated bonds in the fatty acid chains of the biodiesel can also be saturated. HDO products of biodiesel are petrodiesel-like paraffins characterized by a desired viscosity and lubricity, low or no oxygen content, high cetane numbers, enhanced atomization, and good low-temperature properties, which is also known as "green diesel."[65] Additionally, the green diesel formed via the HDO route even exhibits improved properties compared to conventional fossil fuels due to its high cetane number.[71]

It has been reported that during the HDO process, deoxygenation of fatty acid esters can follow three different reaction pathways, based on the carbon number of produced paraffins and the kinds of light gas byproduct,—*hydrodeoxygenation*, *decarbonylation* and *decarboxylation*.[65, 66] The rate of the hydrodeoxygenation reaction and its mechanism are influenced by the nature of feedstock and catalysts used.[65] Oxygen removal includes C=O bond hydrogenation, C-O bond rupture and C-C bond cleavage. Larger hydrocarbons are selectively formed in the presence of a catalyst, which can cause C=O bond hydrogenation, C-O bond cleavage inhibiting, and C-C bond breaking. Additionally, these paraffins can be hydrocracked into shorter-chain alkanes under the high temperature and hydrogen pressure. It was also reported by Filho and Brodzki (1993)[73] that the paraffin formed by hydrodeoxygenation pathway (typically marked with C18) could be isomerized under the high temperature, leading to a better low-temperature properties. The possible pathways during the HDO process are shown in Figure 17.

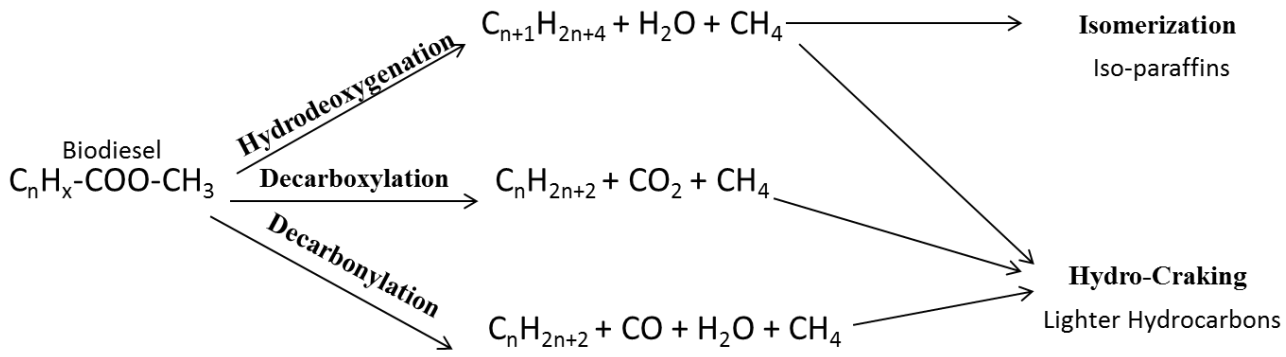


**Figure 17.** The possible pathways in HDO process. In the methyl oleate case, n = 17 and x = 33. In the commercial biodiesel case, n is the mixture of 15 and 17. And $C_{17}H_xCOOCH_3$ is also the major component of the commercial biodiesel produced from soybean oil, which can reach as high as 85 vol%.

The commonly used catalysts in the hydrodeoxygenation process are supported noble and sulfide or reduced metal catalysts.[66] Compared to a high valued noble metal catalyst, supported

sulfide or reduced metal catalysts, such as Pd, Ni, Co and Mo, are much more favorable. In previous study, supported sulfide metal catalysts such as sulfide $CoMo/Al_2O_3$ and sulfide $NiMo/Al_2O_3$ were widely applied in the HDO process for their high activity and good selectivity.[66] However, the formation of sulfur-contaminated products and the reduction of the catalysts in the low-sulfur reactant limit the application of sulfide catalyst in the industry.[74] Also in more recent works by Zou et al. (2012) [75], water produced during the HDO process was reported to have a significant inhibit effect on the sulfide catalyst. According to that study, 2.5 MPa partial pressure of water can lead to the loss of two-thirds initial activity of a sulfide $NiMo/Al_2O_3$ in 60 h HDO process. Therefore, more attention must be devoted to developing non-sulfided transition metal catalysts, such as the reduced molybdenum.

In this chapter, the activities of four supported reduced molybdenum catalysts ($Mo/Al_2O_3$, $Co\text{-}Mo/Al_2O_3$, Mo/Zeolite, and Co-Mo/Zeolite), which were prepared by the thermal decomposition of ammonium heptamolybdate in the hydrodeoxygenation of biodiesel were studied. The effects of two feedstock sources (methyl oleate and commercial biodiesel B100), five pretreatment temperatures (250, 300, 350, 400, and 450°C), four hydrogen flow rates (20, 30, 40 and 60 mL/min), and five reaction temperatures (250, 300, 350, 400, and 450°C) were investigated to find the optimal conditions of hydrodeoxygenation of biodiesel via these catalysts. The effect of cobalt as a promoter for the reduced molybdenum catalyst was also studied. Additionally, the activities of Co/-Mo catalysts with different supports (γ-alumina and Y-zeolite) as well as the commercial CoMo catalyst (Harshaw CoMo catalyst) were compared to get an idea of function of supports.

## 3.2. Literature Review

### 3.2.1 Properties of Biodiesel versus Green Diesel

Biodiesel, as mentioned in Chapter 1, is defined as the alkyl esters of vegetable oils or animal fats, designated B100 as formulated in the biodiesel standard ASTM D6751. The major component of biodiesel is the straight-chain fatty acid profile, which corresponds to the parent oil or fat it is obtained from, dominating its major physical properties. Typically, the most common biodiesel contains 18 carbon atoms, while the second common one contains 16 carbon atoms.[6] There are also some biodiesels that contain significant amounts of fatty acid chains other than the typical C16 and C18 acids. Such biodiesels produced from feedstocks include tropical oils, such as coconut oil, enriched in shorter-chain acids**.** Table 10 shows the fuel property data of some common FAMEs.

**Table 10.** Properties of major components of biodiesel (FAME)

| Compound | Cetane Number | Kinematic Viscosity[a] (40 °C; $mm^2/s$) | Melting Point[b] (°C) | Oxidative Stability[c] (h) |
|---|---|---|---|---|
| **methyl decanoate** | 51.6 | 1.71 | -13.48 | >24 |
| **methyl laurate** | 66.7 | 2.43 | 4.30 | >24 |
| **methyl palmitate** | 81.9 | 4.38 | 28.48 | >24 |
| **methyl stearate** | 101 | 5.85 | 37.66 | >24 |
| **methyl oleate** | 59.3 | 4.51 | -20.21 | 2.79 |
| **methyl linoleate** | 38.2 | 3.65 | -43.09 | 0.94 |
| **methyl linolenate** | 22.7 | 3.14 | -55 | 0.00 |
| **methyl erucate** | 74.2 | 7.33 | -3.05 | - |

a. All kinematic viscosity data from Ref. [76].
b. All melting point data in this column from Ref. [77].
c. Data in this column from Ref. [78]. Data obtained by EN 14112 (Rancimat) test.

The cetane number of biodiesel depends on carbon chain length and degree of unsaturation.[72, 79] The presence of polyunsaturated fatty esters is the cause of oxidative stability problems with biodiesel and the presence of higher amounts of saturated fatty esters is the cause

of cold flow problems, which can be exemplified by the data of methyl stearate and methyl linoleate.

Green diesel, sometimes also called renewable diesel, is used to descript the petrodiesel-like fuels derived from biological sources.[71] Usually the green diesel is a mixture of long straight-chain alkanes and some shorter-chain and isomerized species. Table 11 shows the property data of some main compounds in green diesels. From this table we can find that the cetane number of green diesel is high (> 70), and the low-temperature performance and lubricity are improved. Moreover, according to the study of Aatola et al. (2008)[80], the isomerized compounds in green diesel showed better low-temperature performance than that of long straight-chain compounds. The cloud point (CP) of isomerized compound investigated for exhaust emissions testing was given as 7°C, while the CP of petrodiesel was usually stated to be between -5 and -25°C.

**Table 11** Properties of major components of green diesel

| Compound | Cetane Number | Kinematic Viscosity[a] (40 °C; $mm^2/s$) | Melting Point[b] (°C) |
|---|---|---|---|
| **Dodecane** | 80 | 1.46 | -9.57 |
| **Hexadecane** | 100 | 2.93 | -18.12 |
| **Heptadecane** | 105 | 3.01 | -22.0 |
| **Octadecane** | 110 | 3.45 | -28.2 |

a. All kinematic viscosity data from Ref. [76].
b. All melting point data in this column from Ref. [77].

Green diesel was also reported to have a lower flash point, which is a reflection of the boiling points of the individual components.[71] For example, the boiling point of methyl palmitate is 417 °C and that of methyl decanoate is 224 °C, while that of hexadecane is 287 °C and that of decane is 174 °C. This lower flash point can benefit the performance of engine when dealing with green diesel.

It is also of interest to assess the effect of individual components of biodiesel and green diesel, as well as the petrodiesel, on regulated exhaust emissions, which are nitrogen oxides ($NO_x$), particulate matter (PM), hydrocarbons (HC) and carbon monoxide (CO). Work was done by Knothe et al. (2006)[81] with a 2003 model year engine (14 L, six-cylinder, turbo-charged, intercooled, and exhaust gas recycling) showed that both the green diesel and biodiesel have better exhaust emissions performance than petrol diesel. When compared to petrodiesel, biodiesel has a PM reduction of 73–83%, while the green diesel's PM reduction is 45–50%. In the nitrogen oxides case, compared to petrodiesel, $NO_x$ exhaust emissions were increased by 12.5% using methyl soyate, about 6% with technical grade methyl oleate and slightly reduced (4–5%) with the saturated esters methyl palmitate and methyl laurate, while the green diesels have a reduction of 15 - 16%. This worked is depicted in more detail in Figure 18.

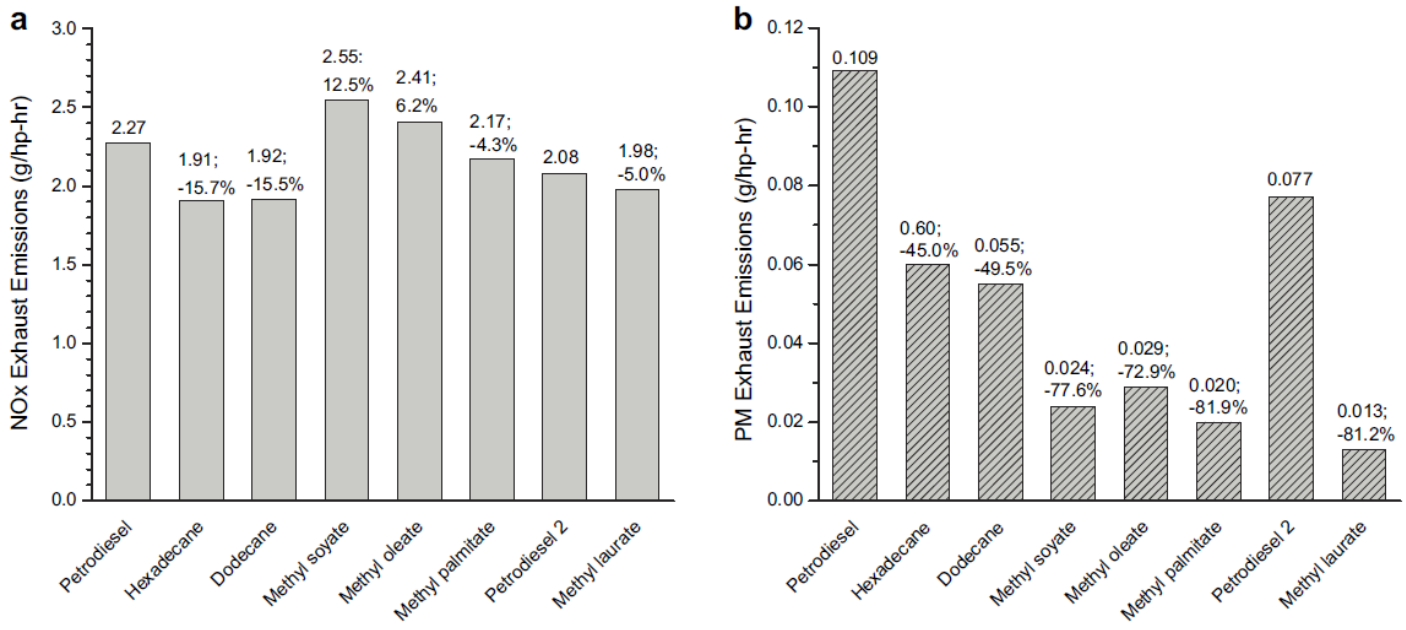


**Figure 18.** NOx and PM exhaust emissions of petrodiesel, biodiesel and some neat components. (3.1.a is $NO_x$ emissions, and 3.1.b is PM emissions). The inscribed numbers show the level of these exhaust emission species and the numbers in parentheses indicate fuel consumption changes for the other fuels relative to petrodiesel. Petrodiesel 2 refers to a second test of the petrodiesel reference fuel relating only to methyl laurate due to a new turbocharger on the test engine.[81]

Other studies also proved that green diesel has a HC emission reduction of 0–25% and CO emission reduction of 28–50% versus petrodiesel, while biodiesel has an HC emission reduction of 30–54% and CO emission reduction of 15–25% versus petrodiesel.[71] In summary, both biodiesel and green diesel has improved regulated exhaust emissions, and green diesel can do better in $NO_x$ and CO emissions.

3.2.2 Methods for the Production of Green Diesel

Currently, there are many technologies to improved biodiesel to green diesel, such as catalytic cracking, emulsification, steam reforming, super-critical upgradation, gasification-Fischer-Tropsch (gasification-F–T) synthesis, and hydrodeoxygenation (HDO).[65, 71] Of these methods, gasification-F-T synthesis and HDO process are two most promising.

3.2.2.1 Fischer-Tropsch Method

Fischer–Tropsch's (F–T) synthesis is a process developed by Franz Fischer and Hans Tropsch in the 1920s that includes a set of chemical reactions through which a mixture of hydrogen and carbon monoxide (syngas) is converted into long chain liquid hydrocarbons (Figure 19a**)**.[82] Huber, Iborra and Corma (2006)[83] provided to combine this F–T synthesis with a previous biomass gasification step to produce green diesel. During this technology, a raw material of biomass or biodiesel will first be thermochemically transformed into a gaseous mixture ($H_2$ and CO) through a series of chemical reactions with a catalyst, a controlled amount of air and high temperatures (800–900°C or even higher). Then this bio-syngas will be converted into green diesel by a traditional F-T synthesis. The strategy map is shown in Figure 19b.

(a)

$$(2n+1)\,H_2 + n\,CO \xrightarrow[150-300\ ^{o}C]{\text{Catalyst}} C_nH_{2n+2} + n\,H_2O$$

(b)

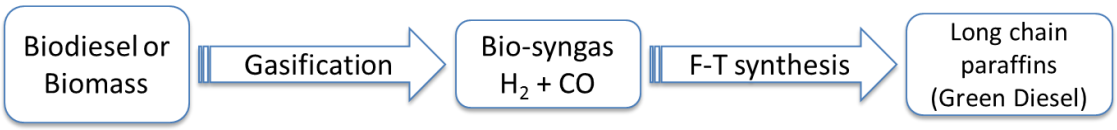


**Figure 19.** Strategy maps of F-T method. (a) Reactions in the F-T step, while n is a positive integer representing the length of the hydrocarbon chain; (b) strategy maps of F-T in green diesel production.

Gasification step usually operates at high temperatures (800–900 ºC or even higher) and regardless of their type and configuration, their operation consists of four steps: drying, pyrolysis/devolatilization, reduction, and combustion.[81] In the drying section, the feedstock biodiesel or biomass is stripped of its moisture content (usually high for raw biomass feedstocks). In the pyrolysis zone, volatiles are removed in the form of light hydrocarbons, CO, and $CO_2$. During this section, some liquid long-chain hydrocarbons are also formed, which is also known as tar. The reduction zone serves as the main process where the raw materials are completely gasified using oxygen from the air and/or steam in order to form the syngas product through a series of endothermic reactions. In this section, catalysts such as cobalt or iron are required. Lastly, in the combustion section, the residual char matrix is further burned producing more gaseous products and the necessary heat for the reactions in the reduction zone. The produced bio-syngas will then be transported into the F–T synthesis section after a cleaning and purification step.

The F–T synthesis process is usually operated in a temperature range of 150–300 ºC and at an elevated pressure of some tens of atmospheres, both of which inhibit the formation of short chain hydrocarbons, such as methane. The chemical conversion of syngas into hydrocarbons is

mostly catalyzed by transition metal-based catalysts, the most common of which being cobalt and iron. Previous studies proved that cobalt catalysts reach their optimal operation at high $H_2$:CO ratios (close to 2), while iron-based catalysts can handle a syngas feed with a lower $H_2$:CO ratio due to their inherent ability to promote the water-gas shift reaction, through which more hydrogen is produced.[84] Additionally, all F–T catalysts are well-known for their sensitivity to sulfur.[85] Thus, a carefully designed desulfurization step prior to the F–T reaction is deemed necessary in order to avoid catalyst poisoning.

The thermochemical transformation of biodiesel or biomass into green diesel through the F–T synthesis route relies on the combination of well-established technologies such as gasification, purification, desulfurization, and subsequent F–T synthesis.[82] The conjunction of multiple processes creates a lucrative new process for biofuels production but at the same time a rather difficult system for process design studies and management. Moreover, the high temperature and pressure required in this process as well as a complicated catalyst system will increase the cost of final green diesel.[82,85] These all limit the application of F–T methods in the laboratory level.

3.2.2.2 Hydrodeoxygenation Method

Hydrodeoxygenation (HDO) is a process by which a feedstock that contains double bonds and oxygen moieties is converted to hydrocarbons by saturation of the double bonds and removal of oxygen into water.[65, 66] The feedstocks of HDO process can be vegetable oil, biodiesel, or other bio-oils obtained from wood and wood residues. Recently, Mohammad and Hari (2013)[65] published a review on the overview of catalytic hydrodeoxygenation to produce paraffin based-biofuels. They illustrated the importance of different feedstocks and their

advantages and disadvantages, as shown in Table 12, and hydrodeoxygenation of bio-oils is reported to be the most suitable method to upgrade bio-oils.

**Table 12.** Comparison between gasification/FT process and HDO method[65]

| Plant Type | Effective Scale Output | Particle Scale Output | Biomass Input |
|---|---|---|---|
| **HDO** | >400 ML | 150-400 ML | 0.2-0.4 Mt/year pongamia oil |
| **G/FT** | >2000 ML | 400ML | 1.8 Mt/year lignocellulose |

Industrialization of the HDO process was first done by Neste Oil in Porvoo, Finland, using vegetable oils as primary feedstock in the 1990s.[86] Although HDO is an efficient method to obtain fuel from bio-based feedstocks, it has not received considerable importance as the petroleum feeds generally contains 98 wt% carbon and hydrogen, 1.8 wt% sulfur, and only 0.1wt% oxygen. Besides the feedstocks, optimization of the catalyst can be the most challenging task. For efficient design of the HDO process, choice of catalyst, optimization of reaction temperature, hydrogen pressure and catalyst loading is highly essential. And information on the supply-demand structure for the diesel substitute products in a local community and process economics are also mandatory for the commercialization of the HDO process. The next few sections will introduce the hydrodeoxygenation process in detail.

3.2.3 Mechanism of Hydrodeoxygenation

The aim of the hydrodeoxygenation process is to upgrade bio-oils by removing the oxygen content as water. Previous study proved the rate of the HDO reaction and its mechanism are influenced by the nature of feedstocks used.[65] Oxygen removal includes C=O bond hydrogenation, C-O bond rupture, and C-C bond cleavage, and larger hydrocarbons are

selectively formed in the presence of a catalyst, which can cause C=O bond hydrogenation, C-O bond cleavage inhibiting, and C-C bond breaking. Generally, this removal of oxygen during the HDO process can follow three different reaction pathways, based on the carbon number of produced paraffins and the kinds of light gas byproduct, —*hydrodeoxygenation (HDO)*, *decarbonylation (DCO)* and *decarboxylation (DCO$_2$)* which is shown in Figure 17. The hydrodeoxygenation pathway results in the formation of hydrocarbons with chains of the same number of carbons with the feedstock, along with water and methane. Decarbonylation/ decarboxylation pathway produces paraffin with one carbon less than that of the corresponding fatty acid and liberates $CO_2$ or CO.

A proposed reaction network for the hydrodeoxygenation of palm oil was brought by Srifa *et al*. (2015)[87], (Figure 20). Four monometallic catalysts (Co, Ni, Pd, and Pt) supported on γ-$Al_2O_3$ were tested, and the result reaction network is similar to that of oleic acid. Firstly, the double bonds in palm oil were hydrogenated to saturated triglycerides, and subsequently cleaved to stearic acid via a hydrolgenolysis process. In the HDO pathway, the stearic acid could react to yield alcohols, and subsequently hydrocarbons with byproduct water. While in $DCO_2$ and DCO pathways, stearic acid would first be transformed into intermediate octadecanal via a hydrogenation process, and subsequently transformed into hydrocarbons with byproducts $CO_2$ and CO, respectively. Moreover, they proved that the rate limiting step of the $DCO_2$ and DCO pathways for the production of green diesel by palm oil is the low equilibrium concentrations of intermediate octadecanal, the amount of which is mainly dominated by the availability of oxygen vacancy sites of the catalyst. Toba et al. (2011)[88] got a similar conclusion on the hydrodeoxygenation of sunflower oil over sulfide NiMo and CoMo catalysts supported on γ-

$Al_2O_3$. However, to the best of author's knowledge, there is no research being done on the reaction network for hydrodeoxygenation of biodiesel.

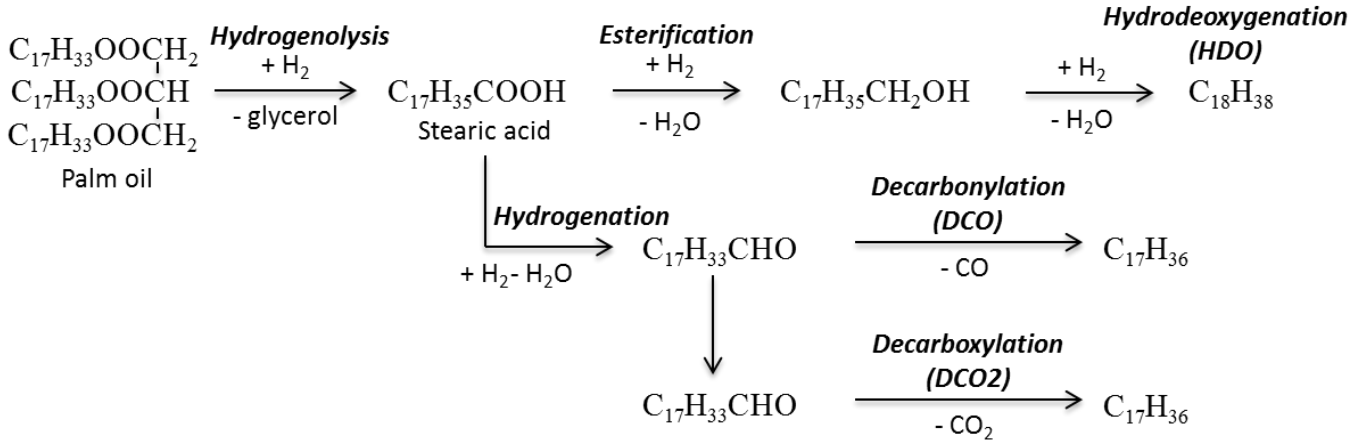


**Figure 20.** Proposed reaction network for hydrodeoxygenation of palm oil.[87]

Additionally, the n-paraffins produced from hydrodeoxygenation can be isomerized into iso-paraffins, which results in a far lower freezing point and a higher cetane number.[65, 71] The decarbonylation/decarboxylation pathway can only produce n-alkanes, which was characterized with high cetane number but poor cold properties. Thus, the hydrodeoxygenation pathway is preferred in the upgradation of bio-oils. In the case of biodiesel upgradation, currently the common commercial biodiesel are based on the soybean oil, of which the fatty acid chain contains carbon number of 18. The green diesel produced by hydrodeoxygenation pathway also has the carbon number of 18, while product of the decarbonylation/decarboxylation pathway has the carbon number of 17. In the biodiesel upgradation research, the mass ratio of C18 product divided by C17 product is usually applied to compare the selectivity of HDO catalysts.

Studies by Prasad and Bakhshi (1985)[89] showed that the routes in HDO process depend on the reaction temperature, hydrogen pressure, liquid hourly space velocity, and most importantly, the catalyst used. The choice of catalyst is complicated and explained below.

### 3.2.4 Catalysts for Hydrodeoxygenation

#### 3.2.4.1 Sulfide Metal or Reduced Metal

Typically current commonly used catalysts in the hydrodeoxygenation process are supported noble and sulfide or reduced transition metal catalysts.[66, 72] Figure 21 summarizes the reported supported metal catalysts in the hydrodeoxygenation process. Compared to high valued noble metal catalyst, sulfide or reduced metal catalysts are much more favorable.

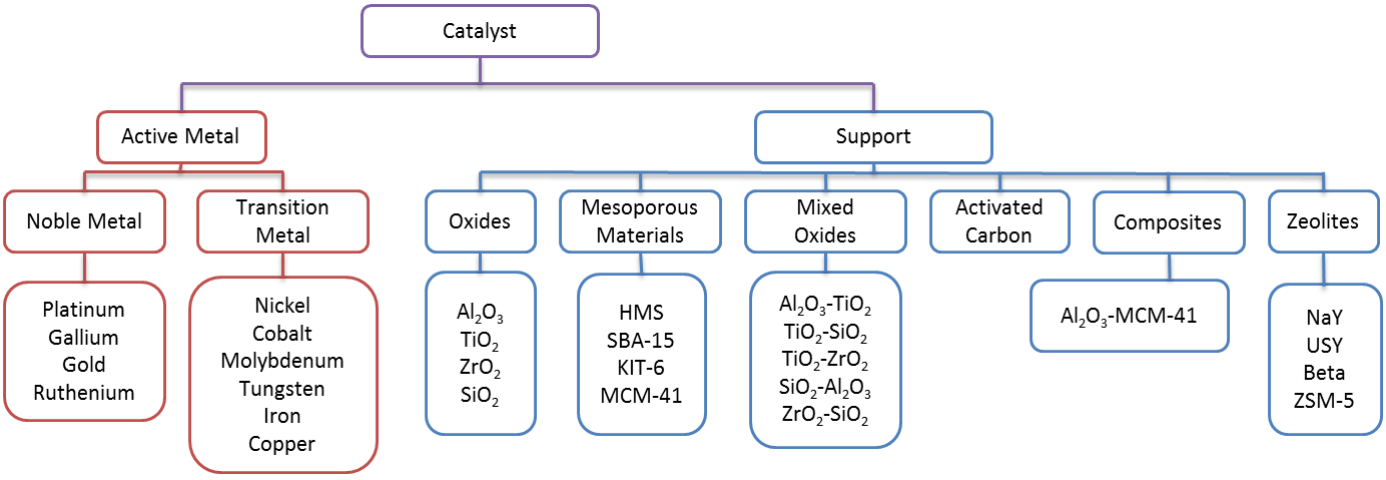


**Figure 21.** Catalyst developments for hydrodeoxygenation process.[66]

Transition metallic sulfides of nickel, cobalt and molybdenum are proven to be efficient catalysts for hydrotreating reactions, such as hydrodesulfurization (C-S), hydrodenitrogenation (C-N), as well as hydrodeoxygenation (C-O).[72] The sulfidation process of catalyst is carried out at high temperature (280–350ºC) using hydrogen sulfide ($H_2S$) or carbon disulfide ($CS_2$). Senol and Viljava (2007)[90] reported that the usage of $H_2S$ as sulfiding agent is more beneficial than $CS_2$ due to decrease in hydrogen consumption and coke formation. The sulfide metal was proved to be efficient in hydrodeoxygenation process by several researchers. Ki *et al*. (2013)[91] reported that a final conversion of 95% can be achieved in the soybean oil into green diesel with the

catalyst Co-Mo sulfide supported on $SiO_2$-$Al_2O_3$. A highest final conversion of 99.99% was also achieved by Anand and Sinha (2012)[92] for jatropha oil into green diesel with the catalyst Co-Mo sulfide on $Al_2O_3$.

Despite the high efficiency of sulfide metal, there are several disadvantages limiting the application in the industry. First, high oxygen (>30 wt%) and low sulfur content (<3 wt%) of the feed (such as biodiesel or vegetable oil) can cause oxidation of the active catalyst phase, thus deactivating the sulfide catalyst, which leads to a short lifetime of the catalyst (<48 h).[72] The second is the high sulfur content in the final green diesel produced with the sulfide catalyst.[65, 71] In the United States, diesel fuel should have less than 15 ppm of sulfur content for transportation usage, which means the green diesel produced with sulfide catalyst requires an additional desulfurization process.[93] Also in more recent studies, water produced during the HDO process was reported to have a significant inhibiting effect on the sulfide catalyst. In Laurent and Delmon's study (1994)[94], 2.5 MPa partial pressure of water can lead to the loss of two-thirds initial activity of a sulfide NiMo/ $Al_2O_3$ in 60 h HDO process. Therefore, more attention must be devoted to developing non-sulfided transition metal catalysts, such as the reduced nickel or molybdenum.

3.2.4.2 Choice of Support

Choice of support is also a key factor for determining the hydrodeoxygenation activity of different catalysts. The most common and conventional support is γ-$Al_2O_3$. γ-$Al_2O_3$, which has many beneficial properties such as low cost, high stability, and most important, moderate/slight acidity which benefits the hydrodeoxygenation pathway in the HDO process.[66, 72] Alternative materials such as $SiO_2$, active carbon, $TiO_2$, $ZrO_2$, $Nb_2O_5$, zeolites and various metal oxides were also used in HDO reactions. Due to the selectivity of pathways, hydrodeoxygenation reactions

have been traditionally carried out using moderate-highly acidic support materials such as oxides of alumina, silica, zirconia; these materials have high ionic potential. One interesting fact about using activated carbon as support is that their activity depends on the preparation method and hence, tailoring of their activity is a possibility.[72] This unique property can make activated carbon a suitable choice as a support material for HDO reactions. Recently Bui et al. (2011)[95] compared the support effects (zirconia, titania, and $Al_2O_3$) for CoMo sulfide catalyst on the hydrodeoxygenation of guaiacol. It was concluded that the performance of zirconia support was better than titania and $\gamma$-$Al_2O_3$ in terms of HDO conversion and product selectivity.

Catalyst design for HDO reactions can be done by altering the host lattice (support) and seeing the influence on the guest metal ion on catalytic activity.[66, 72] When the host lattice changes, the interaction and the co-ordination environment of the guest ion will also change. The primary advantage of using porous support is that the extent of availability of active metal for catalytic reactions can be controlled. Also preparation methods can govern the diffusion limitations to obtain well-distributed metal catalysts.

He and Wang (2012)[96] also proved that support materials which offer intermediate metal-oxygen bond strength are considered to be the best support materials. Strong metal-oxygen bonding causes difficulty in the creation of oxygen vacant sites on the catalyst material to adsorb oxygen containing compounds. Weak metal-oxygen bonding makes the abstraction of oxygen from the feed challenging. Conclusively, moderate to slightly acidic supports such as zeolite, $TiO_2$, $ZrO_2$, and especially $Al_2O_3$, have gained great importance and their usage is highly recommended for hydrodeoxygenation systems.

3.2.4.3 Promoter Effect

Over the past years, cobalt, tungsten and nickel have been used as promoters for catalyst improvement in hydrodeoxygenation reactions.[66] Promoters and supported metal can form bimetallic or multi-metallic catalysts. These bimetallic or multi-metallic catalysts are reported to show better catalytic activity than single-metal catalysts due to two effects: (1) ensemble effect caused by the influence of geometry, and (2) ligand effect due to the influence of electronic interactions, which means promoters can donate ions to the whole catalyst to weaken the metal-oxygen bond increasing the activity of catalyst.[97]

Moreover, promoters can alter the catalyst geometry by increasing the number of stacks. Usage of promoters such as cobalt (Co) and lanthanum (La) were reported to increase selectivity of the catalyst (>90%) towards oxygen free products.[98] Additionally, Romero and Richard (2010)[99] studied the hydrodeoxygenation of 2-ethylphenol using unpromoted Mo/Al2O3, CoMo/Al2O3, and NiMo/Al2O3 catalysts. It was concluded that using promoters increased the deoxygenation rate. Moreover, nickel was reported to promote only hydrogenation, but cobalt promoted both hydrogenation and direct deoxygenation reactions. From their results, it could be seen that the incorporation of active metal and the promoter seems to increase the BET surface area of the support material.

Use of promoters such as boron was also reported to create new Lewis and Bronsted acid sites, increasing the overall acidity of the catalyst material, which benefits the HDO process.[66] The addition of phosphorous also has similar effect as boron. In Lewandowski and Sarbak's research (2000)[100], the presence of boron alters the oxide structure of molybdenum. It helps in increasing the octahedral molybdate density in comparison to tetrahedral $MoO_4^{2-}$ species, thus promoting the activity of the catalyst.

One of the major factors that need to be considered during the choice of promoter is promoter–support interaction. Based on the catalyst activation conditions and the oxidation state of the metal, some promoters (such as Ni) can form strong chemical bond with support (such as $Al_2O_3$) which reduces the activity of the catalyst. The amount of promoter used is also a crucial parameter reported by Ferdous, Dalai and Adjaye (2004).[101] In their study, excess usage of Ni (promoter) can also possibly result in the formation of Ni-γ-$Al_2O_3$ (promoter-support interaction), thus lessening the availability of active sites (Ni-Mo-S) for catalytic reactions.

**3.3. Experimental Section**

3.3.1 Materials and Equipment

Commercial biodiesel B100 (soybean oil based) was purchased from the Diesel Direct Company, Stoughton, MA. Methyl oleate (>98%), HPLC grade 2,2,4-trimethylpentane (iso-octane), ACS grade (>98%) ammonium heptamolybdate, ACS grade ammonium hydroxide solution (28.0-30.0 wt% $NH_3$), (ACS grade (>98%) cobalt nitrate hexahydrate, and ACS grade sodium Y zeolite powder were purchased from the Sigma-Aldrich Company, St. Louis, MO. γ-alumina was purchased from the Davison Chemical Company, Washington D.C. Commercial CoMo and Nickel catalysts were purchased from the Harshaw Chemical Company, Cleveland, OH.

Ultra high purity (>99%) compressed hydrogen gas, compressed helium gas, and compressed air gas were purchased from the Air Gas Company, Dover, NH. The pressure-lock 0.5 mL syringe was purchased from Valco Instruments Company, Baton Rouge, LA. Glass wool was purchased from Acros Organics, Geel, Belgium.

3.3.2 Catalyst Preparation

3.3.2.1 Mo/γ-alumina

15 g of ammonium heptamolybdate was dissolved into 50 mL water and 15 mL ammonium hydroxide solution to form a uniform solution. 25 g of γ-alumina was added into this solution and blanketed under nitrogen gas at room temperature (25ºC) for 24 h. The equilibrated γ-alumina was separated by filtration (Whatman, 90 mm, Cat. No. 1001-090) and then calcined in an oven at 400ºC for 2 h. This calcining procedure thermally decomposed the ammonium heptamolybdate into $MoO_3$ immobilized on γ-$Al_2O_3$. Finally all prepared Mo/γ-$Al_2O_3$ samples were cooled under nitrogen gas and stored at room temperature for future use. The surface area of catalysts was evaluated by the Brunauer-Emmett-Teller method (BET), and the loading of molybdenum was characterized by the X-ray Photoelectron Spectroscopy method (XPS), as described in part 3.3.

3.3.2.2 CoMo/γ-alumina

5 g of cobalt nitrate hexahydrate was dissolved in 40 mL water to form a solution at room temperature (25ºC) and 150 rpm. Then 15 g of Mo/γ-alumina made in part 3.2.1 was added to this solution and blanketed in air at room temperature for 48 h. Finally the solid catalyst was collected by filtration (Whatman, 90 mm, Cat. No. 1001-090) and dried in a vacuum desiccator at room temperature for 24 h. The CoMo/γ-alumina catalyst was characterized by BET and XPS, as described in part 3.3, and then stored at room temperature for future use.

3.3.2.3 Mo/Y-zeolite

15 g of ammonium heptamolybdate was dissolved in 50 mL water and 15 mL ammonium hydroxide solution at room temperature, and 150 rpm. 25 g of sodium Y zeolite powder was added to this solution and blanketed under nitrogen gas at room temperature for 24 h. The equilibrated Y zeolite powder was separated by filtration and then calcined in an oven at 400ºC for 2 h. This calcining procedure resulted in thermal decomposition of the ammonium

heptamolybdate into $MoO_3$ immobilized on Y zeolite. Finally all prepared Mo/Y-zeolite samples were cooled under nitrogen gas and characterized by BET and XPS, as described in part 3.3. The catalyst was then stored at room temperature for future use.

3.3.2.4 CoMo/Y-zeolite

5 g of cobalt nitrate hexahydrate was dissolved in 40 mL water to form a solution. Then 15 g of Mo/Y-zeolite made in part 3.2.1 was added to this solution and blanketed in air at room temperature for 48 h. Finally the solid catalyst was collected by filtration (Whatman, 90 mm, Cat. No. 1001-090) and dried in a vacuum desiccator at room temperature for 24 h. The CoMo/Y-zeolite catalyst was characterized by BET and XPS, as described in part 3.3, and stored at room temperature for future use.

3.3.3 Surface Area and Loading Measurement

All the Co-/Mo catalysts made in section 3.2 were evaluated by BET to determine the surface area and by XPS to determine the loading of molybdenum and cobalt. The details of BET and XPS methods are introduced next, and the results are shown in Table 13.

**Table 13.** Results of BET and XPS

| Catalyst | BET Area ($m^2/g$) | $Mo^{3d}$ wt% (g/g) | $Co^{2p}$ wt% (g/g) |
|---|---|---|---|
| **Mo/γ-alumina** | 204 | 18.7 | - |
| **CoMo/γ-alumina** | 206 | 18.3 | 4.6 |
| **Mo/Y-zeolite** | 112 | 16.6 | - |
| **CoMo/Y-zeolite** | 111 | 16.4 | 3.4 |

3.3.3.1 BET Area Measurement

The BET was determined by $N_2$ adsorption at -195ºC using a Quantasorb analyzer (Quantachrome, model: NOVA 2200E). Nitrogen partial pressure was changed by regulating the flow rate of $N_2$ in a $N_2$/He mixture. The incremental volumes adsorbed were detected by a thermal conductivity detector. The corresponding calibration constant was used to convert peak area to adsorbed $N_2$ volume.

3.3.3.2 XPS Loading Measurement

XPS is a surface-sensitive quantitative spectroscopic technique that measures the elemental composition at the parts per thousand range, empirical formula, chemical state and electronic state of the elements that exist within a material. XPS spectra were obtained by irradiating the sample with a beam of X-rays while simultaneously measuring the kinetic energy and number of electrons that escape from the top 0 to 10 nm of the material being analyzed. Usually XPS requires high vacuum (P ~$10^{-8}$ millibar) or ultra-high vacuum (P < $10^{-9}$ millibar) conditions. The loading of catalysts were calculated with the data for mass of Co and Mo, as well as the total mass tested.

3.3.4 Equipment System Setup and Reaction Procedure

3.3.4.1 Reaction System Setup

Typically, the catalytic HDO process contains three steps: (i), pretreatment of the catalyst by hydrogen gas to reduce $MoO_3$ and/or CoO; (ii), reaction step with biodiesel and hydrogen gas, with samples periodically analyzed by gas chromatography (GC); and (iii), cleaning and drying step of catalyst by inert gas. Based on these steps, an auto-sampling bubbler-reactor system was designed and assembled, as shown in Figure 22.

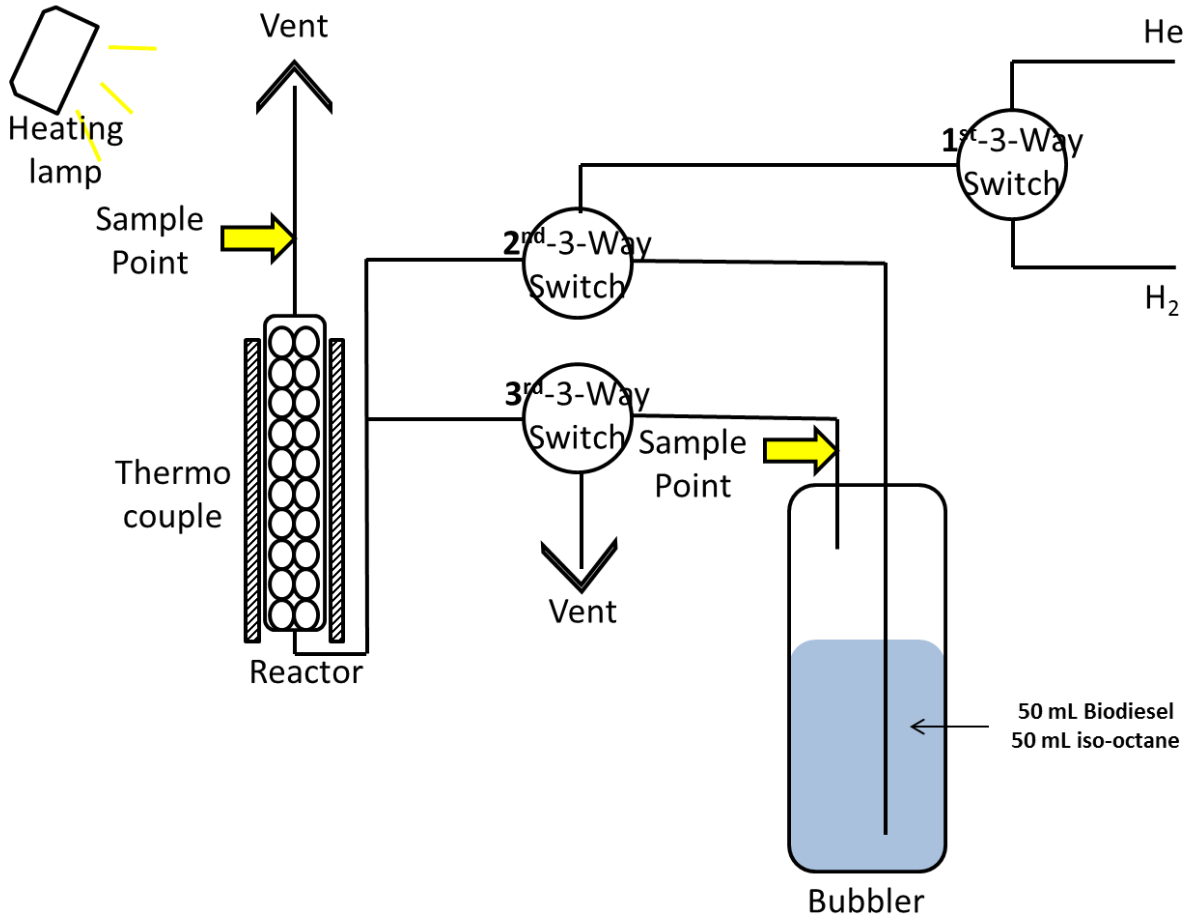


**Figure 22.** Reaction system set up.

The system essentially consisted of a stainless-steel micro-reactor ($\frac{1}{4}\times4\frac{1}{4}$ in.) and a stainless-steel bubbler ($1\frac{1}{4}\times4\frac{1}{4}$ in.) equipped with three 3-way switches that permitted *in situ* pretreatment, reaction, and activity measurement of the catalyst. The lines between the bubbler, the microreactor, and the line downstream of the reactor were stainless-steel coil ($\frac{1}{4}$ in.) wrapped with heating tape to prevent condensation of reactants. There also were heating lamps around the whole system to provide a constant temperature environment. All the sample points were covered with silica septa and the samples were taken by a gas-proof pressure-lock syringe and analyzed by gas chromatography (Hewlett Packard 5890). Typically the reactor was loaded with

0.5 g of catalyst (Co-/Mo alumina, Co-/Mo zeolite, or commercial catalyst) as well as glass wool, and the bubbler was loaded with 50 mL biodiesel or methyl oleate and 50 mL iso-octane. The detail of valves set in every reaction step will be described in the next section.

3.3.4.2 Pretreatment Step

In this step, the first 3-way valve was set to connect the hydrogen gas to the system, and the second valve was set to connect the inlet gas directly to the reactor. The third valve was set to connect the bubbler to the vent, as shown in Figure 23. 60 mL/min of the hydrogen gas flowed through the microreactor to reduce the Co-/Mo catalyst. The temperature of reactor was set at 400ºC and the reaction was carried out for 1 h.

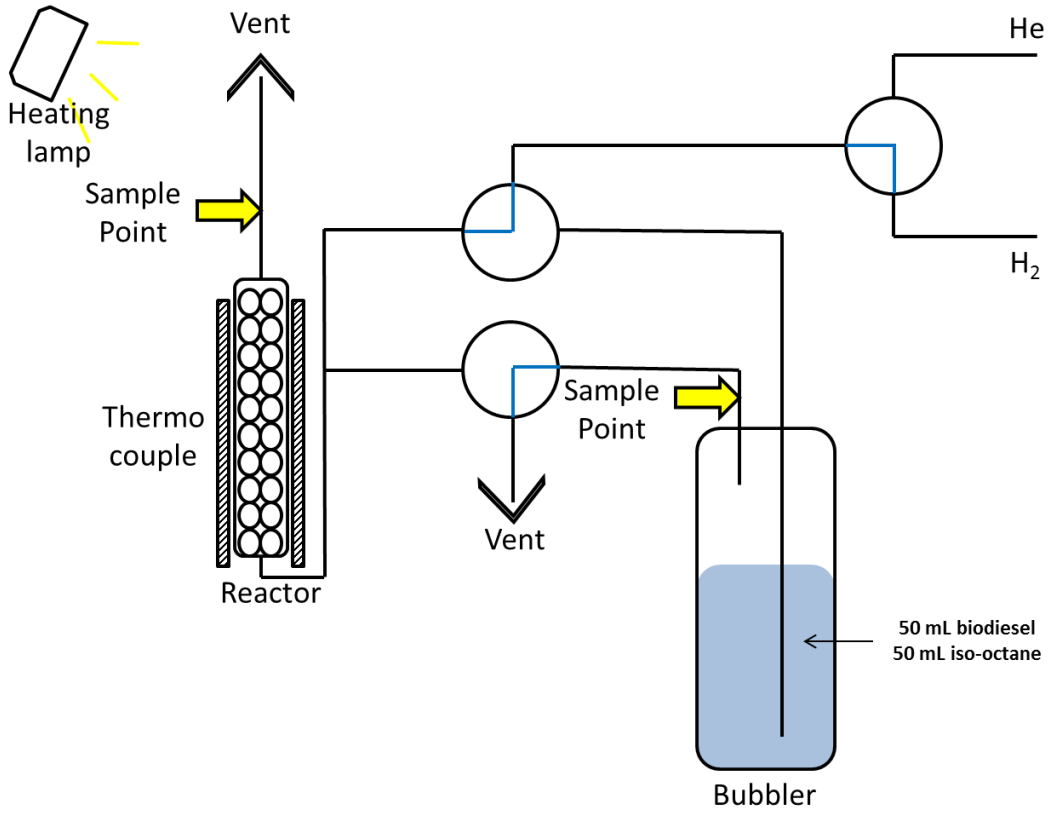


**Figure 23.** Valves set-up for pretreatment step.

3.3.4.3 Reaction Step and Samples Analysis

In this step, the first[t] 3-way valve was set to connect the hydrogen gas to the system, the second valve was set to connect the inlet gas to the bubbler, and the third valve was set to connect the outlet of bubbler to the reactor, as shown in Figure 24. Typically the reactor temperature was set at 400ºC and the hydrogen flow rate was set at 60 mL/min. 0.2 mL of gas sample of the final product was taken by a gas-proof pressure-lock syringe at a reaction time of 90 min. The inlet samples (at outlet of bubbler) of 0.2 mL were also taken before and after the reaction step. All samples were analyzed by gas chromatography (GC. Hewlett Packard 5890, detector: FID).

In the analysis step, helium gas was used as a carrier for the GC and the flow rate was set at 2.52 mL/min. Hydrogen and compressed air were used for the FID, and the flow rates were set at 30.8 mL/min and 300 mL/min, respectively. The injector temperature of GC was 180ºC and the detector temperature was 350ºC. The initial temperature of the GC oven was set at 180ºC, and this temperature was kept for 2 min. Then the oven temperature was increased to 220ºC at a gradient of 10ºC/min. The final temperature of 220ºC was kept for 30 min. The data were transferred to a computer with the help of Peak96. The data files were analyzed by software Origin_8 to calculate the areas of all peaks. With the help of a calibration line (shown in Appendix A), the concentration of initial biodiesel, final biodiesel, C18 green diesel, and C17 green diesel can be calculated from the area results. Finally, the total conversion of biodiesel, green diesel's C18/C17 ratio (for the pathway selectivity) can be calculated from these data, as shown in Appendix B.

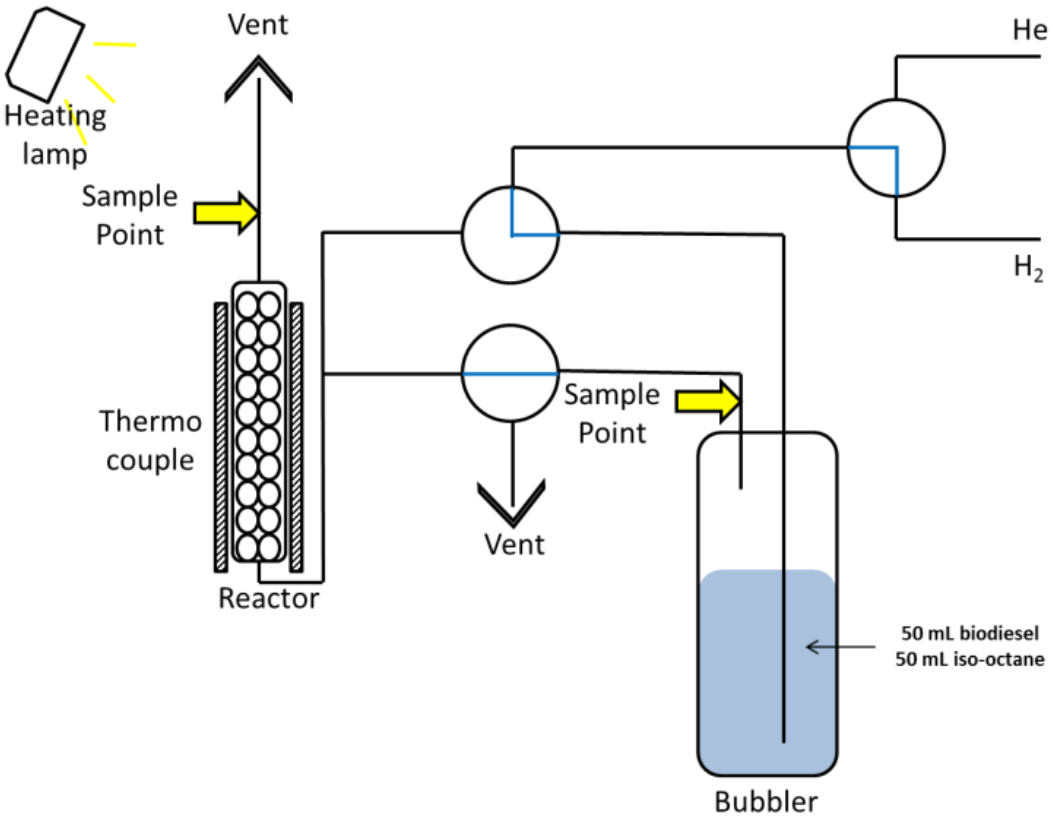


**Figure 24.** Valves set-up for reaction step.

3.3.4.4 Post-Reaction Cleanup Step

In this step, the first 3-way valve was set to connect the helium gas to the system, the second valve was set to connect the inlet gas directly to the reactor, and the third valve was set to connect the bubbler to the vent, as shown in Figure 25. 20 mL/min of helium gas was used to blow out all reactant residues as well as water produced in the reaction. The temperature of reactor was kept at 200ºC; this step lasted for 1 h.

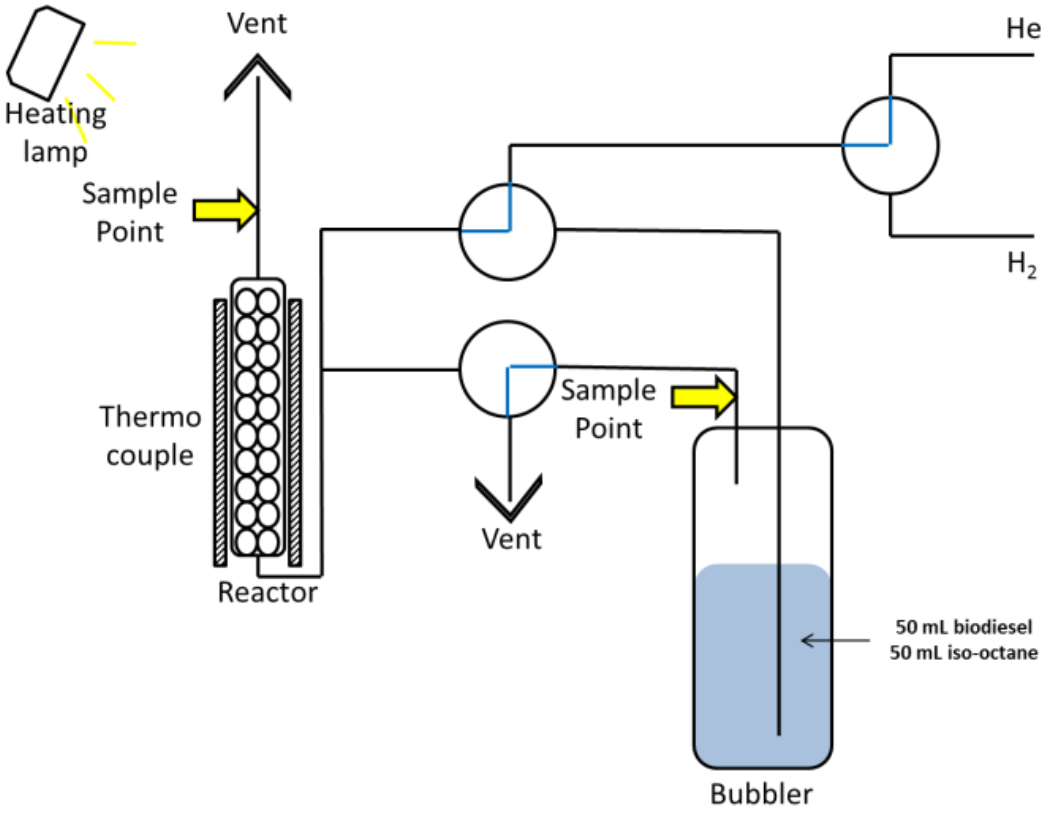


**Figure 25.** Valves set-up for post-reaction cleanup step.

### 3.3.5 Catalysts Activity Investigation

#### 3.3.5.1 Effect of Feedstock

In this experiment, two sources of biodiesel (ACS grade methyl oleate from Sigma-Aldrich and commercial biodiesel B100 from DieselDirect) were investigated. Typically, 50 mL of biodiesel (methyl oleate or commercial biodiesel B100) and 50 mL of isooctane were loaded into the bubbler, and 0.5 g of commercial Harshaw CoMo catalyst was loaded into the reactor. The pretreatment temperature was set at 400ºC and the pretreatment hydrogen flow rate was set at 60 mL/min. The reaction temperature was set at 400ºC and hydrogen flow rate during the reaction step was also set at 60 mL/min. The final product samples were taken at 5 min, 45 min,

and 90 min. Reaction inlet samples were taken before and after the reaction step. Samples were tested by GC and the conversions were calculated.

3.3.5.2 Effect of Pretreatment Temperature

In this experiment, 50 mL of commercial biodiesel B100 and 50 mL of isooctane were loaded into the bubbler, and 0.5 g of hydrodeoxygenation catalyst (Mo/$\gamma$-$Al_2O_3$, CoMo/$\gamma$-$Al_2O_3$, Mo/Y-zeolite, CoMo/Y-zeolite, or commercial Harshaw CoMo catalyst) was loaded into the reactor. Five pretreatment temperatures (250, 300, 350,400, and 450ºC) were investigated. Typically, the pretreatment hydrogen flow rate was set at 60 mL/min, the reaction temperature set at 400ºC, and hydrogen flow rate during the reaction step was also set at 60 mL/min. The final product sample was taken at 90 min. Reaction inlet samples were taken before and after the reaction step. Samples were tested by GC and the conversions (overall conversion, C17 conversion, and C18 conversion) were calculated. Conversions of different pretreatment temperatures were then compared.

3.3.5.3 Effect of Hydrogen Flow Rates

In this experiment, 50 mL of commercial biodiesel B100 and 50 mL of isooctane were loaded into the bubbler, and 0.5 g of CoMo/$\gamma$-$Al_2O_3$ catalyst was loaded into the reactor. The pretreatment temperature was set at 400ºC and the pretreatment hydrogen flow rate was set at 60 mL/min. The reaction temperature was set at 400ºC. Four hydrogen flow rates (20, 30, 40, and 60 mL/min) during the reaction step were investigated. The final product sample was taken at 90 min. Reaction inlet samples were taken before and after the reaction step. Samples were tested by GC and the conversions were calculated. Mass of biodiesel in the inlet sample and conversions of different hydrogen flow rates were then calculated and compared.

3.3.5.4 Effect of Reaction Temperature

In this experiment, 50 mL of commercial biodiesel B100 and 50 mL of isooctane were loaded into the bubbler, and 0.5 g of hydrodeoxygenation catalyst ($Mo/\gamma\text{-}Al_2O_3$, $CoMo/\gamma\text{-}Al_2O_3$, Mo/Y-zeolite, CoMo/Y-zeolite, or commercial Harshaw CoMo catalyst) was loaded into the reactor. Typically, the pretreatment temperature was set at 400ºC, the pretreatment hydrogen flow rate set at 60 mL/min, and the hydrogen flow rate during the reaction step was set at 60 mL/min. Five reaction temperatures (250, 300, 350,400, and 450ºC) were investigated. The final product sample was taken at 90 min. Reaction inlet samples were taken before and after the reaction step. Samples were tested by GC and the conversions were calculated and compared.

3.3.5.5 Continuous Usage of Catalysts

In this experiment, 50 mL of commercial biodiesel B100 and 50 mL of isooctane were loaded into the bubbler, and 0.5 g of catalyst ($Mo/\gamma\text{-}Al_2O_3$ or $CoMo/\gamma\text{-}Al_2O_3$) was loaded into the reactor. The pretreatment temperature was set at 400ºC, the pretreatment hydrogen flow rate set at 60 mL/min, the reaction temperature set at 400ºC, and the hydrogen flow rate during the reaction step was set at 60 mL/min. The final product sample was taken at the reaction time of 60, 120, 180, 240, 300, 360, and 420 min. Reaction inlet samples were taken before and after the reaction step. Samples were tested by GC and the conversions were calculated and compared.

**3.4. Results and Discussions**

3.4.1 Effect of Feedstock

Commercial biodiesel is a complicated mixture of fatty acid methyl esters. Typically the commercial biodiesel based on soybean oil has 49–57 vol% of the component methyl oleate ($C_{17}H_{33}O_2CH_3$), 18–30 vol% methyl linoleate ($C_{17}H_{31}O_2CH_3$), 8–13 vol% methyl palmitate ($C_{15}H_{31}O_2CH_3$), as well as small amounts of methyl stearate ($C_{17}H_{35}O_2CH_3$) and methyl

linolenate ($C_{17}H_{29}O_2CH_3$). Evaluation of commercial biodiesel is usually a complex task, and ACS grade methyl oleate is typically used as the model of biodiesel.

In this research, ACS grade methyl oleate and commercial biodiesel B100 were used to run the hydrodeoxygenation process with the catalyst commercial CoMo catalyst. The use of methyl oleate can verify the function of the assembled bubbler-reactor system, as well as the quality of commercial biodiesel purchased. Moreover, the results of methyl oleate can also determine the products' (C17 and C18 products) retention time in the GC image. The results of overall methyl oleate/biodiesel conversions are shown in Figure 26.

From this result we can find that the overall conversions of methyl oleate and commercial biodiesel are almost the same, with methyl oleate a little higher than commercial biodiesel (60.6% versus 57.5%). Additionally, the C18/C17 ratios of the final product are found to be almost the same (13.93 versus 13.91).This result proves that the commercial biodiesel we used are of high quality and rich with methyl oleate component. The small difference in conversion is probably due to the impurity of commercial biodiesel.

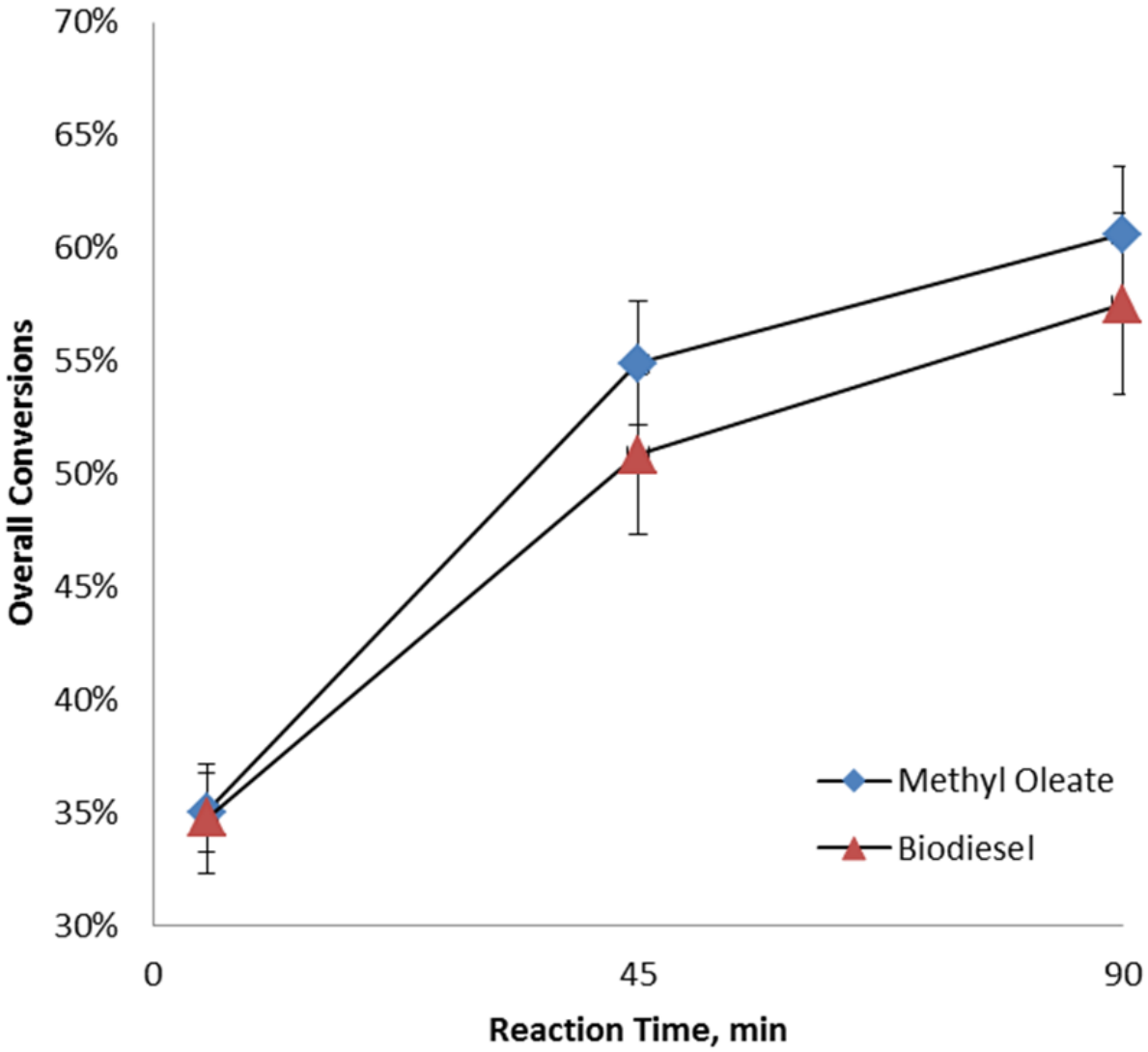


**Figure 26.** Overall methyl oleate/biodiesel conversions (diamond methyl oleate, triangle commercial biodiesel). Catalysts loadings were 0.5±0.007 g, and reduction and reaction temperature was set as 400 °C.

### 3.4.2 Effect of Pretreatment Temperature

Pretreatment is an important step to promote and maintain the activity of the catalyst. In the catalytic HDO process, pretreatment of the catalyst by hydrogen at a certain temperature can reduce the active metal and provide the activity electrons used in further reaction steps. This reduction procedure is mainly affected by the temperature; thus, study of the pretreatment temperature is important and necessary.

In this research, five pretreatment temperatures (250, 300, 350,400, and 450ºC) were investigated in the HDO process with different catalysts. The results of Co-/Mo on γ-alumina are shown in Figure 27, and the results of Co-/Mo on Y-zeolite are shown in Figure 28.

From the results we find that the highest overall conversion for Co-/Mo on γ-alumina and Mo/Y-zeolite was achieved at a pretreatment temperature of 400ºC, while in the CoMo/Y-zeolite case, the conversion with the pretreatment temperature of 350ºC is a little higher than at 400ºC. This is probably due to the nature of the catalyst. The activation energy of the Mo-O-Si component in Y-zeolite supported catalysts is less than that of the Mo-O-Al component in γ-alumina supported catalysts[68], resulting in a lower optimal pretreatment temperature during the reduction reactions. The results of product C18/C17 ratio proved that the pretreatment temperature has no influence on the pathway selectivity of catalysts.

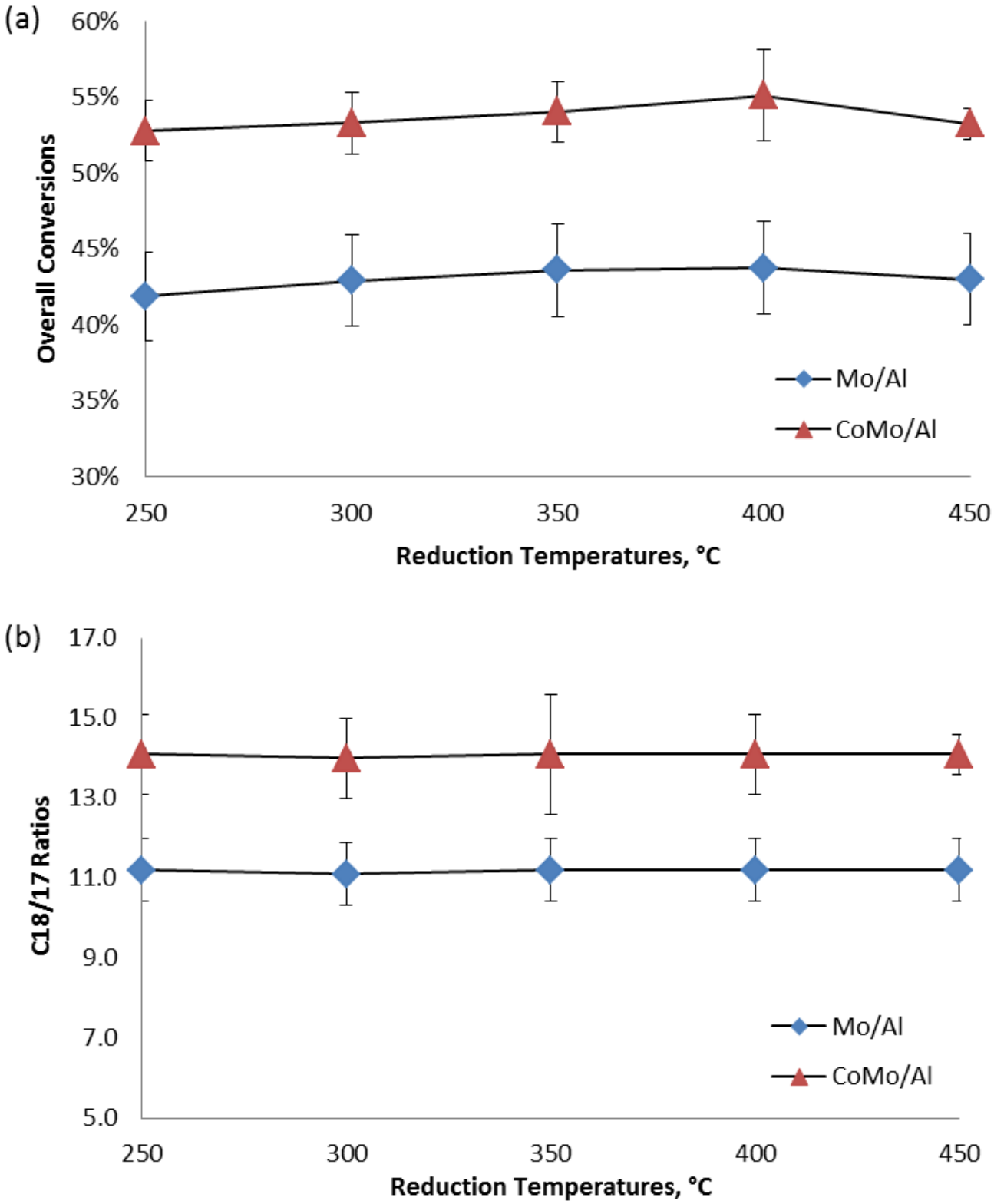


**Figure 27.** Effect of pretreatment temperature with Co-/Mo on γ-alumina (diamond Mo/γ-$Al_2O_3$, triangle CoMo/γ-$Al_2O_3$): (a) overall biodiesel conversion, (b) product C18/C17 ratio. Catalysts loadings were 0.5±0.007 g, and reaction temperature was set as 400 °C.

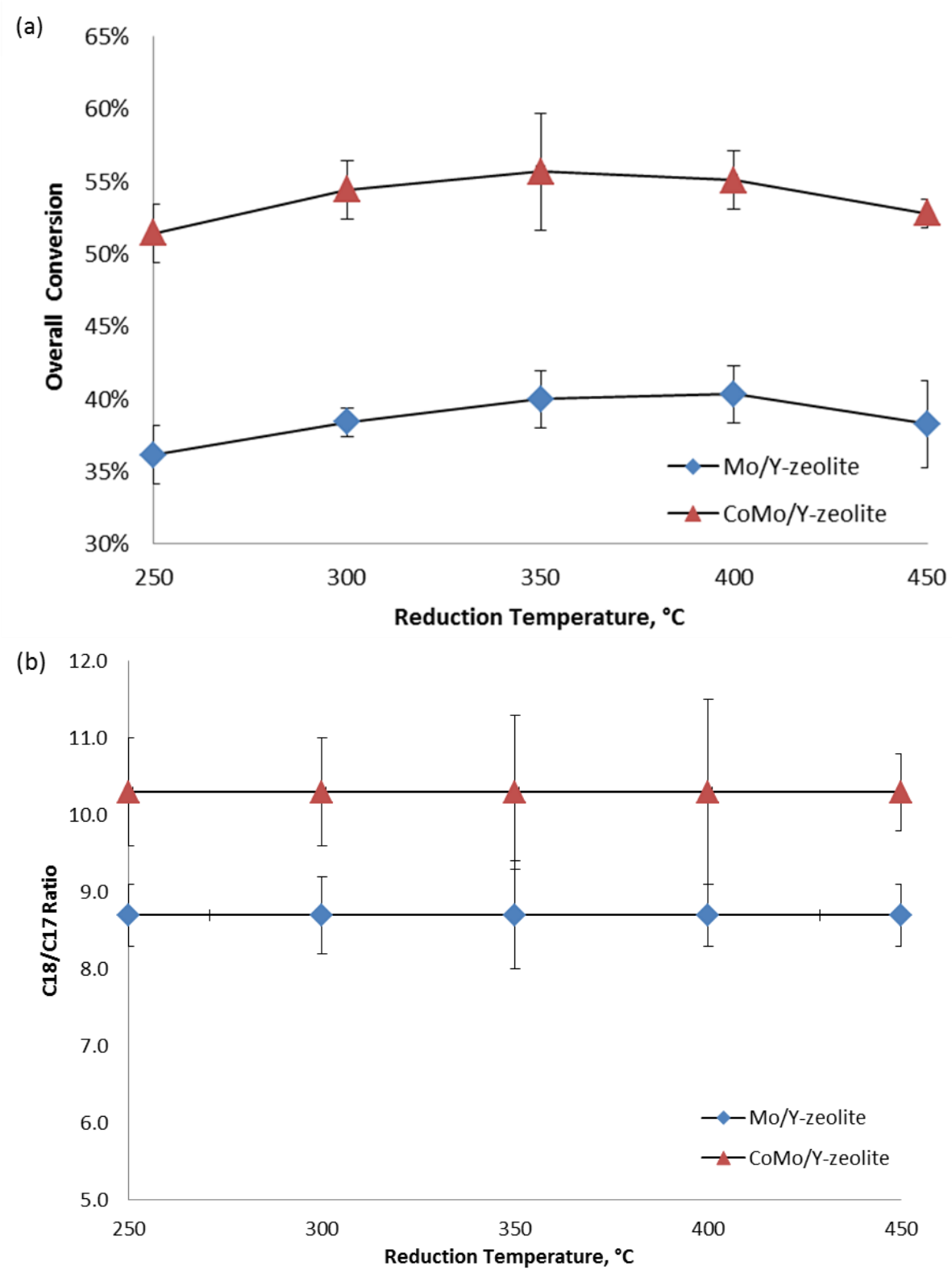


**Figure 28.** Effect of pretreatment temperature with Co-/Mo on Y-zeolite (diamond Mo/Y-zeolite, triangle CoMo/Y-zeolite): (a) overall biodiesel conversion, (b) product C18/C17 ratio. Catalysts loadings were 0.5±0.007 g, and reaction temperature was set as 400 °C.

### 3.4.3 Effect of Hydrogen Flow Rate

Hydrogen pressure plays a key role in hydrodeoxygenation process, especially in overall biodiesel conversion and deoxygenation pathway selection. Additionally, hydrogen gas also works as a carrier gas for biodiesel in the experimental system, so the mass of biodiesel in the system is affected by hydrogen flow rate. In this study, four hydrogen flow rates (20, 30, 40, and 60 mL/min) were investigated with the Mo/$\gamma$-$Al_2O_3$ catalyst. The result of mass of biodiesel input in 2 mL inlet gas sample is shown in Figure 29.

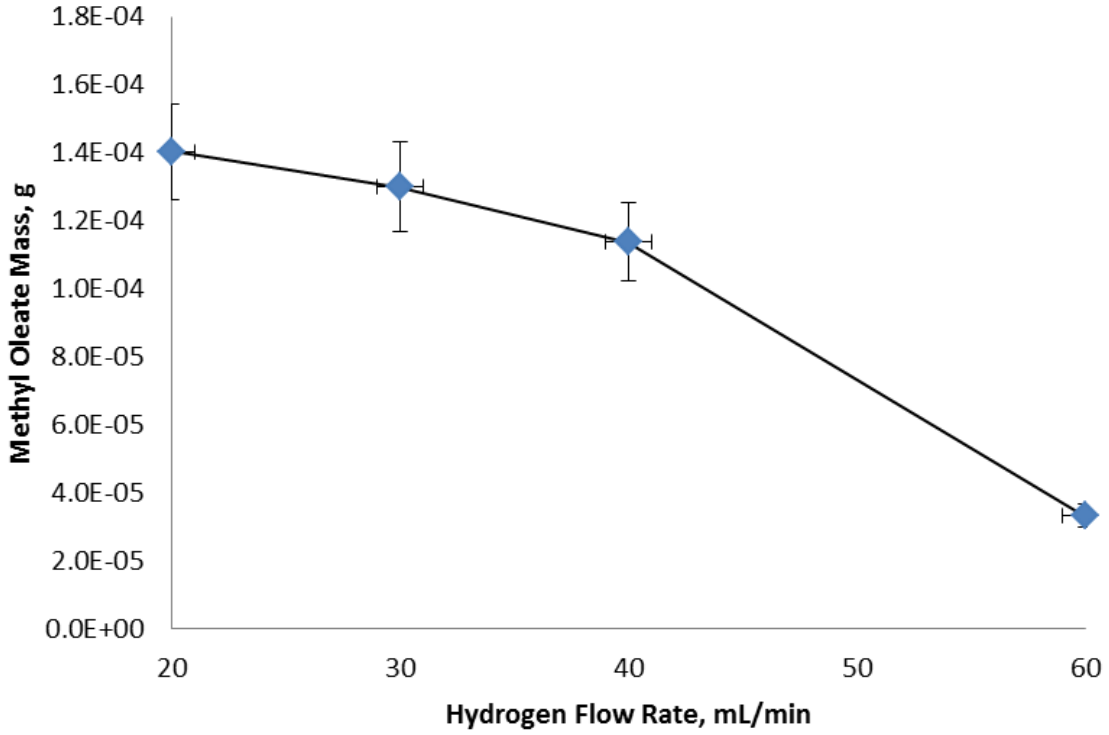


**Figure 29.** Mass of biodiesel input at different hydrogen flow rate. Samples were taken as 2 mL gas by a pressure-proof syringe.

From this data, the hourly volume of oil processed to the volume of catalyst (LHSV) of can be calculated. It is calculated that LHSV of biodiesel decrease from 2.18 $h^{-1}$ to 1.56 $h^{-1}$ when hydrogen flow rate increased from 20 mL/min to 60 mL/min, as shown in Figure 30.

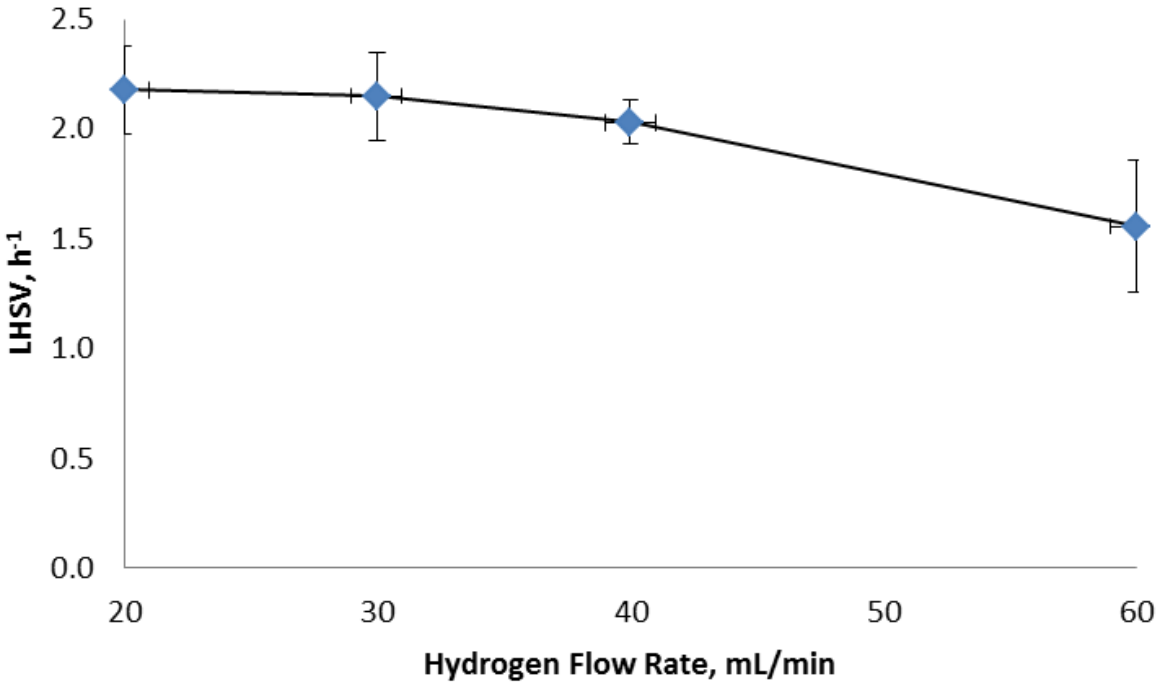


**Figure 30.** LHSV of biodiesel input with different hydrogen flow rate.

Also the overall biodiesel conversions and product C18/C17 ratios with different hydrogen flow rates were determined and are shown in Figure 31**.**

It is clearly found from Figures 29 and 30 that as hydrogen gas flow rate increases, the mass of biodiesel per unit volume of gas decreases, which also means an increase in hydrogen partial pressure. Figure 31a shows that this increased hydrogen pressure can benefit the overall conversion, which increased from 25.7% to 43.7% as the $H_2$ flow rate 20 mL/min to 60 mL/min. There are probably two reasons: (1) because hydrogen is also a carrier gas, higher hydrogen flow rate can produce a higher bulk flow rate that benefits the mass-transfer rate, and (2) the mass of biodiesel per volume of input gas decreases, which results in a higher hydrogen/biodiesel ratio and a higher partial pressure of $H_2$. This benefits the hydrodeoxygenation reaction.

A higher product C18/C17 ratio means that the hydrodeoxygenation pathway also benefits from the higher hydrogen pressure as shown in Figure 31b. The stoichiometry of the reactions indicates that more hydrogen is required in the hydrodeoxygenation pathway than the decarbonylation/decarboxylation pathway. Moreover, from the mechanism of the HDO process, it is clear that more gaseous products are formed in the decarbonylation and decarboxylation pathways, which mean they are more favorable at lower reaction pressures. Thus, higher hydrogen pressure will shift the reaction towards the HDO pathway at the expense of other two pathways. Considering all these benefits, a hydrogen flow rate of 60 mL/min provided the optimal condition and was applied in other experimental runs.

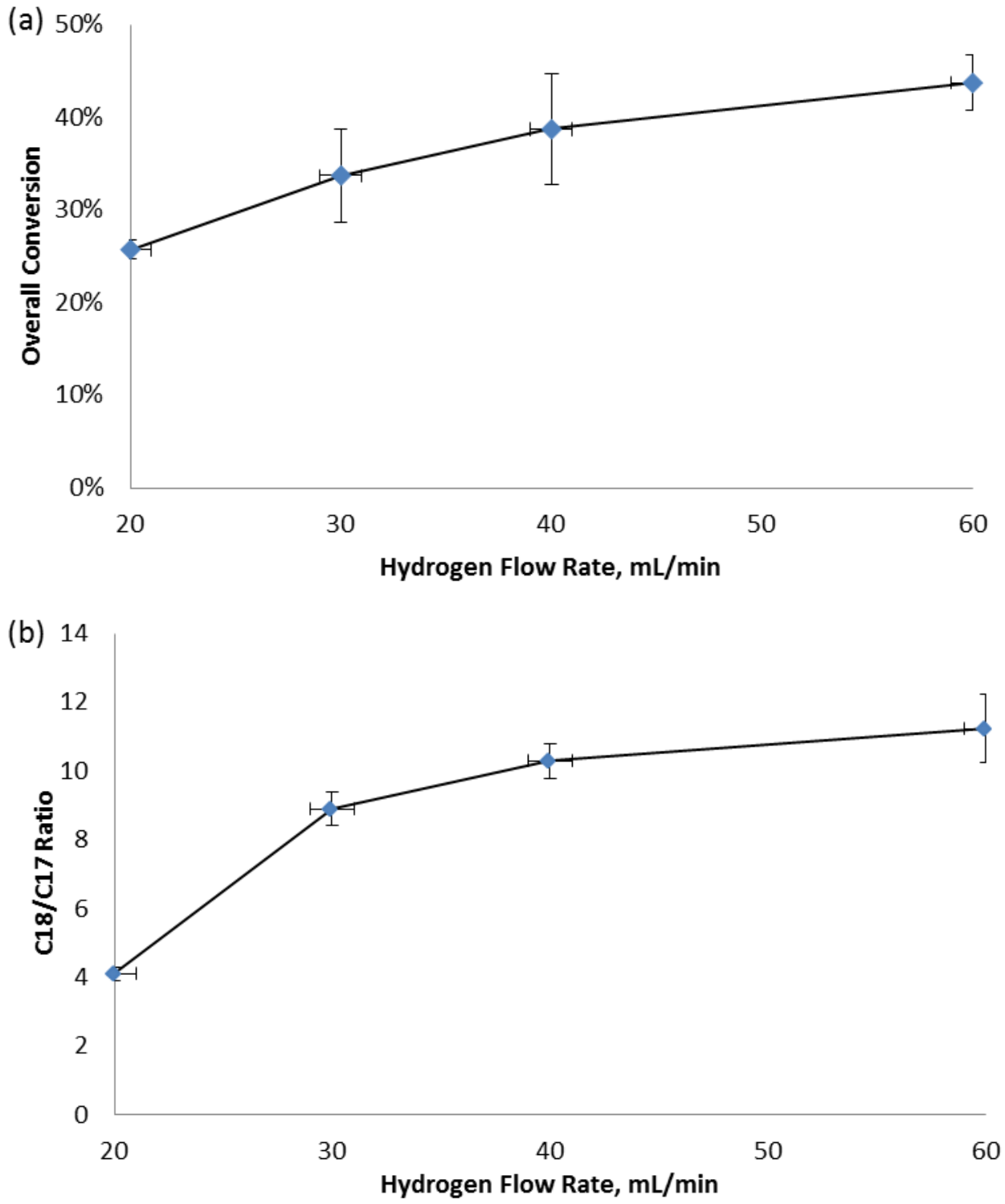


**Figure 31.** Hydrogen pressure effect on HDO process: (a) overall biodiesel conversion, (b) product C18/C17 ratio. Catalysts loadings were 0.5±0.007 g, and reduction and reaction temperature was set as 400 °C.

### 3.4.4 Effect of Reaction Temperature

As indicated in section 4.3, reaction temperature is the most important factor that affects the HDO process and catalyst selectivity. In this study, five reaction temperatures (250, 300, 350,400, and 450ºC) were investigated in the HDO process with different catalysts. The results of Co-/Mo on γ-alumina are shown in Figure 32, and the results of Co-/Mo on Y-zeolite are shown in Figure 33.

From Figures 32a and 33a, the optimal reaction temperature for the HDO process with reduced unpromoted and Co-promoted molybdenum on γ-alumina and Y-zeolite catalyst is 400°C. The main reason is that increase of reaction temperature benefits the reaction rates and equilibrium conversions. Calculation from the stoichiometry of the reactions indicates that the reaction enthalpies (ΔH) of hydrodeoxygenation, decarboxylation, and decarbonylation pathways are 82.5, 31.1, and 72.3 kJ/mol, respectively. Moreover, with increase in temperature, there are more anion vacancies existing in the metal-support component that benefit the reactions.[68] As temperature is increased further, coke formation occurs, which can cover the catalyst's active sites to inhibit the mass-transfer rate and reaction rate. According to Peng et al. (2012)[102], the rate of coke formation significantly increases with temperature increase.

Figures 32b and 33b show that at a temperature of 400°C, the highest product C18/C17 ratio is obtained, which means that temperature of 400°C is the optimal reaction temperature for hydrodeoxygenation of biodiesel. The probably reason is that the rate limiting step of the decarboxylation and decarbonylation pathways for the production of green diesel is the low equilibrium concentrations of intermediate octadecanal ($C_{17}H_{35}CHO$), the amount of which is mainly dominated by the availability of oxygen vacancy sites of the catalyst and limits the overall reaction rates, as introduced in section 3.2.[87] The availability of oxygen vacancy sites of

a catalyst is only dependent on the material used, and not affected by reaction temperature or hydrogen partial pressures. This catalyst-material-dominating limitation means the reaction rates for these two pathways are almost constant and are less promoted by temperature increase than the hydrodeoxygenation pathway, which results in the C18/C17 ratio reaching the highest value when the overall conversion is also the highest. Combining the results of the overall biodiesel conversion and the pathway selectivity, reaction temperature of 400°C is the optimal condition for HDO process catalyzed by Co-/Mo on γ-alumina and Co-/Mo on Y-zeolite. The highest overall biodiesel conversion achieved is 55.8% for CoMo/γ-alumina and 59.3% for CoMo/Y-zeolite.

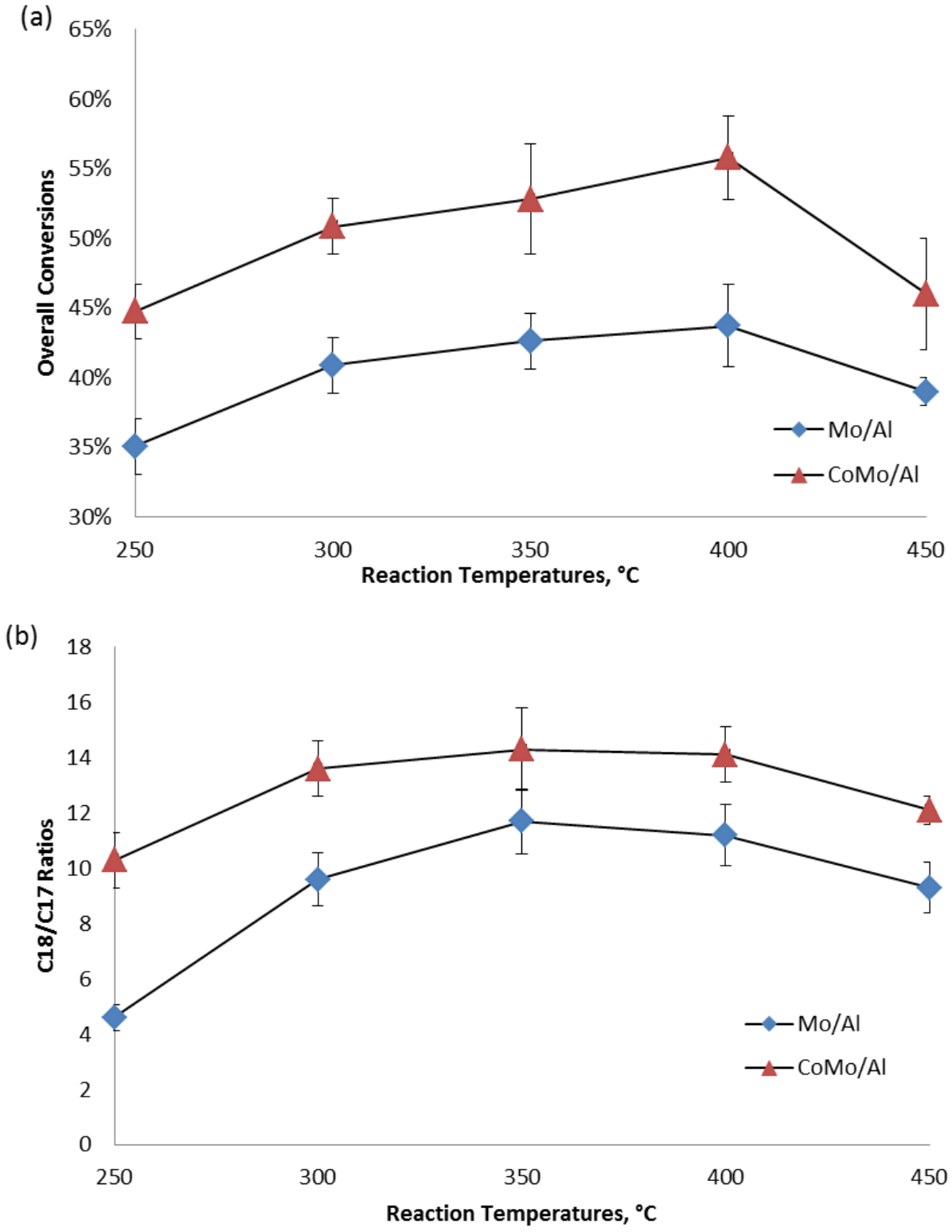


**Figure 32.** Effect of reaction temperatures with Co-/Mo on γ-alumina (diamond Mo/γ-$Al_2O_3$, triangle CoMo/γ-$Al_2O_3$): (a) overall biodiesel conversions, (b) product C18/C17 ratios. Catalysts loadings were 0.5±0.007 g, and reduction temperature was set as 400°C.

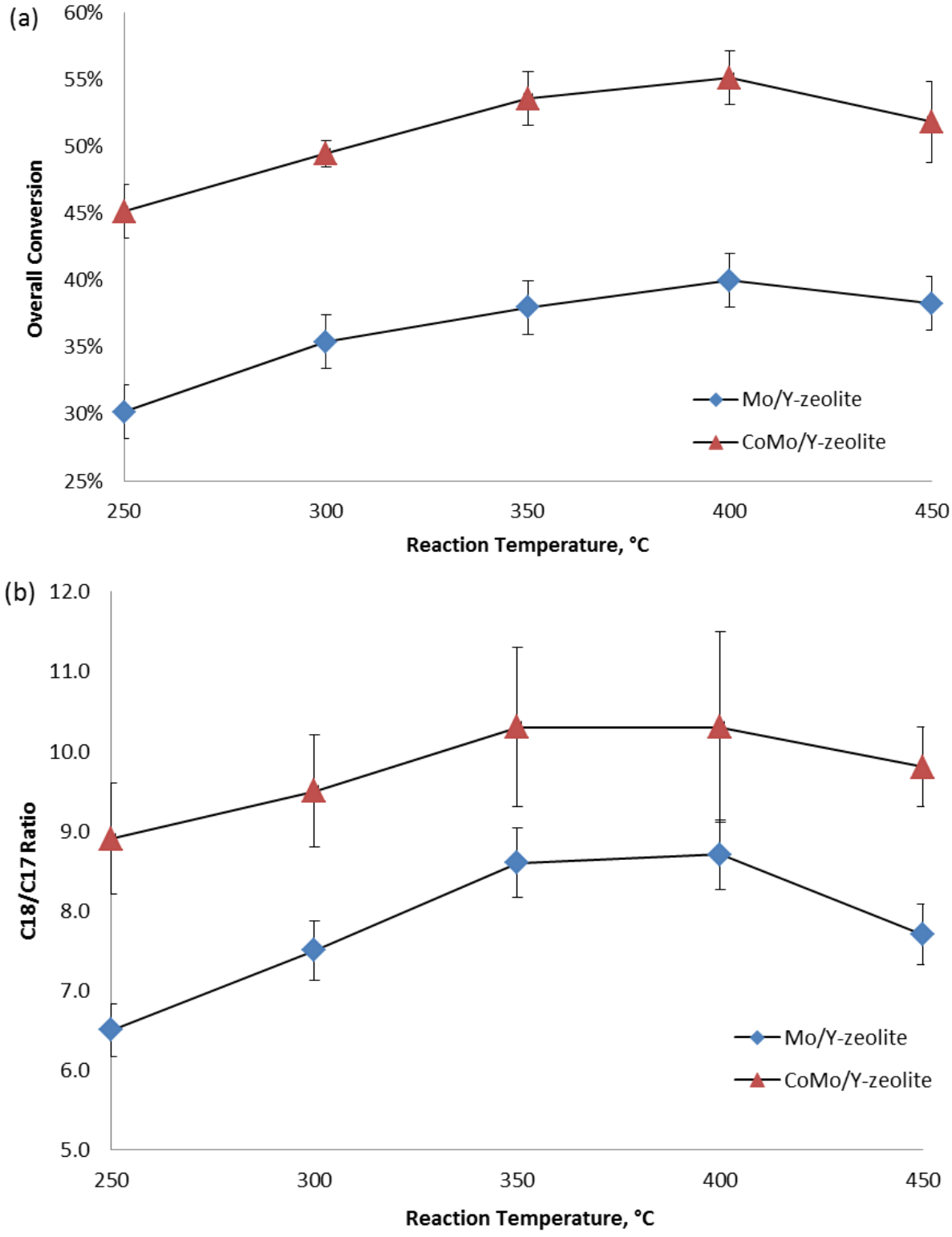


**Figure 33.** Effect of reaction temperature with Co-/Mo on Y-zeolite (diamond Mo/Y-zeolite, triangle CoMo/Y-zeolite): (a) overall biodiesel conversion, (b) product C18/C17 ratio. Catalysts loadings were 0.5±0.007 g, and reduction temperature was set as 400°C.

3.4.5 Effect of Promoters

From the results of section 3.4.2 and 3.4.4, we clearly find cobalt is an effective promoter for reduced molybdenum on γ-alumina and/or Y-zeolite in the hydrodeoxygenation process as well as in pathway selectivity. As introduced in section 3.2, due to two effects: (1) ensemble effect caused by the influence of geometry, and (2) ligand effect due to the influence of electronic interactions, Co working as the promoter can benefit the catalyst activity and selectivity.

Also in this research, an experiment of continuous usage of Mo/γ-$Al_2O_3$ and CoMo/γ-$Al_2O_3$ on HDO process was conducted to investigate the effect of cobalt as promoter on the stability and lifetime of molybdenum catalyst. The result proved that Co as promoter increased the stability of molybdenum catalyst in the HDO process, as shown in Figure 34.

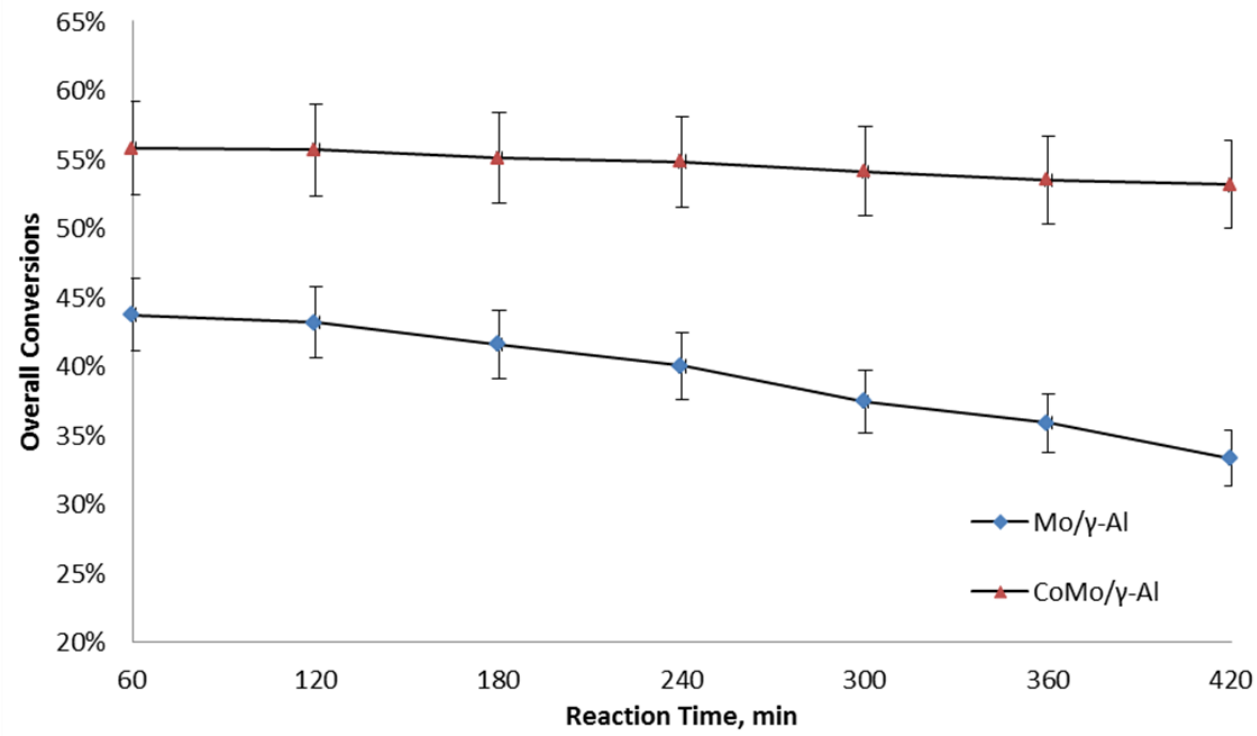


**Figure 34.** Continuous usage of unpromoted and Co-promoted Mo/γ-Al (diamond Mo/γ-Al, triangle CoMo/γ-Al). Catalysts loadings were 0.5±0.007 g, and reduction and reaction temperature was set as 400°C.

3.4.6 Effect of Support

Effect of support was also investigated in this dissertation. The characteristic for two lab-made catalysts, CoMo catalyst (CoMo/γ-alumina and CoMo/Y-zeolite), as well as for the commercial Harshaw CoMo catalyst are shown in Table 14. Results of reactions with these catalysts are shown in Table 15.

**Table 14.** Information of CoMo catalyst on different support

| Support | $MoO_3$, wt% | CoO, wt% | Material | BET area, $m^2/g$ | Packed Shape |
|---|---|---|---|---|---|
| **γ -Alumina** | 18.3 | 4.6 | $Al_2O_3$ | 206 | 1/16 in-Extrudate |
| **Y-Zeolite** | 16.4 | 3.4 | $SiO_2$, $Al_2O_3$ | 111 | Powder |
| **Harshaw** | 15.0 | 3.0 | $Al_2O_3$ | 227 | 1/4 in-Sphere |

**Table 15.** Conversion of biodiesel in different supported catalysts

| Support | Overall Biodiesel Conversion | C18/C17 Ratio |
|---|---|---|
| **γ -Alumina** | 55.8% | 14.1 |
| **Y-Zeolite** | 59.3% | 10.3 |
| **Harshaw** | 66.1% | 13.9 |

The results show that the nature of support material has a significant effect on the HDO activity and especially on pathway selectivity. The CoMo/γ-alumina and Harshaw CoMo on alumina provide better selectivity than CoMo/Y-zeolite. This can be explained by the slight acidity of the γ-alumina support as introduced in section 2.4. We can also find that the overall biodiesel conversion of CoMo/Y-zeolite is a little higher than CoMo/γ-alumina even though its

surface area tested by BET is lower than γ-alumina one. This can be attributed to the difference in particle shape and size. Since CoMo/Y-zeolite is a powder, there is likely less channeling in the reactor compared to γ-alumina.

### 3.5. Conclusions

In this chapter, the activities of four supported reduced molybdenum catalysts ($Mo/Al_2O_3$, $Co\text{-}Mo/Al_2O_3$, Mo/Zeolite, and Co-Mo/Zeolite), which were prepared by the thermal decomposition of ammonium heptamolybdate, in the hydrodeoxygenation of biodiesel were synthesized and characterized. An auto-sampling bubbler-reactor system was designed and assembled. Methyl oleate was used as a model fuel for biodiesel was applied to study the reaction system and provide a comparison with data for commercial biodiesel, B100.

The effects of five pretreatment temperatures (250, 300, 350, 400, and 450 °C), four hydrogen flow rates (20, 30, 40 and 60 mL/min), and five reaction temperatures (250, 300, 350, 400, and 450°C) were investigated to find the optimal conditions of hydrodeoxygenation of biodiesel using different catalysts (Co-/Mo on γ-alumina and Co-/Mo on Y-zeolite). The optimal conditions appear to be a hydrogen flow rate of 60 mL/min, and pretreatment and reaction temperatures of 400°C.The highest overall conversion of biodiesel achieved was 55.8% for CoMo/γ-alumina and 59.3% for CoMo/Y-zeolite.

The effect of cobalt as a promoter for reduced molybdenum catalyst was studied. Continuous usage of Co-/Mo on γ-alumina was also investigated, which proved that the activity, selectivity and stability of CoMo catalyst on HDO processes increased as a result of the promoter. We were able to maintain a relatively high activity of the catalyst for the duration of the experiment, which was 7h.

Factors that affect the catalyst pathway have also been investigated. Higher hydrogen pressure, the presence of a promoter and optimal support, and higher reaction temperature, can lead to a higher C18/C17 ratio, which results in a better green diesel product.

# CHAPTER 4

# SUMMARY

## 4.1 Overview and Conclusions

Worldwide consumption of transportation fuels has increased over the past few decades while petroleum reserves have decreased. Furthermore, climate change and other environmental concerns have led to an urgent need to develop alternative and sustainable fuels, such as biodiesel. Biodiesel is a renewable, non-toxic, and biodegradable alternative fuel with several other desirable characteristic and advantages. Enzymatic production of biodiesel is a promising environmentally-friendly process compared to the current industrial chemical process.

However, there are several technical and economical obstacles in the enzymatic produced biodiesel which significantly affects its commercial viability, such as (i) insufficient availability of large quantities of inexpensive lipase suitable for catalysis, and (ii) bad performance at low temperatures due to its low cetane number. This dissertation has addressed several of these challenges through genetic engineering and hydrodeoxygenation optimization.

In Chapter 2, the challenge of producing large quantities of inexpensive lipase suitable for biodiesel catalysis has been addressed through plant biotechnology and genetic engineering. The genes of lipase with known trans-/esterification activity was cloned from *Thermomyces lanuginosus* and *Candida antarctica*. Cloning involved isolation of total RNA and genome DNA, reverse transcription of mRNA to cDNA, and PCR amplification of lipase gene using specific primers. Three lipase constructs were designed for gene fusion on the C-terminus: (1) entire CDS with signal peptide; (2) deletion of the signal peptide; and (3) addition of the Kozak sequence

after signal peptide removal. The gene was inserted into a cloning vector (pCR8/GW/TOPO) and sequenced to confirm its identity. Each of the gene constructs were then inserted into *Agrobacterium*-compatible plant destination vectors via LR Clonase reaction: pGWB408 which fuses a 6xHis tag, and pMDC83 which fuses GFP and a 6xHis tag. *Agrobacterium tumefaciens* (strain GV3101) was used to transform genes into *Nicotiana tabacum* (tobacco) by *Agrobacterium*-mediated transformation and into *Arabidopsis thaliana* by floral dip method. The transgenic plants were screened using selection media and PCR.

Extraction and purification of the transgenic lipases proved to be more complex and difficult. Green plant tissue contains a myriad of phenolic compounds and secondary metabolites which can interact and deactivate recombinant proteins. Several extraction and purification methods were employed and analyzed by SDS-PAGE and tributyrin assay. The results showed no conclusive evidence for enzymatic activity or presence of lipase. However, there were positive indications that the transgene was being expressed within the transgenic plants.

We showed a proof-of-concept that a lipase gene with high trans/-esterification can be cloned from microbial sources, genetically transformed into a plant host, and over-expressed. Although we were unable to successfully purify the enzyme, we did demonstrate a method to develop an inexpensive biocatalyst for biofuel production that had not previously been attempted. The use of a plant expression system could grant us the versatility and almost unlimited scalability that cannot accomplished by other expression systems.

In Chapter 3, the challenge of the bad performance of biodiesel at low temperatures has been addressed through the hydrodeoxygenation of biodiesel into green diesel. The activities of four supported reduced molybdenum catalysts ($Mo/Al_2O_3$, $Co\text{-}Mo/Al_2O_3$, Mo/Zeolite, and Co-

Mo/Zeolite), which were prepared by the thermal decomposition of ammonium heptamolybdate in the hydrodeoxygenation of biodiesel were synthesized and characterized.

The effects of five pretreatment temperatures (250, 300, 350, 400, and 450°C), four hydrogen flow rates (20, 30, 40 and 60 mL/min), and five reaction temperatures (250, 300, 350, 400, and 450°C) were investigated to find the optimal conditions of hydrodeoxygenation of biodiesel using different catalysts (Co-/Mo on γ-alumina and Co-/Mo on Y-zeolite). The optimal conditions appear to be a hydrogen flow rate of 60 mL/min, and pretreatment and reaction temperatures of 400°C.The highest overall conversion of biodiesel achieved was 55.8% for CoMo/γ-alumina and 59.3% for CoMo/Y-zeolite.

The effect of cobalt as a promoter for reduced molybdenum catalyst was studied. Continuous usage of Co-/Mo on γ-alumina was also investigated, which proved that the activity, selectivity and stability of CoMo catalyst on HDO process increased as a result of the promoter. We were able to maintain a relatively high activity of the catalyst for the duration of the experiment, which was 7h.

Factors that affect the catalyst pathway have also been investigated. Higher hydrogen pressure, the presence of a promoter and optimal support, and higher reaction temperature can lead to a higher C18/C17 ratio, which results in a better green diesel product.

**4.2 Recommendations**

Two recommendations are proposed:

1) Other expression systems to produce recombinant proteins, as stated in Chapter 2, should be examined. In a research environment, it may be more beneficial to use suspended plant cell cultures instead of producing entire lines of transgenic plants. The proteins then can

be tailored to secrete into the medium, which would make extraction and purification much easier and simpler.

2) Other transition metals or noble metals such as W, Ni and Pt can be characterized for the hydrodeoxygenation of biodiesel. As stated in Chapter 3, there are several metals suitable to be applied in the hydrodeoxygenation process, such as tungsten and nickel. Other supports such as activated carbon or mesoporous material MCM-41 can also be tested.

## REFERENCES


1. U.S.A Energy Information Administration, http://www.eia.doe.gov/countries/data.cfm/ (accessed May 4, 2016).
2. Smol J., Climate Change: A Planet in Flux. *Nature* **2012**, 483, 12-15.
3. International Energy Agency, https://www.iea.org/about/faqs/oil/ (accessed Aug 1, 2016).
4. Biodiesel Fact Sheet, http://biodiesel.org/ (accessed May 1, 2016).
5. Meher L., Vidya S., Technical Aspects of Biodiesel Production by Transesterification: A Review. *Renewable and Sustainable Energy Reviews* **2006**, 10(3), 248-268.
6. Vasudevan P., Gagnon M., and Briggs M., Sustainable Biotechnology: Sources of Renewable Energy. *Environmentally Sustainable Biofuels - The Case for Biodiesel, Biobutanol, and Cellulosic Ethanol* **2010**, 2, 102-115.
7. Statistics: The US Biodiesel Industry. http://www.ebb-us.org. (accessed Jun 19, 2015).
8. Biofuel Expansion: Challenges, Risks, and Opportunities for Rural Poor People. United Nations: New York, **2008**.
9. Vasudevan P., Fu B., Environmentally Sustainable Biofuels: Advances in Biodiesel Research. *Waste and Biomass Valorization*. **2010**, 1(1), 47-63.
10. Vicente G., Martinez M., Aracil J., Integrated Biodiesel Production: A Comparison of Different Homogeneous Catalysts Systems. *Bioresource Technology.* **2004**, *92*, 297-305.
11. Nie K., Xie F., Wang, F., Lipase Catalyzed Methanolysis to Produce Biodiesel: Optimization of the Biodiesel Production. *Journal of Molecular Catalysis B: Enzymatic*. **2006**, *43*, 142-147.
12. Gagnon M., Engineering Lipases and Solvents for Trans/-Esterification of Used Vegetable Oils (doctoral Dissertation). University of New Hampshire, **2013**.
13. Vasil, K. A History of Biotechnology: From Cell Theory of Schleiden and Schwann to Biotech Crops, *Plant Cell Rep*. **2008**, 27, 1423-1440.
14. Sijmons P., Dekker B., Schrammeijer B., Christou P., Dale P., Fisher R., Production of Correctly Processed Human Serum Albumin in Transgenic. *Plants. Nature Biology* **1990**, 8, 217-221.
15. Bettini P., Santangelo E., Agrobacterium Rhizogenes RolA Gene Promotes Tolerance to Fusarium Oxysporum F. Sp. Lycopersici in Transgenic Tomato Plants (Solanum Lycopersicum L.) *Journal of Plant Biochemistry and Biotechnology* **2016**, 25(3), 225-233.
16. Macknight R., Laing A., and Bully S., Increasing Ascorbate Levels in Crops to Enhance Human Nutrition and Plant Abiotic Stress Tolerance. *Current Opinion in Biotechnology*, **2017**, 44, 153-160.
17. Rivera, A. L.; Gomez-Lim, M. Physical methods for genetic plant transformation. *Physics of Life Reviews* **2012**, 9(3), 308-345.
18. Klein T. M., Fromm, M., Transfer of Foreign Genes into Intact Maize Cells with High-Velocity Microprojectiles. *Proceedings of the National Academy of Sciences*. **1988**, 85, 12, 4305-4309.
19. Tseng M., Yang M. and Liu C., Plastid Transformation in Cabbage (Brassica Oleracea L. Var. Capitata L.) by the Biolistic Process. *Chloroplast Biotechnology* **2014**, 1132, 355-366.
20. Ribeiro T., Arraes F., Silva M., Lucena M., Macedo L., Artico S., Transgenic Cotton Expressing Cry10Aa Toxin Confers High Resistance to the Cotton Boll Weevil. *Plant*

*Biotechnology Journal* **2017**, 9, 48-56.
21. Roesler K., Shintani D., Targeting of the Arabidopsis Homomeric Acetyl-Coenzyme A Carboxylase to Plastids of Rapeseeds. *Plant Physiology* **1997**, 113(1), 75-81.
22. Karg, S. R.; Kallio, P. T., The Production of Biopharmaceuticals in Plant Systems. *Biotechnology Advances* **2009**, 27 (6), 879-894.
23. Curtis, M. D.; Grossniklaus, U., A Gateway Cloning Vector Set for High-Throughput Functional Analysis of Genes in Plants. *Plant Physiology* **2003**, 133(2), 462-496.
24. Nakagawa, K.; Matsuoka, K., Development of Series of Gateway Binary Vectors, PGWB408, for Realizing Efficient Construction of Fusion Genes for Plant Transformation. *Journal of Bioscience and Bioengineering* **2007**, 104(1), 34-41.
25. Yang Q., Deng M., Zhang L., A Super Twin T-DNA Vector that Allows Independent Gene Expression during Agrobacterium-Mediated Transformation. *Plasmid* **2016**, 87, 58-64.
26. Ye, X., Shen, J., Use of Non-Agrobacterium Bacterial Species for Plant Transformation. **2016**.
27. Moore T., *Lipid Metabolism in Plants*. CRC Press: Bica Raton, **1993**.
28. Bowsher C., Steer M., *Plant Biochemistry*. Garland Science: New York, **2008**.
29. Rangasamy D., Ratledge C., Genetic Enhancement of Fatty Acid Synthesis by Targeting Rat Liver ATP: Citrate Lyase into Plastids of Tobacco. *Plant Physiology* **2000**, 122(4), 1231-1238.
30. Kubala S., Garnczarska M., Wojtyla L., Clippe A., Quinet M., Deciphering Priming-Induced Improvement of Rapeseed (*Brassica napus L.*) Germination through an Integrated Transcriptomic and Proteomic Approach. *Plant Science* **2015**, 231, 94-113.
31. Jako C., Kumar A., Wei Y., Zou J., Barton D., Giblin E., Seed-Specific Over-Expression of an Arabidopsis cDNA Encoding a DIacylglycerol Acyltransferase Enhances Seed Oil Content and Seed Weight. *Plant Physiology* **2001**, 126(2), 861-874.
32. Dianmarca J., Levitan O., Overexpression of a Diacylglycerol Acyltransferase Gene in Phaeodactylum Ttricornutum Directs Carbon Towards Lipid Biosynthesis. *Journal of Phycology* **2017**, 2, 125-133.
33. Zou J., Li Y., Katavic V., Giblin E., Modification of Seed Oil Content and Acyl Composition in the Brassicaceae by Expression of a Yeast Sn-2 Acyltransferase Gene. *The Plant Cell Online* **1997**, 9(6), 909-923.
34. Courchesne N., Parisien A., Enhancement of Lipid Production using Biochemical, Genetic and Transcription Factor Engineering Approaches. *Journal of Biotechnology* **2009**, 141, 2, 31-41.
35. Chen J., Lang C., Antisense PEP Gene Regulates to Ratio of Protein and Lipid Content in Brassica Napus Seeds. *Journal of Agricultural Biotechnology* **1999**, 7(4), 316-320.
36. Kumar V., Sangwan P., Global Scenario of Industrial Enzyme Market. *Industrial Enzymes: Trends, Scope and Relevance*, **2017**.
37. Treichel H., Oliveira D., A Review on Microbial Lipases Production. *Food and Bioprocess Technology* **2010**, 3(2) 182-196.
38. Guruprasad M., Seridevi V., Remash B., A Review on Maize (Zea Mays L.) Transformation for Expression of Insecticidal Proteins. *Crop Research* **2016**, 51, 87-96.
39. Prathumpai W., Lipase production by recombinant strains of Aspergillus niger expressing a lipase-encoding gene from Thermomyces lanuginosus. *Applied Microbiology and Biotechnology* **2004**, 65(6), 714-719.
40. Singh S., Madlala A., Thermomyces lanuginosus: properties of strains and their

hemicellulases. *FEMS Microbiology Reviews* **2003**, 27(1), 3-16.
41. Zhang N., Suen W., Li S., Wei W., Brain S., Improving tolerance of Candida antarctica lipase B towards irreversible thermal inactivation through directed evolution. *Protein Engineering* **2003**, 16(8), 599-605.
42. Zheng Y., Guo X. Song N., Thermophilic lipase from Thermomyces lanuginosus: Gene cloning, expression and characterization. *Journal of Molecular Catalysis B: Enzymatic* **2011**, 69(3), 127-132.
43. Houde A., Kademi A., Leblanc D., Lipases and their industrial applications. *Applied Biochemistry and Biotechnology* **2004**, 118(1), 155-170.
44. Laugesen K., The Novozymes Report 2011: Bagsvaerd **2012**.
45. Demain A., Vaishnav P., Production of recombinant proteins by microbes and higher organisms. *Biotechnology Advances* **2009**, 27(3), 297-306.
46. Sudbery P., The Expression of Recombinant Proteins in yeast. *Current Opinion in Biotechnology* **1996**, 7(5), 517-524.
47. Yin J., Li G., Select what you need: A Comparative Evaluation of the Advantages and Limitations of Frequently Used Expression Systems for Foreign Genes. *Journal of Biotechnology* **2007**, 127(3), 335-347.
48. Matsumoto, T.; Takahashi, S.; Kaieda, M.; Ueda, M.; Tanaka, A.; Fukuda, H.; Kondo, A. Yeast Whole-Cell Biocatalysts Constructed by Intracellular Overproduction of *Rhizopus oryzae* Lipase is Applicable to Biodiesel Fuel Production. *Applied Microbial Technology*. **2001**, 57(4), 515-520.
49. Bouvier-Nave P., Oelkers P., Expression in Yeast and Tobacco of Plant cDNAa Encoding Acyl CoA:Diacylglycerol Acyltransferase. *European Journal of Biochemistry* **2000**, 267(1), 85-96.
50. Gray D., Overview of Protein Expression by Mammalian Cells. *In Current Protocols in Protein Science*, **2001**.
51. Houdebine L., Production of Pharmaceutical Proteins by Transgenic Animals. *Comparative Immunology, Microbiology and Infectious Diseases* **2009**, 32(2), 107-121.
52. Jayapal K., Wlaschin K., Recombinant Protein Therapeutics form CHO Cells. *CHO Consortium: SBE Special Edition* **2007**, 40-47.
53. Xu J., Dolan M., Medrano G., Plants as Bioproduction Platforms for Recombinant Proteins. *Biotechnology Advances* **2012**, 30, 1171-1184.
54. Yin J., Li G., Select what you need: A Comparative Evaluation of the Advantages and Limitations of Frequently Used Expression Systems for Foreign Genes. *Journal of Biotechnology* **2007**, 127(3), 335-347.
55. Rybickl R., Plant-Produced Vaccines: Promise and Reality. *Drug Discovery Today* **2009**, 14(1-2), 16-24.
56. Yang Z., Wang W., Drew D., Mandel U., Engineering Mammalian Mucin-type O-Glycosylation in Plants. *The Journal of Biological Chemistry* **2012,** 44, 58-63.
57. Webster D., Post-Translation Modification of Plant-made Foreign Proteins, Glycosylation and Beyond. *Biotechnology Advances* **2012**, 30(2), 410-418.
58. Mukherjee, K.D. Plant Lipases and Their Application in Lipid Biotransformations. *Progress of Lipid Research* **1994**, 33, 165-74.
59. Basaran P., Plant Molecular Farming: Opportunities and Challenges. *Critical Review in Biotechnology* **2008**, 28, 153-172.
60. DeScenzo R., Minocha S., Modulation of Cellular Polyamines in Tobacco by Transfer and

Expression of Mouse Ornithine Decarboxylase cDNA. *Plant Molecular Biology* **1993**, 22, 113-127.
61. Golker C., Isolation and Purification. *Enzymes in Industry* **2004**, 2, 50-70.
62. Beisson F., Methods for Lipase Detection and Assay: A Critical Review. *European Journal of Lipid Science and Technology* **2000**, 102(2), 133-153.
63. Pierpoint W., The Extraction of Enzymes from Plant Tissues Rich in Phenolic Compounds. *Plant Molecular Biology* **1996**, 5, 69-80.
64. Hey C., Zhang C., Process Development for Antibody Purification from Tobacco by Protein Affinity Chromatography. *Chemical Engineering & Technology* **2012**, 35(1), 142-148.
65. Mohammad M., Hari T., Overview on the production of paraffin based-biofuels via catalytic hydrodeoxygenation. *Review and Sustainable Energy Reviews* **2013**, 22, 121-132.
66. Arun N., Sharma R., Dalai A., Green diesel synthesis by hydrodeoxygenation of bio-based feedstocks: Strategy for catalyst design and development. *Review and Sustainable Energy Reviews* **2015**, 48, 240-255.
67. Furimsky E., Chemistry of Catalytic Hydrodeoxygenation. *Catalysis Reviews* **1983**, 25(3), 421-458.
68. Furimsky E., Catalytic hydrodeoxygenation. *Applied Catalysis A: General* **2000**, 199, 147-190.
69. Lopes D., Neto A., Potential Crops for Biodiesel Production in Brazil: A Review. *World Journal of Agricultural Sciences* **2011**, 7, 206-217.
70. Liu C., Liu J., Zhou G., Tian W., Rong L., A Ceaner Process for Hydrocracking of Jatropha Oil into Green Diesel. *Journal of the Taiwan Institute of Chemical Engineers* **2013**, 44, 221-227.
71. Knothe G., Biodiesel and Renewable Diesel: A Comparison. *Progress in Energy and Combustion Science* **2010**, 36, 364-373.
72. Yakovlev V., Khromora S., Development of New Catalytic Systems for Upgraded Biofuels Production from Bio-Crude-Oil and Biodiesel. *Catalysis Today* **2009**, 144, 362-366.
73. Filho G., Brodzki D., Formation of Alkanes, Alkylcykloalkanes and Alkylbenzenes during the Catalytic Hydrocracking of Vegetable Oils. *Fuel* **1993**, 72, 543-549.
74. Furimsky E., Deactivation of Hydrodeoxygenation Catalysts. *Catalysis Today* **1999**, 381-495.
75. Zuo H., Liu Q., Wang T., Ma L., Zhang Q., Zhang Q., Hydrodeoxygenation of Methyl Palmitate over Supported Ni Catalysts for Diesel-Like Fuel Production. *Energy Fuels* **2012**, 26, 3747-3755.
76. Knothe G., Steidley K., Kinematic Viscosity of Biodiesel Fuel Components and Related Compounds. Influence of Compound Structure and Comparison to Petrodiesel Fuel Components. *Fuel* **2005**, 84, 1059-1065.
77. American Society for Testing and Materials (ASTM) Standard D6751. Standard Specification for Biodiesel Fuel Blend Stock (B100) for Middle Distillate Fuels. West Conshohocken, PA: ASTM, **2010**.
78. European Committee for Standardization. Standard EN 14214. Automotive Fuels: Fatty Acid Methyl Esters (FAME) for Diesel Engines, Requirements and Test Methods.
79. Puckett A., Caudle B., Ignition Qualities of Hydrocarbons in the Diesel-Fuel Boiling Range. *U.S. Bureau of Mines* **1948** [Information Circular No. 7474].

80. Aatola H., Larmi M., Sarjovaara T., Mikkonen S., Hydrotreated Vegetable Oil (HVO) as a Renewable Diesel Fuel: Trade-Off between NOx, Particulate Emission, and Fuel Consumption of a Heavy Duty Engine. In: SAE Technical Paper Series 2008-01-2500, **2008**.
81. Knothe G., Sharp C., Ryan T., Bagby M., Exhaust Emissions of Biodiesel, Petrodiesel, Neat Methyl Esters, and Alkanes in a New Technology Engine. *Energy Fuels* **2006**, 20, 403-408.
82. Damartizs T., Zabazitou A., Thermochemical Conversion of Biomass to Second Generation Biofuels through Integrated Process Design: A Review. *Review and Sustainable Energy Reviews* **2011**, 15, 366-378.
83. Huber G., Iborra A., Corma A., Synthesis of Transportation Fuels from Biomass: Chemistry, Catalysts and Engineering. *Chemical Reviews* **2006**, 106, 4044-4098.
84. Van Steen E., Schulz H., Polymerization Kinetics of the Fischer–Tropsch CO Hydrogentation Using Iron and Cobalt Based Catalysts. *Applied Catalysis A: General* **1999**, 186, 309-320.
85. Kapteijn F., Deugd R., Moulijn J., Fischer–Tropsch Synthesis Using Monolithic Catalysts. *Catalysts Today* **2005**, 105, 350-356.
86. Zeman N., Neste Oil Starts Construction on Europe's Largest Renewable Fuels Plant. *Biodiesel Magazine* **2009**, 13, 15-21.
87. Srifa A., Faungnawakij K., Itthibenchapong V., Assabumrungrat S., Roles of Monometallic Catalysts in Hydrodeoxygenation of Palm Oil to Green Diesel. *Chemical Engineering Journal* **2015**, 278, 249-258.
88. Toba M., Abe Y., Kumamochi H., Osako M., Mochizuki T., Hydrodeoxygenation of Waste Vegetable Oil over Sulfide Catalysts. *Catalysis Today* **2011**, 164, 533-537.
89. Prasad Y., Bakhshi N., Effect of Pretreatment of HZSM-5 Catalyst on its Performance in Canola Oil Upgrading. *Applied Catalysis A: General* **1985**, 18, 71–85.
90. Senol O., Viljava T., Effect of Sulfiding Agents on the Hydrodeoxygenation of Aliphatic Esters on Sulfide Catalysts. *Applied Catalysis A: General* **2007**, 326, 236-244.
91. Ki S., Young J., Hong S., Lee Y., Kim J., Supercritical $CO_2$ Purification of Waste Cooking Oil for High-yield Diesel-like Hydrocarbons via Catalytic Hydrodeoxygenation. *Fuel* **2013**, 111, 510-518.
92. Anand M., Sinha A., Temperature-Dependent Reaction Pathways for the Anomalous Hydrocracking of Triglycerides in the Presence of Sulfided CoMo-Catalyst. *Bioresource Technology* **2012**, 126, 148-155.
93. United States Environmental Protection Agency Act 1990, https://www.epa.gov/laws-regulations/summary-clean-air-act/ (accessed May 1, 2017).
94. Laurent E., Delmon B., Influence of Water in the Deactivation of a Sulfided NiMoγ-$Al_2O_3$ Catalyst during Hydrodeoxygenation. *Journal of Catalysts*. **1994**, 146, 281-290.
95. Bui V., Laurenti D., Delichere P., Geantet C., Hydrodeoxygenation of Guaiacol: Part II: Support Effect for CoMoS Catalysts on HDO Activity and Selectivity. *Applied Catalysis B: Environmental* **2011**,101, 246-255.
96. He Z., Wang X., Hydrodeoxygenation of Model Compounds and Catalytic Systems for Pyrolysis Bio-oils Upgrading. *Catalysis for Sustainable Energy* **2012**, 1, 28-52.
97. Trimm D., Design of Industrial Catalysts. Elsevier Scientific Publishing Company. The Netherlands,1980.

98. Wang W., Yang Y., Luo H., Amorphous Co–Mo–B Catalyst with High Activity for the Hydrodeoxygenation of Bio-oil. *Catalysis Communications* **2011**, 12, 436-440.
99. RomeroY., Richard F., Hydrodeoxygenation of 2-Ethylphenol as a Model Compound of Bio-Crude over Sulfided Mo-Based Catalysts: Promoting Effect and Reaction Mechanism. *Applied Catalysis B: Environmental* **2010**, 98, 213-223.
100. Lewandowski M., Sarbak Z., Effect of Boron addition on Hydrodesulfurization and Hydrodenitrogenation Activity of NiMo/Al2O3 Catalysts. *Fuel* **2000**, 79, 487-495.
101. Ferdous D., Dalai A., Adjaye J., Aseries of $NiMo/Al_2O_3$ Catalysts Containing Boron and Phosphorus PartII. Hydrodenitrogenation and hydrodesulfurization using heavy gas oil Derived from Athabasca Bitumen. *Applied Catalysis A: General* **2004**, 260, 153-162.
102. Peng B., Zhao C., Centeno I., Fuentes G., Jentys A.,Lercher J., Comparison of Kinetics and Reaction Pathways for Hydrodeoxygenation of C3 Alcohols on $Pt/Al_2O_3$. *Catalysis Today* **2012**, 183, 3-9.

# APPENDICES

APPENDIX A: GC CALIBRATION CURVES

APPENDIX B: CALCULATION OF GREEN DIESEL YIELD

APPENDIX C: MANUFACTURER'S PROTOCOLS

APPENDIX D: PH-STAT CALIBRATION

# APPENDIX A

## GC CALIBRATION CURVES

As illustrated in Chapter 3, in this study methyl oleate was selected as the biodiesel standard for GC analysis. *iso*-Octane was selected as dilute solvent to get different concentration of methyl oleate and *iso*-octane solution.

Calibration curves were prepared as follows:

(i) 20 µl methyl oleate was added into 2 ml *iso*-octane to get the "specimen 0"; (ii) After adequate shaking of specimen 0, 0.8 ml mixture was extracted and mixed with 1 ml *iso*-octane to get the "specimen 1"; (iii) 1 ml of mixture specimen 1 was extracted and mixed with 1ml *iso*-octane to get "specimen 2"; (iv) 1 ml of mixture was extracted from specimen 2 and mixed with 1 ml *iso*-octane to get "specimen 3"; (v) 1 ml of mixture was extracted from specimen 3 and mixed with 1 ml *iso*-octane to get "specimen 4."

Except the specimen 0, the mass concentration of specimen 1-4 was calculated by Equation A.1:

$$W_i = \frac{W_{i-1} * m_i}{m_i * (1 - W_{i-1}) + I_i} \qquad \text{(Equation A.2)}$$

$W_i$ (g/g) and $W_{i-1}$ (g/g) is the mass concentration of specimen i and specimen i-1, respectively; $m_i$ (g) is the weight of mixture extracted from specimen i-1; $I_i$ (g) is the weight of *iso*-octane added to the mixture. While concentration of specimen 0 is calculated by weight of methyl oleate divided by added *iso*-octane.

30 µl samples of specimen 1-4 were extracted and test by GC machine. Software *Origin* is used for calculating the area of peaks. Finally, these area values were correlated with the corresponding the mass concentration to the calibration curve as shown in **Figure A.1**. In this study, calibration curve was tested every week with $R^2 > 0.95$.

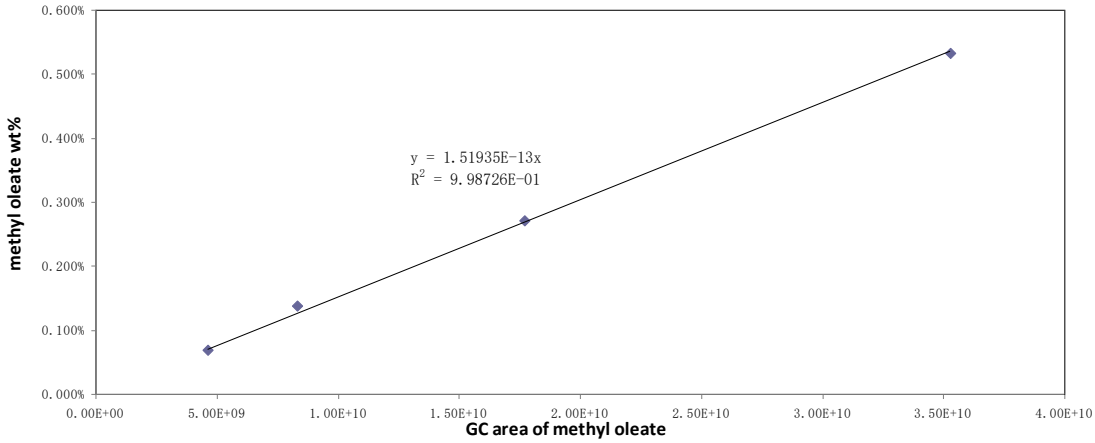


**Figure A.1.** The calibration curve for methyl oleate.

# APPENDIX B

## CALCULATION OF GREEN DIESEL YIELD

As indicated in Chapter 3, 2 mL of gas sample from the bubbler outlet or reactor outlet was injected into the GC via a 10 mL pressure-lock syringe. The resulting curve was designated as FAME inlet and outlet, as well as heptadecane and octadecane outlet. The area of peaks was integrated by *OriginPro*. A sample calculation of green diesel conversion is shown below:

- FAME inlet GC area = $6.29 \times 10^{7}$
- FAME outlet GC area = $2.56 \times 10^{7}$
- Heptadecane GC area = $4.16 \times 10^{6}$
- Octadecane GC area = $1.83 \times 10^{7}$
- Calibration cure slope of FAME = $1.52 \times 10^{-13}$
- Calibration cure slope of heptadecane = $1.52 \times 10^{-13}$
- Calibration cure slope of octadecane = $1.52 \times 10^{-13}$
- FAME inlet mass = $(6.29 \times 10^{7})*(1.52 \times 10^{-13}) = 9.88 \times 10^{-6}$ g
- FAME outlet mass = $(2.52 \times 10^{7})*(1.52 \times 10^{-13}) = 3.83 \times 10^{-6}$ g
- Heptadecane outlet mass = $(4.16 \times 10^{6})*(1.42 \times 10^{-13}) = 5.91 \times 10^{-7}$ g
- Octadecane outlet mass = $(1.83 \times 10^{7})*(3.01 \times 10^{-13}) = 5.51 \times 10^{-6}$ g

Overall green diesel conversion =[ (FAME inlet mass) - (FAME outlet mass) ] / (FAME inlet mass) = [$(9.88 \times 10^{-6}$ g) - $(3.83 \times 10^{-6}$ g) ] / $(9.88 \times 10^{-6}$ g) = 59.30%

C18/C17 Ratio = (Octadecane outlet mass) / (Heptadecane outlet mass) = $(5.51 \times 10^{-6}$ g) / $(5.91 \times 10^{-7}$ g) = 9.3 g/g

## APPENDIX C

## MANUFACTURER'S PROTOCOLS

The protocols used in Chapter 2 were conducted in accordance with the following manufacturer's protocols:

1. PCR8/GW/TOPO TA Cloning Kit (Invitrogen, Cat. No. 45-0642)

**Introduction**

This quick reference sheet is provided for experienced users of the TOPO® Cloning procedure. If you are performing the TOPO® Cloning procedure for the first time, we recommend that you follow the detailed protocols provided in the manual.

| Step | Action |
|---|---|
| Produce PCR product | Produce PCR products using *Taq* polymerase and your own protocol. End the PCR reaction with a final 7 to 30 minute extension step. |
| Perform the TOPO® Cloning Reaction | 1. Set up one of the following TOPO® Cloning reactions using the reagents in the order shown. For electroporation, dilute Salt Solution 4-fold to prepare Dilute Salt Solution. |

| Reagent | Chemical Transfection | Electroporation |
|---|---|---|
| Fresh PCR product | 0.5 to 4 µl | 0.5 to 4 µl |
| Salt Solution | 1 µl | -- |
| Dilute Salt Solution | -- | 1 µl |
| Water | to a final volume of 5 µl | to a final volume of 5 µl |
| TOPO® Vector | 1 µl | 1 µl |
| Total volume | 6 µl | 6 µl |

2. Mix gently and incubate for 5 minutes at room temperature.
3. Place on ice and proceed to transform One Shot® chemically competent *E. coli*, below.

| | |
|---|---|
| Transform One Shot® Chemically Competent *E. coli* | 1. For each transformation, thaw one vial of One Shot® *E. coli* cells on ice.<br>2. Add 2 µl of the TOPO® Cloning reaction into a vial of One Shot® chemically competent *E. coli* and mix gently.<br>3. Incubate on ice for 5 to 30 minutes.<br>4. Heat-shock the cells for 30 seconds at 42°C without shaking. Immediately transfer the tube to ice.<br>5. Add 250 µl of room temperature S.O.C. Medium.<br>6. Incubate at 37°C for 1 hour with shaking.<br>7. Spread 10-50 µl of bacterial culture on a prewarmed LB agar plate containing 100 µg/ml spectinomycin, and incubate overnight at 37°C. |

**Control Reaction**

We recommend using the Control PCR Template and the Control PCR Primers included with the kit to perform the control reaction. See the protocol on pages 19-20 for instructions.

2. Gateway LR Clonase II Enzyme Mix (Introgen, Cat. No. 11791-020)

## Performing the LR Recombination Reaction

**Introduction**

Once you have produced an entry clone containing your gene of interest, you are ready to perform an LR recombination reaction between the entry clone and the appropriate pDEST™ vector, and to transform the reaction mixture into Library Efficiency® DH5α™ to select for an expression clone. It is important to have everything you need set up and ready to use to ensure that you obtain the best results. We suggest that you read this section and the one entitled **Transforming Library Efficiency® DH5α™ Cells**, page 21 before beginning. We also recommend that you include a positive control (see below) and a negative control (no LR Clonase®) in your experiment.

**Positive Control**

The pENTR™-gus plasmid is included in the *E. coli* Expression System with Gateway® Technology for use as a positive control for LR recombination and expression. Use of the pENTR™-gus entry clone in an LR recombination reaction with a pDEST™ vector will allow you to generate an expression clone containing the gene encoding β-glucuronidase (*gus*).

**LR Clonase® II Enzyme Mix**

LR Clonase® II enzyme mix is supplied with the kit (Cat. no. 11824-026 only) or available separately from Invitrogen to catalyze the LR recombination reaction. The LR Clonase® II enzyme mix combines the proprietary enzyme formulation and 5X LR Clonase® Reaction Buffer previously supplied as separate components in LR Clonase® enzyme mix into an optimized single-tube format for easier set-up of the LR recombination reaction. Use the protocol provided on page 20 to perform the LR recombination reaction using LR Clonase® II enzyme mix.

**Note:** You may perform the LR recombination reaction using LR Clonase® enzyme mix, if desired. To use LR Clonase® enzyme mix, follow the protocol provided with the product. **Do not** use the protocol for LR Clonase® II enzyme mix provided in this manual as reaction conditions differ.

**Materials Needed**

- Purified plasmid DNA of your entry clone (50–150 ng/µl in TE, pH 8.0)
- pDEST™ vector (Box 1, 150 ng/µl in TE, pH 8.0)
- LR Clonase® II Enzyme Mix (Box 2, keep at –20°C until immediately before use)
- TE Buffer, pH 8.0 (10 mM Tris-HCl, pH 8.0, 1 mM EDTA)
- Proteinase K solution (supplied with the LR Clonase® II Enzyme Mix; thaw and keep on ice until use)
- pENTR™-gus positive control (50 ng/µl in TE, pH 8.0)

*continued on next page*

# Performing the LR Recombination Reaction, continued

## Setting Up the LR Recombination Reaction

Follow this procedure to perform the LR recombination reaction between your entry clone and the destination vector. If you want to include a negative control, set up a separate reaction but omit the LR Clonase® II enzyme mix.

1. Add the following components to 1.5 ml microcentrifuge tubes at room temperature and mix.

| Component | Sample | Positive Control |
|---|---|---|
| Entry clone (50–150 ng/reaction) | 1–7 µl | – |
| Destination vector (150 ng/µl) | 1 µl | 1 µl |
| pENTR™-gus (50 ng/µl) | – | 2 µl |
| TE Buffer, pH 8.0 | to 8 µl | 5 µl |

2. Remove the LR Clonase® II Enzyme Mix from –20°C and thaw on ice (~ 2 minutes).
3. Vortex the LR Clonase® II Enzyme Mix briefly twice (2 seconds each time).
4. To each sample above, add 2 µl of LR Clonase® II Enzyme Mix. Mix well by pipetting up and down.

   **Reminder:** Return LR Clonase® II Enzyme Mix to –20°C immediately after use.
5. Incubate reactions at 25°C for 1 hour.

   **Note:** For most applications, 1 hour will yield a sufficient number of colonies for analysis. Depending on your needs, the length of the recombination reaction can be extended up to 18 hours. For large plasmids (≥ 10 kb), longer incubation times will yield more colonies.
6. Add 1 µl of Proteinase K solution to each reaction. Incubate for 10 minutes at 37°C.
7. Proceed to **Transforming Library Efficiency® DH5α™ Cells**, next page.

   **Note:** You may store the LR reaction at –20°C for up to 1 week before transformation, if desired.

3. His-Spin Protein Miniprep Kit (Zymo Research, Cat. No. P2002)

## Description

The **His-Spin Protein Miniprep™** provides researchers with a fast His-tagged protein purification technology. The simplified procedure is based on our innovative protein purification chemistry and custom designed fast spin columns. Up to 1 mg of His tagged protein can be purified in 5 minutes and eluted in as little as 100 ul of **His-Elution Buffer**. The purified protein can be used directly for enzymatic assays, protein biochemical analyses, SDS-PAGE and other applications. The product has been optimized for maximal protein purity: a single protein band is visible by Coomassie blue staining on SDS-PAGE gel (Figure 1.). The straightforward spin – wash – elute protocol dramatically simplifies protein purification:
get results in minutes, not hours.

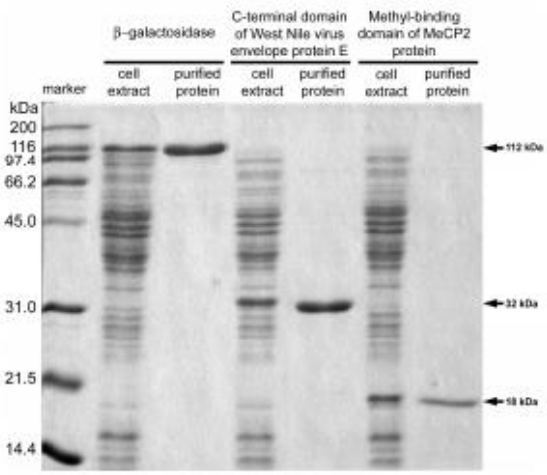


Figure 1. *E. coli* cell extracts, containing indicated proteins expressed as a N-terminal hexahistidine fusion, as well as the proteins purified using His-Spin Protein Miniprep™ were analyzed by SDS-PAGE on a 15% gel, and stained with Coomassie Blue®. The recombinant proteins were purposely expressed to a low level to demonstrate efficiency of the His-Spin Protein Miniprep™.

## Protocol

**NOTE:** The procedure can conducted in cold or at room temperature. Use cold buffers and work on ice for sensitive proteins. Pay attention to centrifugation times: times listed include the time needed for acceleration. Centrifugal steps are carried out in standard tabletop microcentrifuge at maximum speed, usually corresponding to 13,000 to 15,000 g. Read the **SAMPLE PREPARATION** section below to make sure that the samples are in correct buffer before loading on the column.

1. Transfer 250 ul of **His-Affinity Gel** to the Zymo-Spin P1 column (make sure the resin is fully resuspended by shaking/vortexing the bottle before pipetting) and place the column into a collection tube.

   Use 1 ml pipette tip to transfer the **His-Affinity Gel**.; 200 ul-size (usually yellow) or smaller automatic pipette tips have small opening and may not be large enough for the affinity gel particles.

2. Centrifuge for 5-10 seconds.

   Ensure that the **His-Affinity Gel** is completely drained. Some older centrifuge models may require longer time of centrifugation. Do not over-dry the gel by long centrifugation times.

3. Add 150-300 ul of protein sample and resuspend the gel by shaking or tapping the column. Resuspend the gel a few more times during a two minute incubation period.

   It is important to allow the gel and your sample to interact for at least two minutes. If sample volume is larger than 200 ul, an additional 1-2 minutes binding time may be needed to improve yields of purified protein.

4. Centrifuge the column/collection tube 5-10 seconds. Discard the flow-through and place the column back in the collection tube.

5. Add 250 ul of **His-Wash Buffer** and resuspend the gel. Centrifuge 5-10 seconds.

6. Repeat the above wash step (step #5) one more time. Discard the collection tube.

7. Place the Zymo-Spin P1 column into a standard microcentrifuge tube. Add 150 ul of **His-Elution Buffer** to the column and resuspend the gel.

   Elution volumes can be between 100-200 ul. 150 ul of His-Elution Buffer elutes virtually all the column-bound protein. Smaller elution volumes are also possible and may yield more concentrated protein, but the elution efficiency may be compromised.

8. Centrifuge 5-10 seconds to elute the purified protein.

The eluate now contains the purified protein. The eluted protein is suitable for many applications. Use 1-10 ul for SDS-PAGE and Coomassie blue staining analysis. Store the purified protein at appropriate temperature.

## Sample preparation

**His-Binding Buffer** is recommended for sample preparation. Cells expressing the polyhistidine-tagged protein may be directly resuspended in the **His-Binding Buffer** and lysed by standard methods including sonication, repeated freeze-thaw cycles, french press, etc. Other commercial protein extraction buffers (such as BugBuster® from EMD Biosciences or CelLytic from Sigma) are also compatible with the **His-Spin Protein Miniprep**™ system and can be used after adjusting pH and imidazole concentration to values similar to those in the **His-Binding Buffer**.
Any cell extract or other complex protein mixtures can be used as a starting material as long as the proteins are soluble. pH value of the loaded sample should be between 7.5 and 8.0 . Too high or low pH can result in decreased protein yields and/or quality. The sample should not contain higher concentrations of imidazole or histidine (OK up to 10 mM) and should be completely devoid of metal-chelating agents, such as EDTA or EGTA, and strong reducing agents such as DTT. β-mercaptoethanol may be present up to 15 mM. If you are not sure what is in your sample, you can dilute the starting material with one volume of the **His-Binding Buffer** before proceeding with the purification process.

**EXAMPLE PROCEDURE** for protein purification from *E. coli* cell lysates: harvest 10 ml of grown culture and resuspend in 1 ml of **His-Binding Buffer**. Lyse the cells by sonication (or other methods) and centrifuge at ≥ 12,000 g at 4°C for 5 minutes to remove cell debris. Use 150 ul of the supernatant for protein purification.

4. SDS-PAGE (BioRad, Cat. No. 4521061)

1. **Prepare the gel:**
    i. Remove Gel from storage pouch and remove comb by placing both thumbs on the ridge of the comb and push upward in one smooth, continuous motion
    ii. Remove the tape: Pull gently to remove the green tape from the bottom of the cassette. If necessary, use the opening key or comb to help remove the tape at the corners
    iii. Rinse the wells: Use a syringe, wash bottle, or disposable transfer pipette to rinse the wells with running buffer (Reagent D). Straighten the sides of the wells, if necessary

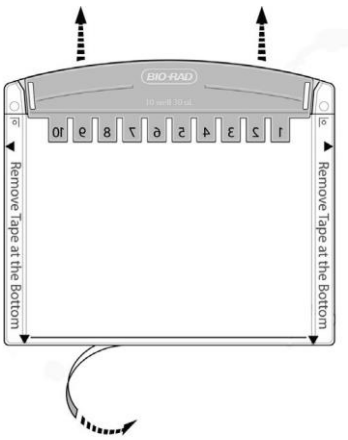


2. **Preparing Mini-PROTEAN Tetra Cell assembly:**
    i. Set the electrode assembly to the open position on a clean, flat surface
    ii. Place the gel cassettes into the electrode assembly. Two cassettes are required to create a functioning assembly
        i. Place the first cassette with the short plate facing inward and so the gel rests at a 30° angle away from the center of the electrode assembly. Make sure the electrode assembly remains balanced and does not tip over
        ii. Place the second gel or buffer dam on the other side of the electrode assembly, again by resting the gel on the supports. The gels rest at 30° angles, one on either side of the electrode assembly, tilting away from the center of the frame
    iii. Gently push both gels toward each other, making sure that they rest firmly and squarely against the green gasket that is built into the electrode assembly. Align the short plates to ensure the edge sits just below the notch at the top of the green gasket
    iv. While gently squeezing the gel cassettes (or cassette and buffer dam) against the green gaskets (maintaining constant pressure and with both gels in place), slide the green arms of the clamping frame one at a time over the gels, locking them into place
    v. The wing clamps of the electrode assembly lift each gel cassette up against the notch in the green gasket, forming a seal. Check again that the short plates sit just below the notch at the top of the green gasket.
    vi. Place the electrophoresis module into the tank and fill the buffer chambers with 1x running buffer (Reagent D):
        i. 200 ml in the inner buffer chamber
        ii. 550 ml (1–2 gels) or 800 ml (3–4 gels, or >200 V) in the outer buffer chamber
3. <u>Prepare Sample</u>: Add 5.5 µL purified protein sample with 5.5 µL Laemmli sample buffer with β-mercaptoethanol (Reagent E), vortex & centrifuge
    i. Heat samples at 95 °C for 5 minutes in the Thermomixer
4. Load Wells using the Loading Guide (10-W)
    i. 15 µL Prestained SDS-PAGE Standard
    ii. 20 µL of sample
5. Running SDS-PAGE
    i. Place lid onto Tetra Cell and plug leads into power supply.
    ii. Turn on power supply to 200V and run for 25 – 45 minutes.
6. After electrophoresis is complete
    i. Turn off the power supply and disconnect the electrical leads
    ii. Remove the lid from the tank and remove the gels from the cell. Pour off and discard the running buffer

iii. To open the cassette, align the arrow on the opening lever with the arrows marked on the cassette and insert the lever between the cassette plates at all four locations. Apply downward pressure to break each seal. Do not twist the lever
iv. Pull the two plates apart from the top of the cassette, and gently remove the gel

7. Perform Gel Staining Procedure

**Gel Staining Procedure:**

1. 1st Wash:
    i. Once SDS-PAGE is performed and is removed IAW SDS-PAGE Procedure (Step 7), wash the gel with 200 mL of $ddH_2O$ for 5 minutes for a total of 3 times
2. Staining:
    i. Remove all water from the staining container and add 50 mL of Bio-Safe Coomassie Stain (enough to completely cover gel) and gently shake for 1 h.
    ii. Protein bands should be visible within 20 min and reach a maximum at 1 h
3. 2nd Wash:
    i. Rinse the gel with 200 mL of $ddH_2O$ for 5 minutes for a total of 3 times, will remove background and allow for proper visualization of the bands.
    ii. Rinse gel in 200 mL of $ddH_2O$ (covers gel) for at least 30 minutes. Can add a folded Kimwipe to assist in stain removal. Background SDS in the gel may cause background staining and interfere with band intensity while the gel is in the stain
    iii. Stained gels can be stored in water.
4. Take a picture of the gel with camera

**Reagent Preparation Instructions:**

A. **Running Buffer:** Dilute 100 mL 10x stock SDS-PAGE running buffer with 900 mL $ddH_2O$.
B. **Sample Buffer:** Add 950 µL Laemmli Sample Buffer to 50 µL β-mercaptoethanol.

5. Lipase Activity Test - Tributyrin Assay (ChiralVison)

**METHOD:**

This method describes the procedure to determine the activity of enzyme in tributyrin units per gram enzyme (TBU/g).

**PRINCIPLE**

The method is based on the speed at which the enzyme hydrolyzes tributyrin at pH 7.5. The butyric acid which is formed is titrated with sodium hydroxide and the consumption of the latter recorded as a function of time.

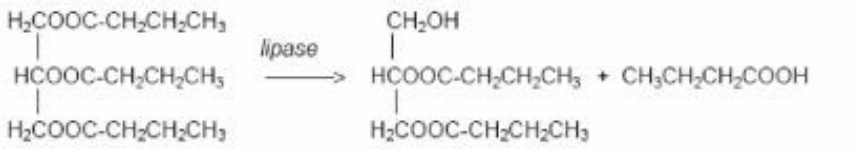


(tributyrin) (butyric acid)

Analysis conditions:

| | |
|---|---|
| Temperature: | 40°C ± 1°C |
| pH: | 7.5 |
| Substrate: | tributyrin (glycerol tributyrate) |
| Reaction time: | at least 3 minutes, up to 30 minutes. (Only the linear response is used to calculate the slope.) |

**3. DEFINITION OF UNITS**

1 TBU (lipase unit) is the amount of enzyme which releases 1 µmol titratable butyric acid per minute under the given standard conditions.

**4. APPARATUS**

pH-stat titration system, eg. Metrohm titrator, comprising:

- Metrohm 665 Dosimat
- Metrohm 614 Impulsomat
- Tamson waterbath
- pH electrode
- magnetic stirrer
- double wall vessel (100 ml)

**4. REAGENTS AND SUBSTRATES**

**4.1 Chemicals**

Sodium hydroxide (NaOH), (prepare 0.1 M solution), Sigma S5881
Glycerol tributyrate (tributyrin), e.g. Sigma-Aldrich 113026

Potassium dihydrogen phosphate p.a. ($KH_2PO_4$), (prepare 0.1 M solution) e.g. Sigma P2222

Buffer solution pH 7.0, e.g. Radiometer 943-112
Buffer solution pH 4.01, e.g. Radiometer 943-111

**5. PROCEDURE**

add to a 100 ml double walled reaction vessel (kept on 40 °C) equipped with a magnetic stirrer bar:

20 ml 25 mM Pi buffer pH 7.3 (= 5 ml 100 mM Pi buffer pH 7.3 + 15 ml demineralized water)
200 microliter tributyrin

stir for 2 minutes
switch on titrator (use 0.1 M sodium hydroxide)
adjust pH to 7.5

*if a blanc reaction runs, monitor the base consumption per minute, for 3 minutes.*

add enzyme (~30 units maximum). *Make sure to take a representative sample containing all particle sizes, specific activity may vary with particle size.*

wait until the first 100 µl base is added
reset and monitor the base consumption for 5 minutes, record each 0.5 minutes and calculate ml titrant / min

wash the vessel with ethanol, then water, dry with paper

**6. CALCULATION**

The measurements for the enzyme standards are used to plot a standard curve with enzyme activity as the x-axis and the associated mean slope (ml/min) as the y-axis. The data must be fitted to a straight line. The mean slope for the different dilutions of the samples is then used to read off the corresponding enzyme activity values from the standard curve. The activity of each sample is then calculated as follows:

$$\text{Sample activity (in TBU/g)} = \frac{\text{ml titrant/min} * \text{molarity of titrant} * 1000}{\text{sample weigth (g)}}$$

**Unit definition**

1 TBU unit = 1 µmol butyric acid released per minute / g enzyme

# APPENDIX D

## PH-STAT CALIBRATION

In this research, lipase from Thermomyces lanuginosus (Sigma-Aldrich, Cat. No. L0777-50ML) was used as the activity standard for the tributyrin assay, as stated in Chapter 2. The solution of lipase was diluted with 100 mM potassium phosphate buffer (pH 7.3) in order to obtain a concentration of 500 U/g. Various amounts were analyzed by the pH-stat in orer to generate a calibration curve, as shown in Figure D1.

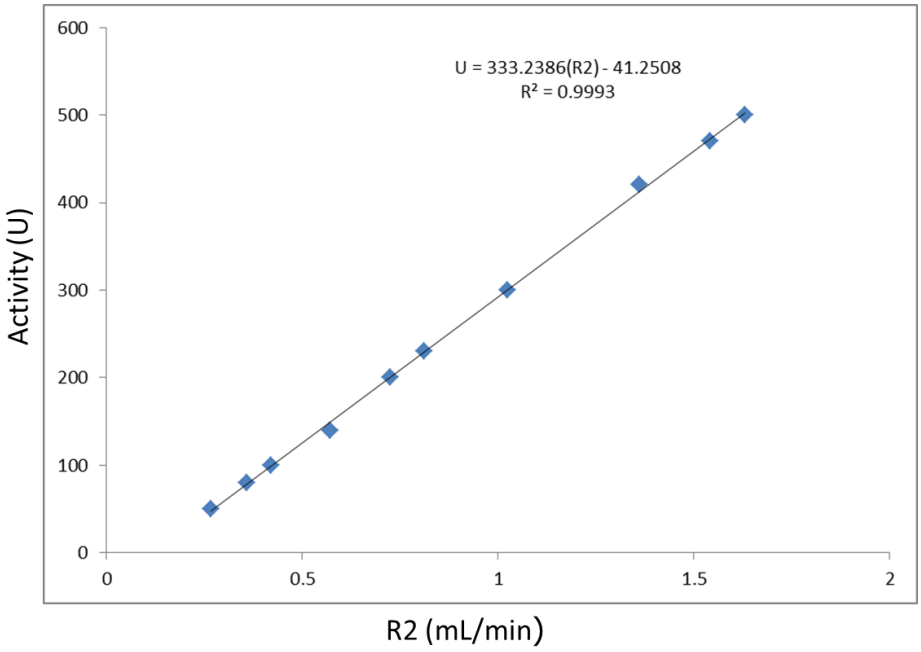


**Figure D1**. pH-stat calibration line.